PNNL-27237

Pacific Northwest
NATIONAL LABORATORY

Proudly Operated by Battelle Since 1965

Snohomish Public Utility District MESA-1

An Assessment of Battery Technical Performance

January 2018

V Viswanathan
A Crawford
J Alam
P Balducci
D Wu
T Hardy
K Mongird

U.S. DEPARTMENT OF ENERGY

Prepared for the U.S. Department of Energy
under Contract DE-AC05-76RL01830

DISCLAIMER

This report was prepared as an account of work sponsored by an agency of the United States Government. Neither the United States Government nor any agency thereof, nor Battelle Memorial Institute, nor any of their employees, makes **any warranty, express or implied, or assumes any legal liability or responsibility for the accuracy, completeness, or usefulness of any information, apparatus, product, or process disclosed, or represents that its use would not infringe privately owned rights**. Reference herein to any specific commercial product, process, or service by trade name, trademark, manufacturer, or otherwise does not necessarily constitute or imply its endorsement, recommendation, or favoring by the United States Government or any agency thereof, or Battelle Memorial Institute. The views and opinions of authors expressed herein do not necessarily state or reflect those of the United States Government or any agency thereof.

PACIFIC NORTHWEST NATIONAL LABORATORY
operated by
BATTELLE
for the
UNITED STATES DEPARTMENT OF ENERGY
under Contract DE-AC05-76RL01830

Printed in the United States of America

Available to DOE and DOE contractors from the
Office of Scientific and Technical Information,
P.O. Box 62, Oak Ridge, TN 37831-0062;
ph: (865) 576-8401
fax: (865) 576-5728
email: reports@adonis.osti.gov

Available to the public from the National Technical Information Service
5301 Shawnee Rd., Alexandria, VA 22312
ph: (800) 553-NTIS (6847)
email: orders@ntis.gov <http://www.ntis.gov/about/form.aspx>
Online ordering: http://www.ntis.gov

This document was printed on recycled paper.
(8/2010)

PNNL-27237

Snohomish Public Utility District MESA-1

An Assessment of Battery Technical Performance

V Viswanathan
A Crawford
J Alam
P Balducci
D Wu
T Hardy
K Mongird

January 2018

Prepared for
the U.S. Department of Energy
under Contract DE-AC05-76RL01830

Pacific Northwest National Laboratory
Richland, Washington 99352

Executive Summary

Energy storage integration into the U.S. grid has been gathering momentum, especially as renewable generation penetration increases. Several states have storage procurement targets to deal with a variety of issues such as afternoon ramping requirements, frequency regulation/control, and time shifting of renewable energy. The technical attributes of energy storage to provide benefits to stakeholders, comprised of multiple utilities and their customers, were investigated, funded jointly by the Snohomish Public Utility District (SnoPUD), Washington Clean Energy Fund (CEF) and the U.S. Department of Energy Office of Electricity Delivery and Energy Reliability (DOE-OE).

Motivation for this Work

SnoPUD purchases approximately 76 percent of its electricity, net of slice sales, from the Bonneville Power Administration (BPA) and provides balancing payments to BPA to account for differences in net load and scheduled net load. SnoPUD is using the 2MW/1 MWh battery energy storage system (BESS) called MESA-1 "to learn about energy storage and how it can be used to integrate renewable generation resources into its resource portfolio" (Zyskowski 2015). MESA-1 is located at the Hardeson Substation in Everett, Washington. In addition to load balancing, BESS performance was evaluated when following duty cycles or engaged in modes to provide arbitrage, capacity, distribution upgrade deferral, and power factor (PF) correction. These use cases or services were identified as applicable for MESA-1 and were defined based on utility- and site-specific characteristics. Since BESSs are quite diverse in their characteristics, it was important to first characterize the performance and performance stability of MESA-1 over time using a DOE-OE standardized baseline test procedure for energy storage, which includes energy capacity measurements, response time, internal resistance, and generic duty cycles for the aforementioned use cases. After conducting the baseline tests, the BESS performed the various use cases listed. Outcomes of these analyses will be beneficial for SnoPUD to understand the performance of the MESA-1 BESS at its current state and to apply these results in designing appropriate operational strategies.

Summary of Work Performed

This report investigates the technical performance of the SnoPUD MESA-1 BESS facility, consisting of two battery sub-systems 1a and 1b, based on a number of baseline and use case tests. Baseline tests were intended to assess the general technical capability of the BESS (e.g., stored energy capacity, ramp rate performance, ability to track variable charge/discharge commands, direct current (DC) battery internal resistance) while the use case tests were intended to examine the performance of the BESS while engaged in specific economic services (e.g., arbitrage, power factor correction). Parameters that are important for understanding BESS performance when subjected to actual field operation for achieving economic benefits (e.g., round trip efficiency (RTE) with and without rest, with and without auxiliary loads, auxiliary power consumption, signal command tracking performance, temperature variations, parasitic power loss during power electronics switching during rest, state of charge (SOC) excursions, non-uniformity of power flow between the battery subsystems) were analyzed using test results. In addition, the results and lessons presented herein would also be beneficial for any task or effort that needs technical assessment on similar and different types of BESS based on field deployment results, since the assessment methodology remains the same.

Key Questions Addressed

The following questions were addressed:

1. What is the RTE of the BESS? This analysis determined RTE for the BESS under various scenarios – ambient temperature, charge-discharge power levels, with and without rest periods, with and without auxiliary consumption
2. How does the BESS perform during baseline and use case testing? A thorough analysis of BESS performance was carried out using metrics developed in the DOE-OE Energy Storage Performance Protocol, and additional metrics identified in this project.
3. What was the percent of time the BESS was not available? An analysis was done on the percent of time the BESS was not available, and the reasons were attributed to one of the following:
   a. BESS system issues
   b. Site controller issues
   c. Human error
   d. BESS reserved for demand response for BPA.
4. What are some of the issues identified in this project that are not very obvious? The internal resistance of the DC battery was determined, along with power flow distribution and cumulative energy throughput for 1a and 1b, to identify reasons for RTE trends and potential catalysts for battery degradation. The seasonal effect on auxiliary power consumption was determined. The effect of inverter switching state during rest on battery self-discharge was determined.

Key Outcomes

The MESA-1 BESS was subjected to reference performance or baseline testing, including various rates of charge and discharge, internal resistance measurements, and response time/ramp rate measurements. Duty cycles were developed for various use cases, and the BESS performance was analyzed accordingly.

Outcome 1

The BESS performance during baseline and use case testing was analyzed. During baseline capacity tests, the performance increased with increasing power up to 1,000 kW. The RTE[1] ranged from 66 to 91 percent, depending on the power, and whether the rest periods and auxiliary consumption were included. The BESS retained its energy content during post Cycle 1 and Cycle 2 capacity tests, with a similar RTE range. The RTE at C/4 rate[2] was lowest for baseline tests, because of higher auxiliary power consumption during summer.[3] The RTE had a range of 69 to 87 percent during the baseline peak shaving test, which was carried out at a constant C/4 rate charge, and varying discharge rates of C/4, C/2, and C rate. When auxiliary consumption during rest periods were excluded, the RTE rose by 3 to 5 percent, with the highest increase for baseline tests performed in summer with higher auxiliary load. When the auxiliary consumption was excluded throughout the test period, the RTE increased by 6 to 16 percent, with the

[1] The RTE is simply the ratio of discharge energy to charge energy, ensuring the BESS SOC is brought back to the initial SOC.
[2] C rate corresponds to discharging or charging the BESS at C kW, where C is the rated energy of the BESS. For example, the MESA-1 BESS rated energy is 1000 kWh. Hence, C rate discharge or charge corresponds to 1000 kW.
[3] The EPRI Energy Storage Integration Council (ESIC) identified seasonal testing of auxiliary load for further studies at the ESIC Cleveland meeting in November 16, 2017.

difference increasing at a decreasing rate. At less than or equal to C rate, the increase in RTE was highest for baseline tests, which had auxiliary load.

The BESS was discharged between 92.5 percent and 7.5 percent SOC, which corresponds to 85 percent depth of discharge (DOD). The estimated discharge energy at 100 percent DOD was calculated by dividing the measured energy by the DOD of 85 percent. Including the auxiliary losses, 970 kWh was delivered at the C rate. Excluding auxiliary consumption of 30 kW, the energy delivered is 1,015 kWh.

The arbitrage use case resulted in an RTE of 53 to 91 percent, depending on power, and whether rest and auxiliary loads were included. This supports the conclusion that there is no single RTE that represents BESS performance. Assuming an artificially high RTE makes the BESS more attractive than it actually is, especially for use cases such as arbitrage whose benefits are directly tied to the BESS RTE, in addition to the high/low price differential.

A similar RTE range was observed for the capacity and load shaping tests. For the PF Correction test, the volt-amperes-reactive (vars) requested during Cycle 2 were lower than during Cycle 1, possibly because Cycle 1 testing was done in winter, with a higher need for PF correction. For Cycle 1, the required vars is lower when the BESS is in the discharge mode. The rate of SOC decrease during PF correction mode was 25 times higher than when the BESS was at rest without the PCS switching. This needs to be taken into account when weighing the benefits of PF correction service provided by the BESS.

RTE for the BESS as a whole unit across a range of power levels was determined, as were the RTE for MESA-1a and MESA-1b individually. The BESS RTE peaks at 1,000 kW, in line with the MESA-1a RTE trend, while the MESA-1b RTE, due to lower internal resistance, increases with power levels. Long rest periods, with associated auxiliary losses, reduced the BESS RTE. This effect is further magnified when the BESS is at rest at low SOC, with the power conversion system (PCS) in a switching mode consuming parasitic power.

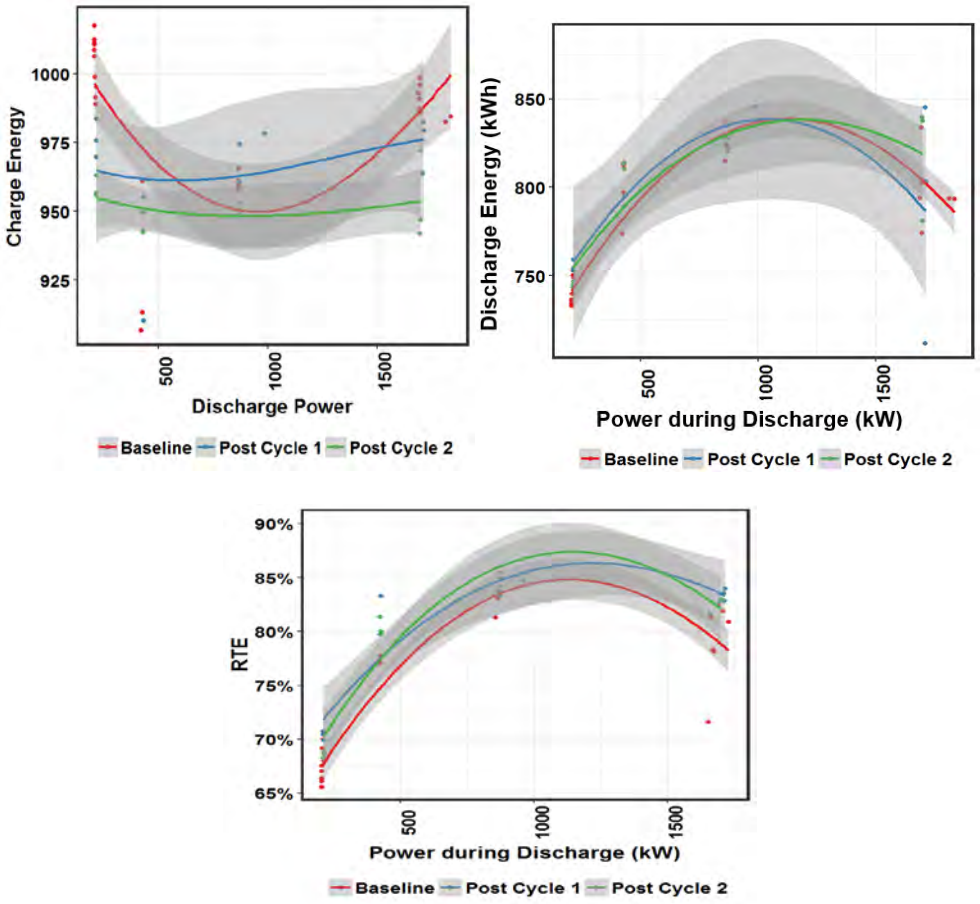

Figure ES.1. Charge, Discharge Energy and Roundtrip Efficiency at Various Power Levels

Outcome 2

A thorough analysis of BESS performance was carried out using metrics developed in the DOE-OE Energy Storage Performance Protocol, and additional metrics identified in this project. As stated in Outcome 1, the RTE was highly dependent on the power, rest period, and whether auxiliary consumption is taken into account. The steep drop in SOC when the PCS is in switching state needs to be accounted for when optimally deploying the BESS for various use cases. While the BESS did not switch during rest after charge, when the SOC after discharge was close to its lower limit, the PCS was in switching state in order to ensure the BESS SOC does not go below the lower limit. Hence, it may be preferable to ensure the BESS SOC is at least 5 percent above its lower limit to prevent PCS switching.

Due to data being available only once every 10 seconds, the response time and ramp rate of the BESS could not be determined, other than to conclude the response time was faster than 10 seconds. Signal tracking analysis was difficult because commands could not be provided to the BESS in time increments faster than 15 minutes.

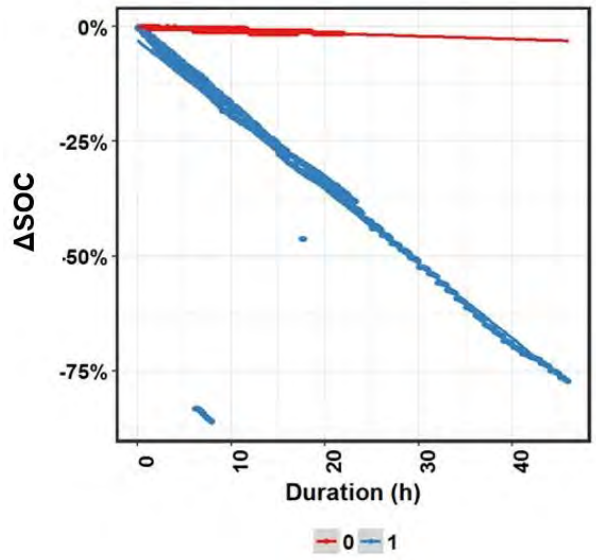

Figure ES.2. Rate of Change of SOC for Volt-Var Runs with BESS in PF Mode (1), and during Rest (0)

Outcome 3

The number of days the BESS was not available for testing was determined. There were 88 days when the BESS was set aside for providing demand response for BPA. Excluding these days, the number of days for testing were 242 from June 20, 2016 to May 20, 2017. The BESS was not available 38 percent of the 242 days, or a total of 92 days. The BESS was not available for 16 days or 7 percent of the time due to BESS related issues, 12 days or 5 percent due to site/DERO-related issues, 6 days or 2.5 percent due to human error, while unknown reasons which could be any of the categories listed contributed 58 days or 24 percent of the time. When the days for DR were counted, the number of days for testing corresponded to 330 days (11 months). The BESS was not available to PNNL for testing 55 percent of the time, with stoppage-related unavailability corresponding to 5 percent due to BESS-related issues, 3.6 percent due to site/DERO -related issues, 1.8 percent due to human error, 18 percent due to unknown reasons, with DR accounting for 27 percent.

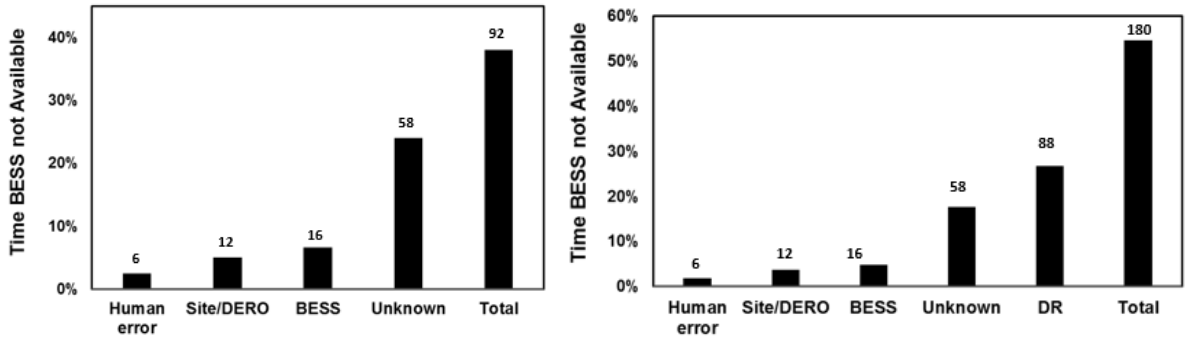

Figure ES.3. Percent Time BESS is Unavailable (left) Excluding BPA DR Days; (right) Including BPA DR days. The number of days unavailable is shown at the top of each bar.

Outcome 4

There were multiple issues identified during testing that were not obvious or necessarily anticipated leading up to testing:

- While the MESA-1b energy content is 6 percent higher than the 1a energy content, the energy available from 1b is 19 percent higher than the energy available from 1a because its SOC range of 5 to 95 percent is higher than the 10 to 90 percent range for 1a. However, the cumulative energy throughput for 1b during testing was 48 percent higher than that for 1a because the 1b SOC was lower than 1a at the start of charge and higher at the start of discharge. Hence, the site controller directs more power to 1b at the start of charge or discharge. For the same reasons, the power at the end of charge and discharge was also higher for 1b, since its SOC limits have not been reached when 1a power starts tapering due to SOC limits being reached. While so far this has not led to increased degradation for 1b, this metric and its effect on 1a and 1b state of health needs to be monitored.[4]
- The 20-s pulse discharge resistance for 1a is greater than 1b, resulting in lower RTE at high power levels for 1a.
- When the BESS is in PF correction mode, the PCS is in switching state. When the PCS is in the switching state, there is power flow across the inverter. This consumes parasitic power, resulting in nearly two orders of magnitude higher rate of SOC decrease. This needs to be accounted for when analyzing benefits from the BESS during the PF correction mode.[5]
- For other use cases where there is only real power flow, the PCS is placed in a switching mode when the BESS SOC is at or within 1-2 percent of its lower SOC limit in order to avoid excursion below the lower SOC limit. This consumes parasitic power. Hence, it would be preferred to maintain the SOC at no less than 5 percent above the BESS lower SOC limit.
- Auxiliary power consumption was less in winter compared to summer.
- The BESS SOC decreased rapidly at the end of charge for rates in the C/4 to C/2 range,[6] dominated by 1a SOC behavior. The BESS increased after charge and decreased after discharge at the C to 2C rate, dominated by 1b SOC behavior. This simply appears to be due to error in SOC measurement by the 1a and 1b battery management system (BMS).[7]
- Spikes at the end of charge and discharge were present, primarily caused by power tapering in 1a necessitating 1b to spike in order to pick up necessary power. At low C rates, this spike results in total power flow exceeding requested power momentarily. Since the spikes do not exceed the PCS rating, no damage to the DC battery is anticipated. However, it is not known what the rapid power pulse does to the PCS hardware.

[4] The EPRI Energy Storage Integration Council (ESIC) identified "state of health definitions and tests" for further studies at the ESIC Cleveland meeting in November 16, 2017.
[5] The EPRI Energy Storage Integration Council (ESIC) identified "SOC loss rate" during "reactive power injection" for further studies at the ESIC Cleveland meeting in November 16, 2017.
[6] A C/x rate is the current in amperes (A) at which the ampere-hour (Ah) capacity of the battery can be discharged in x hours. For example, if the capacity of the battery is 100 Ah, a C/10 rate corresponds to 10 amperes (A).
[7] The EPRI Energy Storage Integration Council (ESIC) identified "SOC calibration procedure" for further studies.

Acknowledgments

We are grateful to Mr. Bob Kirchmeier, who is a Senior Energy Policy Specialist at the Washington Department of Commerce, for providing financial support to PNNL and our utility partners, in addition to his guidance during this project. We are also grateful to Dr. Imre Gyuk, who is the Energy Storage Program Manager in the Office of Electricity Delivery and Energy Reliability at the U.S. Department of Energy, for providing financial support and leadership on this and other related work at PNNL. We wish to acknowledge Philip Craig from BlackByte Cyber Security, the team members from SnoPUD, including Arturas Floria, Kevin Lanum, Will Odell, Kelly Wallace and Jason Zyskowski, and Jason Yedniak from Doosan GridTech.

Acronyms and Abbreviations

1E-1C	1Energy-Intelligent Controller
AC	alternating current
Ah	ampere-hours
BESS	battery energy storage system(s)
BMS	battery management system
BPA	Bonneville Power Administration
BSET	Battery Storage Evaluation Tool
CEF	Clean Energy Fund
CVR	conservation voltage regulation
DC	direct current
DERO	GridTech's Distributed Energy Resources Optimizer
DG	Doosan GridTech
DG-IC	Doosan GridTech-Intelligent Controller
DNP3	Distributed Network Protocol
DOD	depth of discharge
DOE	U.S. Department of Energy
DR	Demand Response
ES	Energy Storage
ESS	Energy Storage Systems
FR	frequency regulation
IEEE	Institute of Electrical and Electronics Engineers
kvar	kilovolt-ampere reactive
kW	kilowatt(s)
kWh	kilowatt-hour(s)
MESA	Modular Energy Storage Architecture
MW	megawatt(s)
MWh	megawatt hour(s)
NWPP	Northwest Power Pool
OCV	open circuit voltage
OE	Office of Energy
PCS	power conversion system
PF	Power Facto
PNNL	Pacific Northwest National Laboratory
PS	peak shaving
PV	photovoltaics
RTE	round trip efficiency

SnoPUD	Snohomish Public Utility District
SOC	state of charge
T	temperature
V	volts
vars	volt-amperes-reactive
W	watt
Wh	watt hour(s)

Contents

Executive Summary iii
Motivation for this Work iii
Summary of Work Performed iii
Key Questions Addressed iv
Key Outcomes iv
Outcome 1 iv
Outcome 2 vi
Outcome 3 vii
Outcome 4 viii
Acknowledgments ix
Acronyms and Abbreviations xi
1.0 Introduction 1.1
1.1 Project Synopsis 1.1
1.2 SnoPUD MESA-1 ..... 1.2
2.0 Battery Performance Test Results 2.1
2.1 Baseline Test Results 2.1
2.2 Internal Resistance Test 2.15
2.3 Peak Shaving Duty-Cycle Results 2.17
2.4 Use Case 1: Energy Arbitrage 2.20
2.4.1 Duty Cycle Summary 2.20
2.4.2 Test Results 2.20
2.5 Use Case 1: System Capacity 2.26
2.5.1 Duty Cycle Summary 2.26
2.5.2 Test Results 2.26
2.6 Use Case 3: Volt/Var 2.30
2.6.1 Duty Cycle Summary 2.30
2.6.2 Test Results 2.30
2.7 Use Case 3: Load Shaping 2.36
2.7.1 Duty Cycle Summary 2.36
2.7.2 Test Results 2.36
2.8 Capacity Stability Test after Cycle 1 and Cycle 2 ..... 2.39
3.0 Lessons Learned 3.1
3.1 Lessons Learned from Test Results 3.1
3.2 Lessons Learned in Design of Test Set-up and Data Transfer 3.4
3.3 Lessons Learned from Test Disruptions and Investigations 3.5
4.0 Conclusions 4.1

5.0 References 5.1
Appendix A A.1

Figures

ES.1 Charge, Discharge Energy and Roundtrip Efficiency at Various Power Levels vi
ES.2 Rate of Change of SOC for Volt-Var Runs with BESS in PF Mode and during Rest vii
ES.3 Percent Time BESS is Unavailable Excluding BPA DR Days; Including BPA DR days vii
1.1 Main Components of the Use Case Analysis Project 1.1
1.2 MESA-1a Module, String, Control System, and MESA-1 Site with all Major Components..... 1.3
1.3 MESA Standard Architecture, and MESA-1 System Connection with Grid 1.4
2.1 Roundtrip Efficiency during Baseline Capacity Tests..... 2.4
2.2 Baseline Capacity Test at 250 kW Charge and Discharge BESS, MESA-1a and 1b..... 2.7
2.3 Reactive Power Flow through 1a and 1b during 250 kW Charge Baseline Capacity Test 2.8
2.4 Baseline Capacity Test at 500 kW Charge and Discharge BESS, 1a and 1b 2.9
2.5 Baseline Capacity Test at 1000 kW Charge and Discharge, BESS, 1a and 1b 2.11
2.6 Baseline Capacity Test at 2000 kW Charge and Discharge, BESS, 1a and b 2.13
2.7 Internal Resistance of a 1.8 Ah Li-ion cell as a Function of Change in SOC during Charge or Discharge Pulse 2.16
2.8 Peak Shaving Tests C/4 Rate Charge, C/4, C/2 and C Rate Discharge..... 2.19
2.9 Energy Arbitrage Runs for Cycle 1, Power and SOC as a Function of Time 2.22
2.10 Energy Arbitrage Runs for Cycle 1, Temperature as a Function of Time..... 2.23
2.11 Energy Arbitrage Runs, Cycle 2, Power and SOC as a Function of Time 2.24
2.12 Energy Arbitrage, Cycle 2, Temperature as a Function of Time..... 2.25
2.13 System Capacity Tests, Cycle 1 ..... 2.28
2.14 System Capacity Tests, Cycle 2 ..... 2.29
2.15 Power Factor Correction Mode, Cycle 1 Reactive Power and total kVA, Real and Reacive Power, SOC 2.31
2.16 Power Factor Correction Mode, Run 2, Cycle 1 Reactive Power and Total kVA, Real and Reacive Power, SOC 2.32
2.17 Power Factor Correction Mode, Run 3, Cycle 1 Reactive Power and Total kVA, Real and Reacive Power, SOC 2.33
2.18 Power Factor Correction Mode, Run 1, Cycle 2 Reactive Power and total kVA, Real and Reacive Power, SOC 2.33
2.19 Power Factor Correction Mode, Run 2, Cycle 2 Reactive Power and Total kVA, Real and Reacive Power, SOC 2.34
2.20 Rate of Change of SOC for Volt-Var Runs with BESS in PF Mode, and during Rest 2.35
2.21 PCS Switching State as a Function of SOC Level after Discharge Real Power, Apparent and Reactive Power..... 2.35
2.22 Load Shaping Results, Cycle 1..... 2.38
2.23 Load Shaping Results, Cycle 2..... 2.38
2.24 Load Shaping Results, Cycle 2..... 2.39
2.25 Load Shaping Results, Cycle 2..... 2.39

2.26 Power, SOC, Temperature and Auxiliary Consumption for Capacity Tests Post Cycle 1 at C/4 Rate; BESS, MESA-1a and 1b 2.43
2.27 Power, SOC, Temperature and Auxiliary Consumption for Capacity Tests Post Cycle 1 at C/2 Rate; BESS, MESA-1a and 1b 2.45
2.28 Power, SOC, Temperature and Auxiliary Consumption for Capacity Tests Post Cycle 1 at C Rate; BESS, MESA-11a and 1b..... 2.47
2.29 Power, SOC, Temperature and Auxiliary Consumption for Capacity Tests Post Cycle 1 at 2C Rate; BESS, 1a and 1b 2.49
2.30 Power, SOC, Temperature and Auxiliary Consumption for Capacity Tests Post Cycle 2 at C/4 Rate; BESS, MESA-11a and 1b 2.51
2.31 Power, SOC, Temperature and Auxiliary Consumption for Capacity Tests Post Cycle 2 at C/2 Rate; BESS, MESA-1a and 1b 2.53
2.32 Power, SOC, Temperature and Auxiliary Consumption for Capacity Tests Post Cycle 2 at C Rate; BESS, MESA-1a and 1b..... 2.55
2.33 Power, SOC, Temperature and Auxiliary Consumption for Capacity Tests Post Cycle 2 at 2C Rate; BESS, MESA-1a and 1b..... 2.57
2.34 Average DC Current during Rest after Charge; after Discharge; 1a, 1b 2.58
2.35 Reactive and Reactive Power Flow during C/4 rate Post Cycle 1 Capacity Test for BESS, Reactive Power Flow for MESA-1a and 1b 2.59
2.36 Auxiliary Power Consumption during Charge and Discharge for Baseline and Post Use Case Tests; BESS, 1a, 1b 2.64
2.37 Relationship between Charge and Discharge Power Levels for BESS 2.65
2.38 Charge Energy at Various Power Levels for Baseline and Post Cycle 1 Includes Rest and Aux, Excludes Rest, Excludes Aux 2.65
2.39 Charge Energy at Various Power Levels for MESA-1a Baseline and Post Cycle 1 Includes Rest and Aux, Excludes Rest, Excludes Aux 2.66
2.40 Charge Energy at Various Power Levels for MESA-1b Baseline and Post Cycle 1 Includes Rest and Aux, Excludes Rest, Excludes Aux 2.67
2.41 Average Temperature for the BESs, 1a and 1b at Various Power Levels 2.68
2.42 Discharge Energy at Various Power Levels for Baseline and Post Cycle 1 Tests Includes Auxiliary Loads, Excludes Auxiliary Loads..... 2.69
2.43 Discharge Energy at Various Power Levels for MESA-1a for Baseline and Post Cycle 1 Tests Includes Auxiliary Loads, Excludes Auxiliary Loads..... 2.69
2.44 Discharge Energy at Various Power Levels for MESA-1b for Baseline and Post Cycle 1 Tests Includes Aux, Excludes Aux 2.70
2.45 RTE at Various Power Levels for Baseline and Post Cycle 1 and Post Cycle 2 ..... 2.72
2.46 Average Temperature as a Function of Power Levels for Baseline and Post Cycle 1 and Post Cycle 2 Tests BESS, MESA-1a, MESA-1b..... 2.73
2.47 Effect of Power and Test Type on Charge or Discharge Energy needed per unit SOC, Combined, MESA-1a, MESA-1b 2.74
2.48 Internal Resistance from Pulse Testing of MESA-1 BESS 10s Pulse, 20s Pulse..... 2.76
2.49 Internal Resistance from Pulse Testing of MESA-1a and MESA-1b..... 2.77

2.50 Voltage as a Function of Charge Current at 8% SOC for Post Cycle 1 and Post Cycle 2 for 1a and 1b 2.78
2.51 Cumulative Discharge Energy Throughput through 1a and 1b 2.79

Tables

2.1 Stored Baseline Energy Capacity and Roundtrip Efficiency at Rated Power 2.1
2.2 Consolidated Results for Baseline Capacity Tests prior to Cycle 1 Use Case Testing 2.3
2.3 Comparison of MESA-1, 1a, and 1b Performance during Baseline Capacity Tests 2.5
2.4 Current through 1a and 1b during Rest after Charge and Discharge during Baseline Capacity Tests 2.14
2.5 Change in SOC during Rest, PCS Switching State, DC Current Flow and Calculated Change for 1a 2.15
2.6 ΔSOC during Rest, PCS Switching State, DC Current Flow and Calculated Δ for 1b 2.15
2.7 Internal Resistance of the ESS for Discharge at 85 and 45% SOC and Charge at 8% SOC 2.16
2.8 Peak Shaving Duty Cycle Results 2.18
2.9 Peak Shaving Duty Cycle Results for MESA-1a 2.18
2.10 Peak Shaving Duty Cycle Results for MESA-1b 2.18
2.11 Energy Arbitrage Cycle 1 Test Results 2.21
2.12 System Capacity Test Results Cycle 1 ..... 2.27
2.13 Load Shaping Test Results 2.37
2.14 Capacity Stability after Cycle 1 ..... 2.40
2.15 Capacity Stability after Cycle 2 ..... 2.41
2.16 Comparison of Baseline Tests and Post Cycle 1 and 2 Tests 2.60
2.17 Change in Performance Metrics with Respect to Baseline 2.62
2.18 Degradation or Improvement in Performance after Cycle 1 and Cycle 2 ..... 2.63
2.19 Internal Resistance of the ESS Post Cycle 1 ..... 2.75
2.20 Internal Resistance of the ESS Post Cycle 2 ..... 2.76
2.21 Cooling Effect of Charging 2.79
A.1 Initial Baseline Capacity Test Results A.1
A.2 Post Peak Shaving and Pulse Testing Baseline Capacity Tests A.2
A.3 Multiple Charge-Discharge Rates July 4 Weekend and Mid July A.3
A.4 Consolidated Results for Baseline Capacity Tests Prior to Cycle 1 Use Case Testing A.6

1.0 Introduction

The Washington State Clean Energy Fund (CEF) was created from funding appropriated by the 2013 Washington State Legislature in the Energy Freedom Program to expand clean energy projects and technologies statewide. The CEF was designed to "provide a benefit to the public through development, demonstration, and deployment of clean energy technologies that save energy and reduce energy costs, reduce harmful air emissions or otherwise increase energy independence for the state." The Washington Legislature appropriated $36 million of the state taxable building construction account for three programs, one of which provided $15 million for smart grid grants to utilities to advance renewable energy technologies by public and private electrical utilities that serve retail customers in the state. Snohomish Public Utility District (SnoPUD), located approximately 20 miles north of Seattle and serving over 341,000 electric customers and 20,000 water customers over 2,200 square miles of service territory, received $7.3 million of CEF funds and used it towards installation of two battery energy storage systems (BESS) and controls integration software. Both of these BESSs were deployed using the Modular Energy Storage Architecture (MESA) and are identified as MESA-1 & MESA-2.

1.1 Project Synopsis

Pacific Northwest National Laboratory (PNNL) was chosen to provide analytical support under the Use Case Analysis Project designed to aid BESS grid integration efforts by providing a framework for evaluating the technical and financial benefits of the energy storage system (ESS), and exploring the role of energy storage in delivering value to utilities and the citizens they serve. This framework, and the tools used to implement it, will evaluate a number of use cases as applied to energy storage projects deployed by the participating utilities under the CEF program. The methodologies that emerge for evaluating multiple storage benefits, and the detailed operational results from utility utilization of energy storage, will have broad national relevance and applicability. There are three main components related to use case testing and evaluation, as outlined in Figure 1.1.

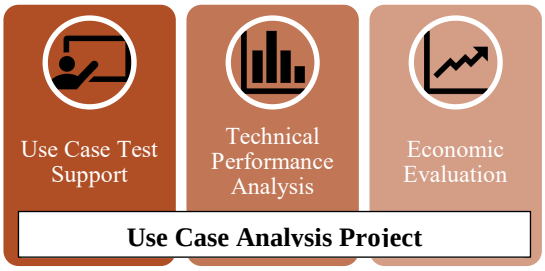

Figure 1.1. Main Components of the Use Case Analysis Project

PNNL provided technical support for baseline and use case testing, including development of protocols and duty cycles to test the ability of the BESS to safely and effectively be used for all applicable use cases. PNNL recommended metrics (e.g., ramp rate, round trip efficiency (RTE), internal resistance) to be evaluated in this task. As the baseline and use case tests were conducted, PNNL analyzed test results against a predefined set of performance metrics to determine the effectiveness of storage for each use case. Finally, PNNL evaluated for each use case and each utility partner the economics of energy storage using commonly used characteristics such as rate of return and payback periods. A use case was developed bundling various services offered by the BESS and was optimized to determine the financial benefit of BESS deployment over the economic life of the unit.

This report documents baseline and use case technical performance of the MESA-1 BESS based on the framework and approaches defined by PNNL in the test plan report, and the lessons learned on the technical aspects of the MESA-1 BESS.

Understanding of the technical features and limitations is essential to performing the economic evaluation of the use cases to which a BESS is subjected. Therefore, technical information on the MESA-1 BESS is provided in the following section.

1.2 SnoPUD MESA-1

The MESA-1 BESS is comprised of 2×1 megawatts (MW), 0.5 MWh lithium-ion battery system installed at SnoPUD's Hardeson Substation. One of the 1 MW banks is manufactured by Mitsubishi and GS Yuasa (MESA-1a), and the other bank is manufactured by LG Chem (MESA-1b).

MESA-1a is composed of modules[8] consisting of 12 cells[9] in series. There are 20 modules in series in a string[10] and 12 strings are connected in parallel. Each of the modules is rated at 50 Ah and 45 Volts (V) Direct Current (DC) (at a nominal cell voltage of 3.7V, the calculated voltage is 44.4 V). Therefore, 12 banks connected in parallel produce 600 ampere-hours (Ah[11]) and 20 modules in series producing 900 VDC results in a nominal energy[12] content of 540 kilowatt-hours (kWh) (533 kWh using 3.7 V nominal cell voltage, or a C rate of 533 kW). The state of charge (SOC) range for MESA 1a is 10 percent to 90 percent SOC, which corresponds to discharge energy of 426 kWh. This limit was set in the control system by the utility. The top pane of Figure 1.2 shows an individual battery module (left) and multiple modules (right) connected in a bank. The bottom pane of Figure 1.2 shows the control panels (left) for the ESS and a wide view of the whole system with for the 1 MW, 0.5 MWh units.

[8] Modules consist of cells connected in series, and may also have parallel strings of these series connected cells, as is the case for the MESA-1b battery.

[9] A cell is the smallest repeating unit in a battery, and consists of a cathode (positive) and an anode (negative) separated by an electronic insulator that allows ion transfer. The cathode and anode may consist of several parallel electrodes to increase cell Ah capacity.

[10] Strings in a BESS are typically connected in parallel, and consist of modules connected in series within each string

[11] Ah is the amount of coulombs, which is a product of amperes x seconds, stored in the battery divided by 3600, where 3600 is the number of seconds in an hour.

[12] Nominal energy content is the Ah capacity of the battery multiplied by the battery nominal voltage which is available from the specifications. Typically, this nominal energy is available at a specific discharge rate.

Figure 1.2. MESA-1a Module, String, Control System, and MESA-1 Site with all Major Components

There are a total of 12 parallel strings in the MESA-1b container. Each string contains 17 modules resulting in a total of 204 modules in the MESA-1b system (17*12=204). Each module has 28 cells, rated at 3.65V (3.0 to 4.2V range) and 27 Ah. The cells are arranged in 2 parallel strings of 14 series connected cells. The energy rating of the system is 560 kWh, with each string rated at 46.6 kWh, each module at 2.7 kWh and each cell at 98.5Wh. The module voltage range is 42.0 to 58.8V. The total calculated energy is 3.7V x 27Ah/cell x 28 cells/module x 17 Modules/String x 12 strings in parallel= 563kWh, or a C rate of 563 kW. The DC Voltage Range for the MESA-1b battery is 714 to 988V. The energy ratio for 1b:1a is 563/533 = 1.06.

The SOC range for MESA-1b is 5 to 95 percent, which corresponds to an energy content of 506 kWh. This limit was set in the control system by the utility. Hence, the maximum energy withdrawn from the MESA-1b battery is 19 percent higher than that from the MESA-1a battery, while its energy content is 6 percent higher. The cumulative energy throughput and average power at the power conversion system (PCS) was quantified for both battery systems. As BESS testing continues, this may be used as one of several tools to provide insights on why one battery degrades faster than the other.

Control system integration of the SnoPUD ESS is performed using MESA standards. At the planning stage, SnoPUD explored different standards for software and control system integration of ESS and experienced a lack of adequate open standards. Therefore, in collaboration with a number of partners, the MESA standard was developed (MESA 2016). The MESA standard is open, non-proprietary, and helps accelerating interoperability, scalability, safety, quality, and affordability in energy storage components and systems. Both BESS units at SnoPUD MESA-1 are built on this standard. There are two major components of the MESA standard as shown in Figure 1.2. One is the MESA-Device that addresses how energy storage components within an energy storage system communicate with each other and other operational components, and is built on the Modbus protocol. The other is the MESA-ESS that addresses

ESS configuration management, ESS operational states, and the applicable ESS functions from the Institute of Electrical and Electronics Engineers (IEEE) 1815 Distributed Network Protocol (DNP3) profile for advanced DER functions.

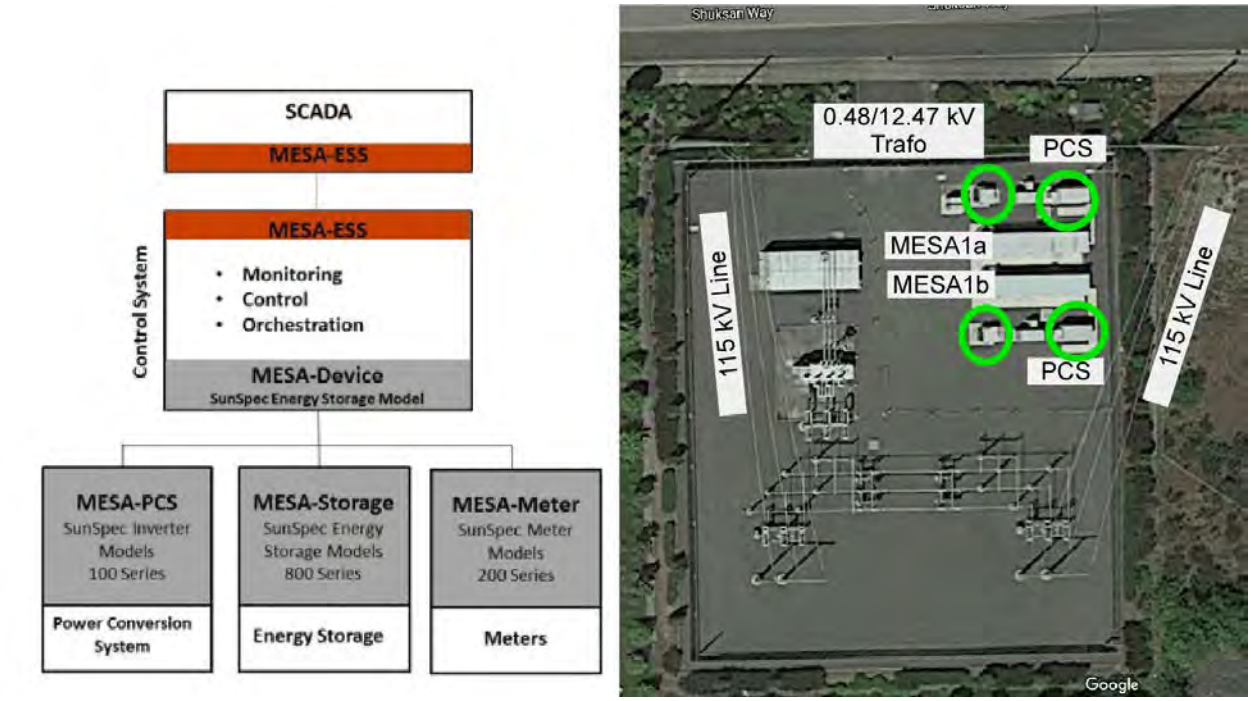

Figure 1.3. MESA Standard Architecture (left), and MESA-1 System Connection with Grid (right)

Control is accomplished by the 1Energy-Intelligent Controller (1E-IC) which has now been acquired by Doosan GridTech and named as DG-IC (Doosan 2016a). This control and communication platform for the ESS includes built-in operating modes that can be configured and fine-tuned to reach maximum economic benefits at changing grid and market conditions. Capabilities of DG-IC can also be extended by creating new operating modes through an Application Programming Interface (API). Built-in operating modes of DG-IC include Market-based Charge/Discharge, Frequency Correction, Forecast Assurance, Power Following, Peak Power Limiting, Power Factor Correction, Volt/VAr, Volt/Watt, Power Smoothing, Islanding, state of charge (SOC) Maintenance. Supervisory control, including optimal control for different use cases for MESA ESSs is performed by Doosan's Distributed Energy Resources Optimizer (DG-DERO) (Doosan 2016a), which is a management system for distributed energy resources that optimally aggregates economic values from fleets of ESS and other resources. The suite of bulk power applications that DERO considers in optimizing storage benefits includes energy arbitrage, and avoiding certain market situations such as energy congestion, unfavorable purchase, and forecast error penalties (Doosan 2016b). Based on historical load and price data, local resource constraints, maintenance events and expected SoC at the start of the day, day ahead schedules for optimal charging and discharging operations, typically looking ahead over the next 24 to 48 hours, are provided by DERO. Recommendations for schedule adjustments at different time horizons are made by DERO in response to changed conditions. Data tags for the energy storage were set based on the SunSpec Alliance Interoperability Specification (SunSpec 2017).

Power conversion is performed by Parker Hannifin 890GT-B inverter. DC link rated voltage is 1200 V DC and Alternating Current (AC) output is provided at 480 V ac. The AC outputs of the Parker Hannifin inverters are stepped up by two 0.48/12.96 kV, 1.5 MVA transformers, as identified in Figure 1.3 (right side), and eventually connected to the utility grid with 115 kV circuits.

2.0 Battery Performance Test Results

During the first phase of tests, the BESS was subjected to baseline testing as described in the DOE-OE Performance Protocol (Viswanathan 2014), with discharge at various C rates[13] for a constant C rate charge. Response time and ramp rate were measured at various SOCs, along with charge and discharge resistance. The results of these tests are presented in this section of the report.

2.1 Baseline Test Results

The energy capacity stability of the ESS shall be reported as a percent of initial performance as determined in accordance with Section 8.4.5 of the Washington Clean Energy Fund: Energy Storage System Performance Test Plans and Data Requirements (Balducci 2017) and as shown in Table 2.1, along with the date of the test upon which the reported value is based and the ambient temperature and barometric pressure encountered during the test.

Table 2.1. Stored Baseline Energy Capacity and Roundtrip Efficiency at Rated Power

	Charge Energy (kWh)	Discharge Energy (kWh)	Cycle Roundtrip Efficiency (%)	Cumulative RTE (%)	Capacity Stability (% of initial energy capacity)
Cycle 1	991	750	75.7		N/A
Cycle 2	1006	736	73.2		N/A
Cycle 3	989	753	76.1		N/A
Cycle 4	995	749	75.3		N/A
Sum cycle 1-4	3980	2991		75.2	
Sum cycle 2-4	2990	2238		74.8	

Table 2.1, shown in the format of the DOE Energy Storage Performance Protocol, is for a constant discharge power of C/4. Baseline capacity tests were done for multiple power levels: 2C, C, C/2, and C/4, where C rate corresponds to 1,000 kWh/1h = 1,000 kW. The limitations for testing were:

1. Commands could be provided only once every 15 minutes.
2. The battery SOC could not be controlled.

Hence, the charge and discharge power levels were selected as close to the desired C rates as possible, taking into account the above constraints. The RTE[14] was calculated for energy flow in and out of the grid including and excluding rest periods, and energy flow at the Power Conversion System (PCS) level, excluding auxiliary losses. As expected, the RTE increases in the following order:

RTE at the grid including rest is lower than the RTE at the grid excluding Rest, which is lower than the RTE at the PCS excluding auxiliary losses.

[13] A C/x rate is the current in amperes (A) at which the ampere-hour (Ah) capacity of the battery can be discharged in x hours. For example, if the capacity of the battery is 100 Ah, a C/10 rate corresponds to 10 amperes (A).
[14] The RTE is simply the ratio of discharge energy to charge energy, ensuring the BESS SOC is brought back to the initial SOC.

Note that for the MESA-1 battery system, auxiliary load is powered by the grid during charge and rest, and by the battery during discharge. Hence, the RTE at the PCS excluding auxiliary losses is the same with and without rest.

Initially, baseline capacity testing was planned only for 2C and C/4 rate charge and discharge. Subsequent to this, baseline capacity tests were repeated at the C/4 rates after peak shaving and pulse test, followed by tests at multiple charge-discharge rates, including C/4, C/2, C and 2C rates. For each rate, three cycles were done, with the mean and cumulative values for C/4, C/2, 1C and 2C rates summarized in Table 2.2. The results for individual runs for all rates tested are included in Appendix A.

There was a one hour rest after each charge and discharge. The mean RTE is simply the average of RTE for each run, while cumulative RTE is the discharge energy divided by charge energy for all the runs combined. Note that at the end of each run, a charge or discharge energy is included to bring the SOC to the initial value. This charge or discharge at the end to bring the SOC to the initial value is actually not carried out, but is the estimated value based on the collected data, and is typically very small, since the BESS starts and ends at the low end of the SOC range for most tests. Note that when rest time and auxiliary losses are included, the maximum discharge energy available from the BESS is 971 kWh at the C rate, while when auxiliary losses are excluded, the maximum energy available from the BESS is 1,000 kWh. To calculate the maximum available energy, the measured energy is divided by the DOD of 82.5 percent (92.5 percent SOC at the end of charge minus 7.5 percent SOC at the end of discharge).

Subsequently, capacity tests were done at multiple charge and discharge rates, including C/4, C/2, C, and 2C rates. The results for all the capacity tests are shown in Appendix A, while consolidated results are shown in Table 2.2. The RTE peaked at 1C rate at 83 percent, with a steep increase from 67 percent at C/4 rate and 77 percent at C/2 rate.

Results are presented for: 1) including rest period and auxiliary load, 2) excluding rest period but including auxiliary load, and 3) including rest period but excluding auxiliary load. The RTE at 2C rate was 82 percent. When the rest period was excluded, the RTE peaked at C-2C rate, at 86.5 percent. The retaining of auxiliary load during operation favors higher C rates, hence the gap between C and 2C rate disappears. Exclusion of auxiliary load resulted in peak efficiency of 91 percent at the 1C rate, with the 2C RTE at 88 percent. Removal of auxiliary loads reflects the electrochemical efficiency of the DC battery, which peaks at 1C. At lower rates, the temperature is low, while at high rates, the polarization losses are higher in spite of higher operating temperature. When excluding auxiliary load, the RTE at C/2 and 2C rate were nearly the same at 88 percent, while the C/4 rate RTE was 83 percent.

Table 2.2. Consolidated Results for Baseline Capacity Tests prior to Cycle 1 Use Case Testing

Type	Duration (h)	Mean Temp. (°C)	Charge Energy (kWh)	Dis-charge Energy (kWh)	RTE (%)	Charge Energy No Rest (kWh)	RTE No Rest (%)	Charge Energy No Aux (kWh)	Dis-charge Energy No Aux (kWh)	RTE No Aux (%)	Average Charge Power (kW)	Average Dis-charge Power (kW)
Mean	9.6	21.4	1129	774	68.3	1079	71.7	1017	845	83.1	273	210
Cumulative	39.7	21.4	4591	3095	67.4	4318	71.6	4094	3380	82.6	273	210
Mean	9.6	21.5	1151	760	66.0	1095	69.3	1017	842	82.8	276	206
Cumulative	28.5	21.5	3484	2279	65.4	3285	69.3	3062	2526	82.5	276	206
Mean	9.6	22.0	1145	761	66.5	1091	69.8	1019	842	82.7	274	207
Cumulative	29.6	22.0	3466	2284	65.9	3273	69.8	3070	2527	82.3	274	207
Mean	6.2	23.9	1086	839	77.3	1025	81.9	998	880	88.1	508	423
Cumulative	17.9	23.9	3219	2511	78.0	3060	82.0	2967	2631	88.6	508	423
Mean	6.2	23.9	1092	836	76.6	1027	81.4	1002	879	87.7	503	421
Cumulative	17.9	23.9	3215	2488	77.4	3047	81.7	2961	2614	88.3	504	421
Mean	3.9	25.6	1048	874	83.3	1008	86.7	984	895	90.9	1008	867
Cumulative	11.9	25.7	3148	2621	83.2	3023	86.7	2953	2685	90.9	1008	867
Mean	3.9	25.6	1053	870	82.6	1008	86.3	984	895	90.9	1008	863
Cumulative	11.9	25.6	3164	2609	82.5	3024	86.3	2953	2683	90.9	1008	863
Mean	2.9	28.3	1032	840	81.4	970	86.6	971	852	87.8	1736	1718
Cumulative	6.9	28.3	2088	1680	80.5	1938	86.7	1944	1705	87.7	1736	1718
Mean	3	28.3	1041	838	80.6	963	87.0	964	852	88.5	1793	1675
Cumulative	8.9	28.3	3086	2513	81.4	2886	87.1	2876	2555	88.8	1828	1675
Mean	5.0	28.9	1103	838	76.1	972	86.2	989	852	86.2	1688	1665
Cumulative	13.4	28.9	3230	2505	77.6	2901	86.4	2934	2547	86.8	1740	1665

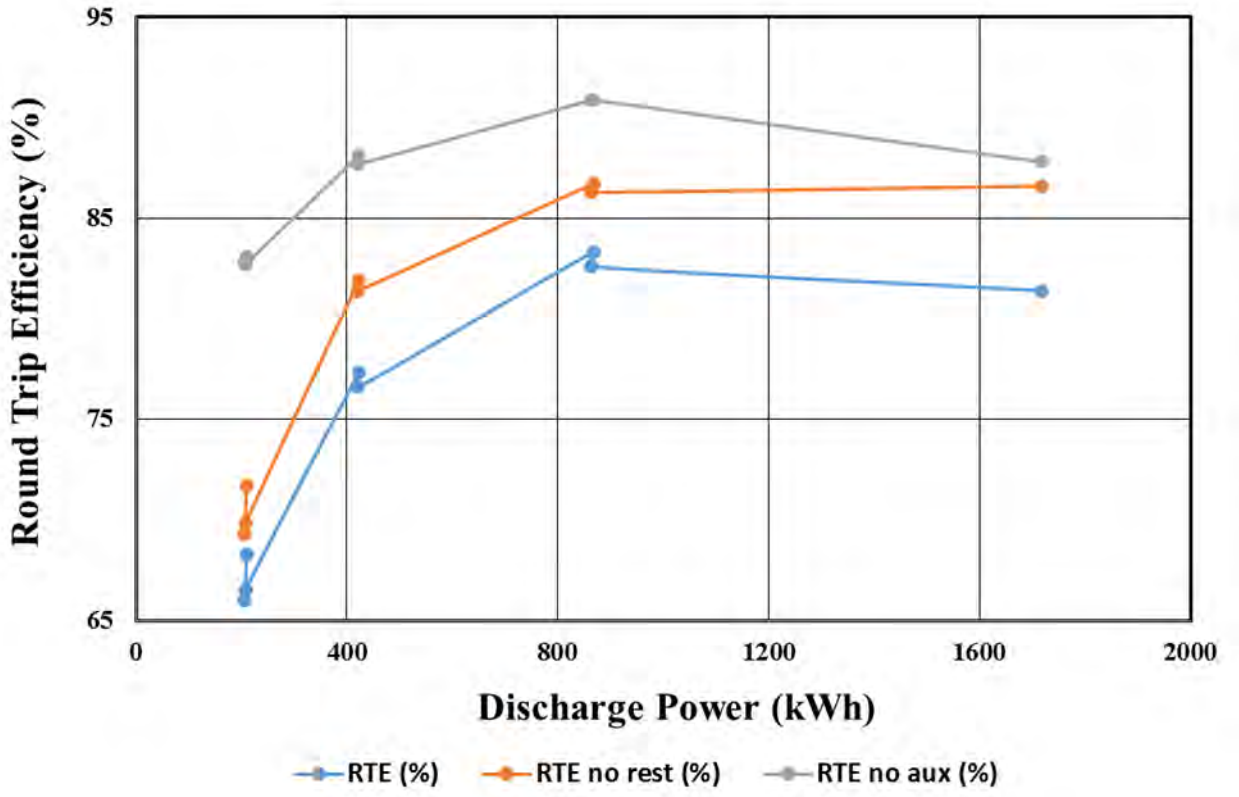

Figure 2.1. Roundtrip Efficiency during Baseline Capacity Tests

The performance of the MESA-1 BESS depends on the performance of MESA-1a and -1b battery systems. The performance of the MESA-1 BESS, along with MESA-1a and -1b batteries are shown in Table 2.3. In this document, MESA-1a and MESA-1b batteries are also referred to as 1a and 1b in the text. The RTE as a function of power without auxiliary load peaks at 1,000 kW for 1a, while the 1b RTE increases with power. This shows 1b to be a high power battery. The RTE at low power for 1a is less than 1b, because 1) the starting SOC during charge is higher, and 2) the starting SOC during discharge is lower, resulting in lower power levels in 1a for charge and discharge. Hence, the auxiliary load is a higher percent of the charge and discharge power for 1a. In reality, the rest period can be set to be lower for lower charge and discharge power levels (lower temperature excursion), thus helping to mitigate auxiliary losses. No effort was made in this analysis to take this into account. This RTE gap disappears when auxiliary load is excluded.

The lower magnitude of charge and discharge power for 1a is probably one reason for its higher RTE without auxiliary load at the C/4 rate. At higher powers, with 1b providing 14% more discharge power, the RTE without auxiliary load for 1b is higher, thus showing it is a high power battery. As noted earlier, the C rate for 1b is 6 percent higher than the C rate for 1a. When auxiliary losses are included, the RTE difference between 1b and 1a is even higher. This is because as discharge and charge power increases, the amount of energy extracted decreases, while the rest period remains constant at 1 hour after charge and discharge. Hence, auxiliary losses during rest become important. Note that for MESA-1a, some runs (in italics) have an unusually low charge energy input, leading to an unusually high RTE. For these runs, there was probably an error in the meter reading for charge power input.

Table 2.3. Comparison of MESA-1, 1a, and 1b Performance during Baseline Capacity Tests

	MESA-1			MESA-1a			MESA-1b		
Start Date	RTE	RTE No Aux	Average Discharge Power (kW)	RTE (%)	RTE No Aux	Average Discharge Power (kW)	RTE (%)	RTE No Aux (%)	Average Discharge Power (kW)
2016/06/23	69.1	83.0	210	64.8	88.2	93	76.4	84.2	120
2016/06/23	67.0	83.1	207	63.9	87.9	93	73.2	84.7	116
2016/06/23	70.0	83.2	211	64.7	88.1	93	77.6	84.8	121
2016/06/24	68.0	83.2	214	65.1	90.3	96	74.0	83.9	120
2016/06/28	65.6	82.5	206	61.8	81.2	91	68.9	83.5	117
2016/06/28	66.1	83.3	206	64.2	81.6	93	67.7	84.6	115
2016/06/29	66.3	82.7	206	62.1	80.7	91	70.0	84.3	118
2016/07/18	65.5	81.8	206	60.8	79.9	94	67.3	83.3	115
2016/07/19	67.5	83.1	208	64.6	82.1	93	70.0	84.0	117
2016/07/19	66.4	83.0	207	63.3	81.7	93	69.1	84.2	116
2016/06/30	77.0	88.8	419	73.5	88.5	182	80.6	90.0	253
2016/06/30	77.7	87.8	424	70.2	85.3	184	80.8	89.0	259
2016/07/01	77.2	87.8	426	73.4	86.4	190	79.2	87.5	252
2016/07/20	76.8	87.7	421	69.8	85.3	184	80.5	90.1	256
2016/07/20	75.8	88.3	421	71.5	84.0	187	76.1	87.8	248
2016/07/21	77.1	87.1	421	70.2	86.0	183	80.6	88.9	257
2016/06/29	83.2	90.8	868	80.7	88.9	385	83.1	89.8	483
2016/06/30	83.8	91.2	868	81.5	90.3	386	84.5	90.5	482
2016/06/30	83.0	90.9	866	81.1	90.5	386	84.5	91.1	480
2016/07/20	83.2	90.7	866	81.3	89.1	386	82.4	89.4	480
2016/07/20	83.2	91.2	865	81.1	90.2	385	83.7	90.4	480
2016/07/20	81.3	90.8	858	80.0	90.5	384	82.3	91.1	474
2016/06/14	81.9	88.7	1708	81.5	89.8	863	82.9	89.5	944
2016/06/14	80.9	86.9	1729	75.2	84.6	868	81.9	87.7	941
2016/06/16	82.4	88.8	1691	80.8	88.7	720	83.3	89.5	971
2016/06/16	81.3	89.0	1663	81.0	88.9	760	81.3	88.8	903
2016/06/16	78.1	87.6	1672	79.7	89.6	776	76.7	85.7	896
2016/07/18	71.6	83.4	1654	67.9	84.3	742	73.5	83.9	912
2016/07/18	78.3	87.4	1670	79.5	86.3	772	76.6	85.0	898
2016/07/18	78.2	87.7	1670	79.1	86.1	774	76.9	85.9	896

Figure 2.2, Figure 2.4, Figure 2.5, and Figure 2.6 show baseline capacity test results for MESA-1, along with results for 1a and 1b. Note that requested power leads the actual power input or output by different amounts, and sometimes, even accounting for the lead, the magnitudes of requested vs. actual power do not match. Since SnoPUD does not include requested power in the data tags provided to PNNL, book-keeping becomes very difficult. Hence, requested power has been omitted from other graphs.

At the C/4 rate (Figure 2.2), the temperature drops during the initial portion of charge and discharge, possibly due to the endothermic nature of the charge process. However, during charge for cycles 2 and 3, this drop is not seen. Hence, it appears that the initial drop during cycle 1 charge is simply due to the thermal mass of the system being large enough that the temperature decrease during rest continues for the first few minutes of charge. The initial temperature drop for 1b is less than for 1a, which is explained by the power flow distribution between 1a and 1b, with 1b supporting charge of 150 kW and 1a charge power being 100 kW initially. Interestingly, during the first few minutes of discharge, the temperature increases, followed by a slight decrease, followed by an increase. MESA-1b shows this behavior, while 1a temperature rises during charge and discharge. Throughout charge and discharge, initial power flow through 1b is higher than 1a. For discharge, crossover of power flow occurs 75% into the discharge duration, after which power flow through 1a is higher, resulting in closing the temperature gap between 1a and 1b. The ΔT (final minus initial temperature) was the same for 1a and 1b at the C/4 rate.

No major trend of auxiliary power consumption exists during charge, rest, and discharge. Note the rapid drop in SOC for 1a after charge. This appears to indicate that the reported 90% SOC at end of C/4 rate charge may be an overestimate. Hence, charge energy/unit change in reported SOC appears to be understated. This seems to be BMS related. Auxiliary power consumption for 1a and 1b are not shown for any of the runs since they are quite close to each other. It should be noted that the BESS SOC behavior during rest after charge is dominated by 1a.

The PCS is in switching[15] mode after discharge, while during rest after charge, the PCS is not in switching mode. The reactive power and DC current flow through 1a and 1b are shown for the C/4 rate in Figure 2.3. As explained later, there appears to be no correlation between the SOC change during rest, and the status of PCS switching or the direction and magnitude of DC power flow through 1a and 1b.

For all rates, there is a spike in power after charge and discharge – a charge spike at the end of charge and discharge spike at the end of discharge. While the spike occurs more for 1b, it does occur for both 1a and 1b. It is not clear if this is hardware or software related. From the power plot for 1a and 1b, it is seen that towards the end of charge and discharge, 1a power tapers, necessitating a rapid pick-up from 1b. This may be one reason for the spikes observed. The reason for both 1a and 1b spiking may be because as 1b spikes, it may reach its power threshold, followed by a rapid taper, necessitating a pick-up from 1a. No matter the reason, these power spikes do not appear to be healthy for the cells.

[15] At this site, auxiliary power is powered during charge and rest by the grid during rest. Hence there is no power flowing through the BESS PCS. However, when the BESS SOC is within 2% of its lower SOC limit, the DC battery needs to be charged. Hence the PCS is connected to the grid, with both real and reactive power flowing. The PCS is in the switching state when there is real or reactive power exchange with the grid.

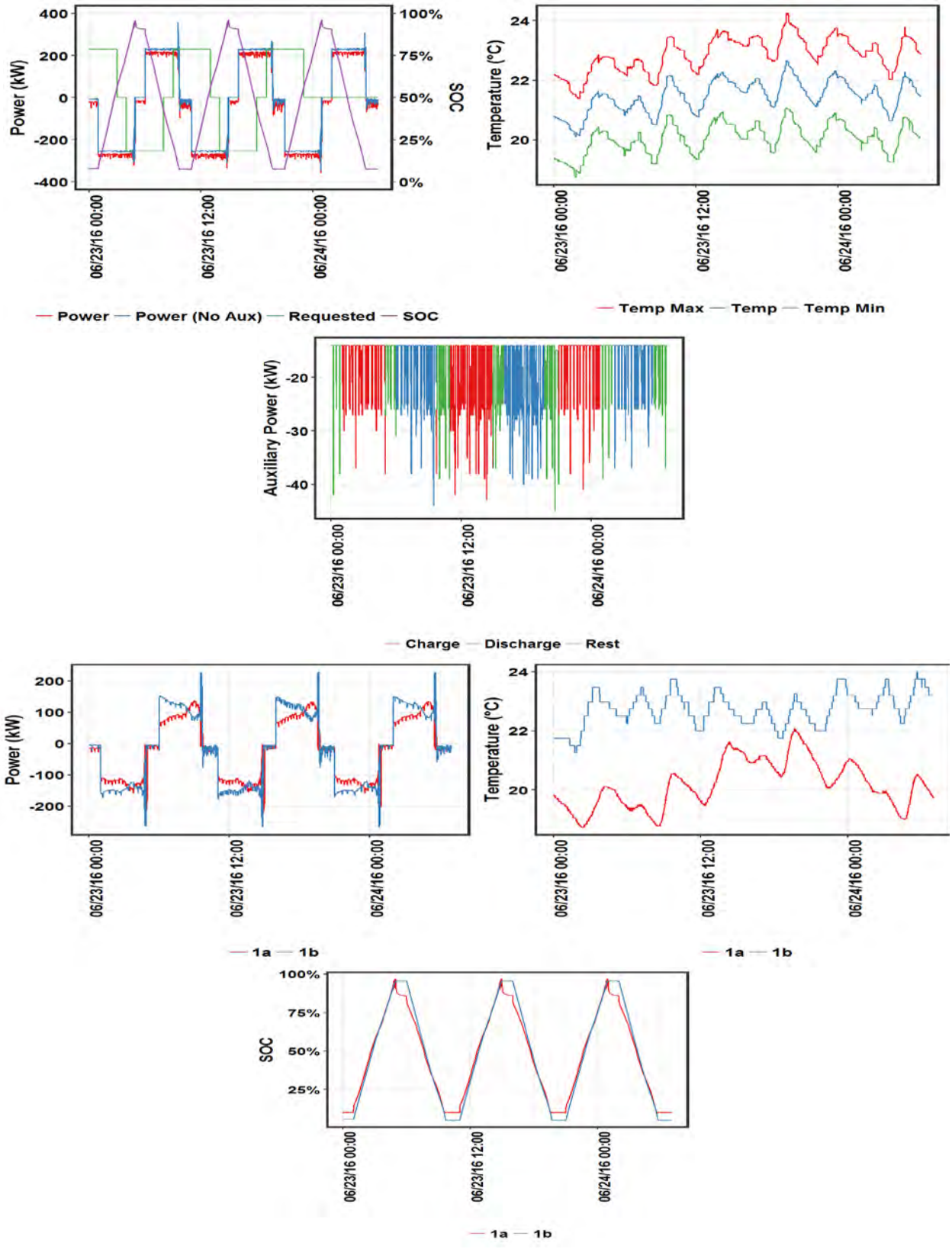

Figure 2.2. Baseline Capacity Test at 250 kW Charge and Discharge. (Top 3) BESS, (Bottom 3) MESA-1a and 1b

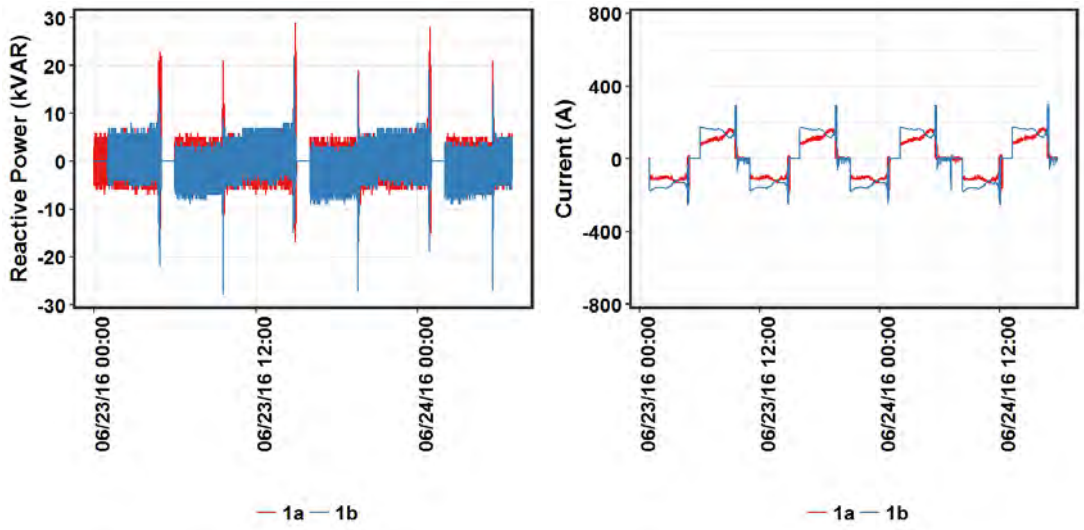

Figure 2.3. Reactive Power Flow through 1a and 1b during 250 kW Charge Baseline Capacity Test

At the C/2 rate, the temperature drops during initial portions of charge and discharge, but less steeply than at the C/4 rate. This shows that the thermal mass of the BESS still allows the decreasing temperature trend during rest to continue initially. As seen for C/4, the temperature during discharge increases, followed by a decrease, and then an increase. This mirrors the behavior of 1b, while 1a temperature increases during charge and discharge. The magnitude of charge power flow through 1b is higher than 1a for the entire duration of charge. During discharge, 1b power flow is higher for the first 90% of discharge, after which the discharge power is equal for both batteries. This results in a higher temperature rise for 1b at the end of the cycling. No major trend exists for the auxiliary power consumption during charge, rest and discharge. Note the rapid drop in SOC for 1a after charge. This appears to indicate that the reported 95% SOC at the end of C/4 rate charge may be an overestimate, with actual SOC in the 85 to 88 percent range. Hence, the charge energy/unit change in reported SOC appears to be understated. As seen from Figure 2.4, the BESS SOC behavior after charge is dominated by 1a. Upon close inspection, 1a continues charging and discharging slightly after 1b operation terminates. Hence at the end of charge, there is a slight spike in 1a SOC. However, this does not explain the slight spike in 1a SOC at the end of discharge.

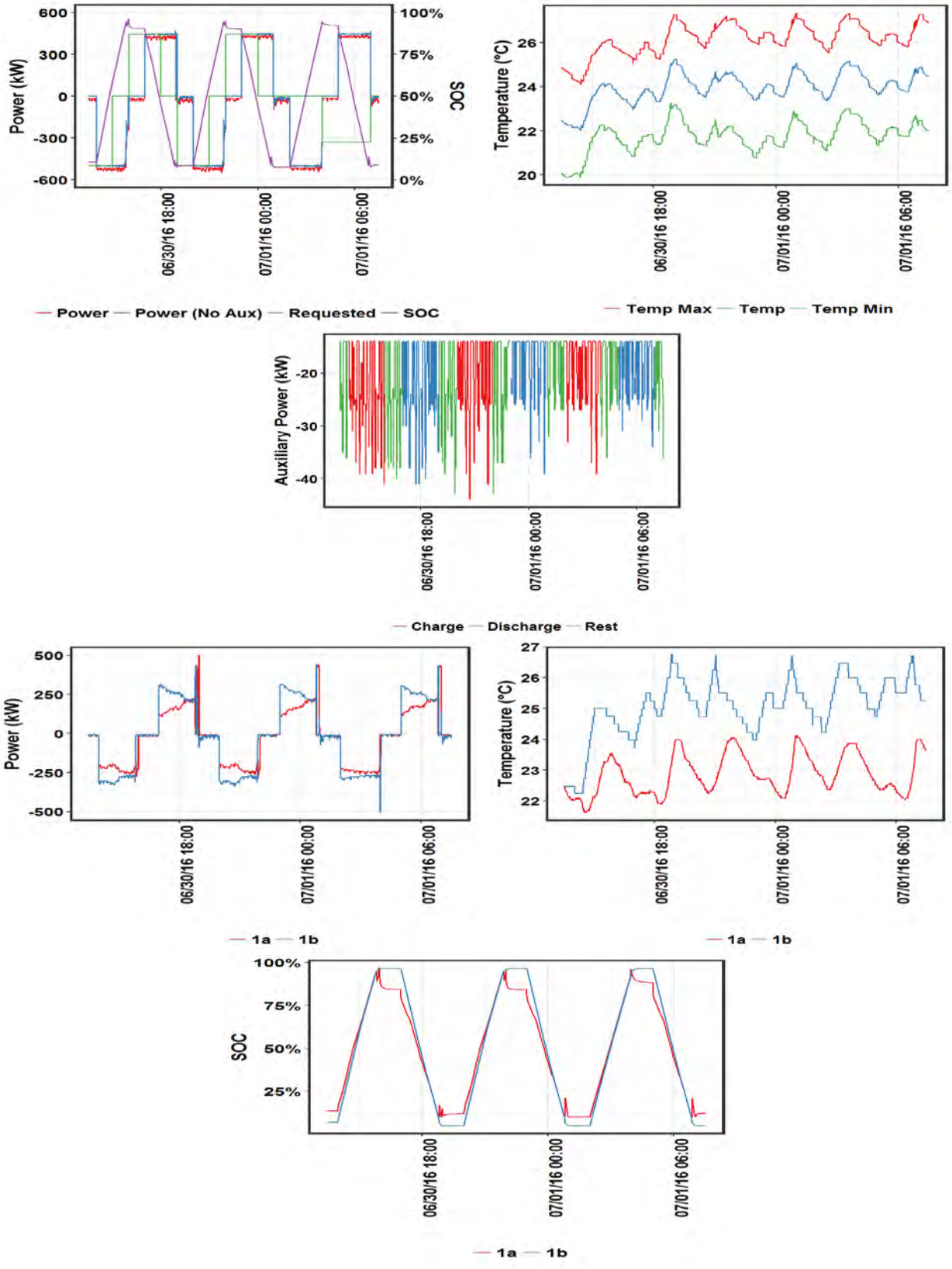

Figure 2.4. Baseline Capacity Test at 500 kW Charge and Discharge. (Top 3) BESS, (Bottom 3) 1a and 1b.

The high power at 1,000 kW overwhelms the BESS thermal mass – temperature rises at the start of charge or discharge, and drops during rest. The power flow through 1b is higher than through 1a for both charge and discharge. The initial charge power is 480 to 500 kW for 1b, 18 percent higher than the 410 to 420 kW range for 1a, while its C rate is 6 percent higher. The power gap narrows as charge proceeds, but towards the end of charge, 1a charge power decreases, while 1b charge power increases, related to power tapering for 1a at high SOC. During discharge, the initial discharge power is 480 kW for 1b, 33 percent higher than the 360 kW power flow for 1a. Throughput discharge, 1b power decreases, while 1a power increases, with the gap narrowing to around 10 to 20 kW. In spite of the lower power flow through 1a, the end of cycle temperature for 1a was 31.7 °C, while for 1b it was 29 °C. Note that the 1a initial temperature was 0.6 °C cooler than 1b initial temperature. This appears to indicate that 1a has a higher internal resistance, and/or the thermal management for 1a allows its temperature to have larger excursions.

The drop in SOC for 1a after charge is less steep than for the C/4 and C/2 rate tests. This appears to indicate the reported 90 percent SOC at the end of C rate charge is close to the real value of 87.5 percent after the drop. The charge power tapers at 87 percent SOC for 1a. This seems to be BMS related. The SOC at the end of discharge increases < 0.5 percent for 1a. For 1b, the SOC after charge increases by 2 percent during rest. This indicates the reported SOC is lower than actual at 1C rate charge, thus corresponding to a higher charge energy per unit change in reported SOC. For 1a, there is taper at the end of charge to ~ 0.5C rate. This could be because the BMS is set to taper to the 0.5C rate per the Acceptance Test Report for 1a when SOC > 80 percent (Figure 8 of 1energy 2015); hence this taper is not present for the C/4 and C/2 runs (which are < or = C/2 rate). This taper during charge is not present for 1b, which indicates that the BMS for 1b does not require tapering until the SOC is very high. Looking closely, it appears that towards the end of charge, there is a slight taper for 1b, when the SOC is close to 95 percent, in line with the Acceptance Report (Figure 8 of 1energy 2016). The SOC at the end of discharge continues to decrease during rest for 1b. This indicates that the reported SOC is higher than the actual SOC at the end of 1C discharge, increasing the discharge energy per unit reported change SOC. This appears to be a characteristic of the 1b BMS. BESS SOC behavior after charge shows a slight dip in SOC initially (due to 1a). After discharge, the BESS SOC decreases during rest (due to 1b). Note that for this run, 1a operation during charge and discharge does not extend beyond 1b (as observed for the C/2 rate test). Hence no spikes in SOC were observed after charge and discharge for 1a.

The power spikes at the end of charge and discharge were absent for the C rate test. Battery 1a power still tapers towards the end of charge, but 1b picks the power smoothly. The power spike appears to be PCS related, and disappears when the PCS is operation at or > 40 percent of rated power.

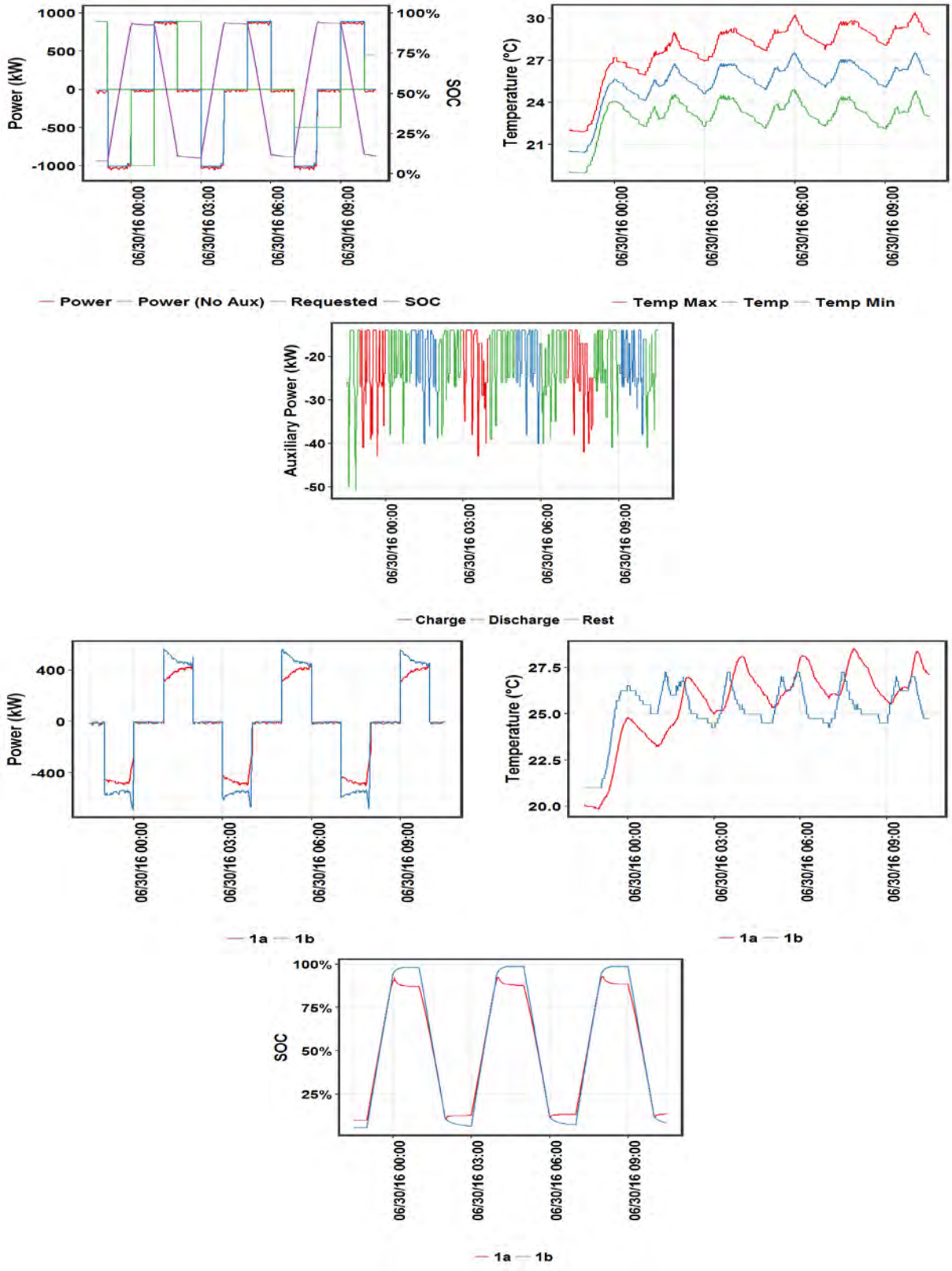

Figure 2.5. Baseline Capacity Test at 1000 kW Charge and Discharge, (Top 3) BESS, (Bottom 3) 1a and 1b

The high power at 2,000 kW overwhelms the BESS thermal mass – the temperature rises at the start of charge or discharge, and drops during rest (Figure 2.6). The auxiliary load is low initially, and increases with test time as temperature increases. As BESS temperature increases and reaches a maximum of 37 °C, auxiliary load remains stable at 42 kW, with a very slight increasing trend, accompanied by a very slight increasing maximum temperature. Charge power was 2,000 kW, while discharge power was 1,750 kW. Hence, during the initial half of charge, since 1b cannot absorb more than 1,000 kW, 1a was forced to support 1000 kW. MESA-1a charge power starts to taper at ~ 55% SOC, and reaches 0.4C at the end of charge. During 1,750 kW discharge, the initial power through 1b is 1000 kW, while power through 1a is 750 kW. The discharge power decreases slightly during discharge for 1b, with the reverse being true for 1a. MESA-1a temperature increases by 14 °C, while 1b temperature increases by 5 °C, in spite of 1a supporting lower average discharge and charge power. This is probably due to higher internal resistance for battery 1a and/or the thermal management for 1a allowing a wider temperature range. For 1a, SOC at the end of charge reaches 86 to 88 percent, and power tapers to 0.4C rate. The drop in SOC after charge is similar to that observed for 1C rate charge. A <1 percent rise in SOC is observed at the end of discharge for 1a – the same as at the end of 1C rate discharge. The SOC behavior for 1b after charge and discharge is the same as observed for 1C rate. The BESS SOC increases at the end of charge, and decreases at the end of discharge, both dominated by 1b behavior. The decrease at the end of discharge is less than at the 1C rate – so the reported SOC at the end of discharge is not as overstated as for the 1C rate.

Note that for this run, 1a operation during charge and discharge does not extend beyond 1b (as observed for the C/2 rate test). Hence no spikes in SOC were observed after charge and discharge for 1a.

The power spikes at the end of charge and discharge were absent for the C rate test, similar to the absence of spikes at the C rate. MESA-1a power still tapers towards the end of charge and discharge, but 1b picks the power smoothly. The power spike appears to be PCS related, and disappears when the PCS is operation at or > 40 percent of rated power.

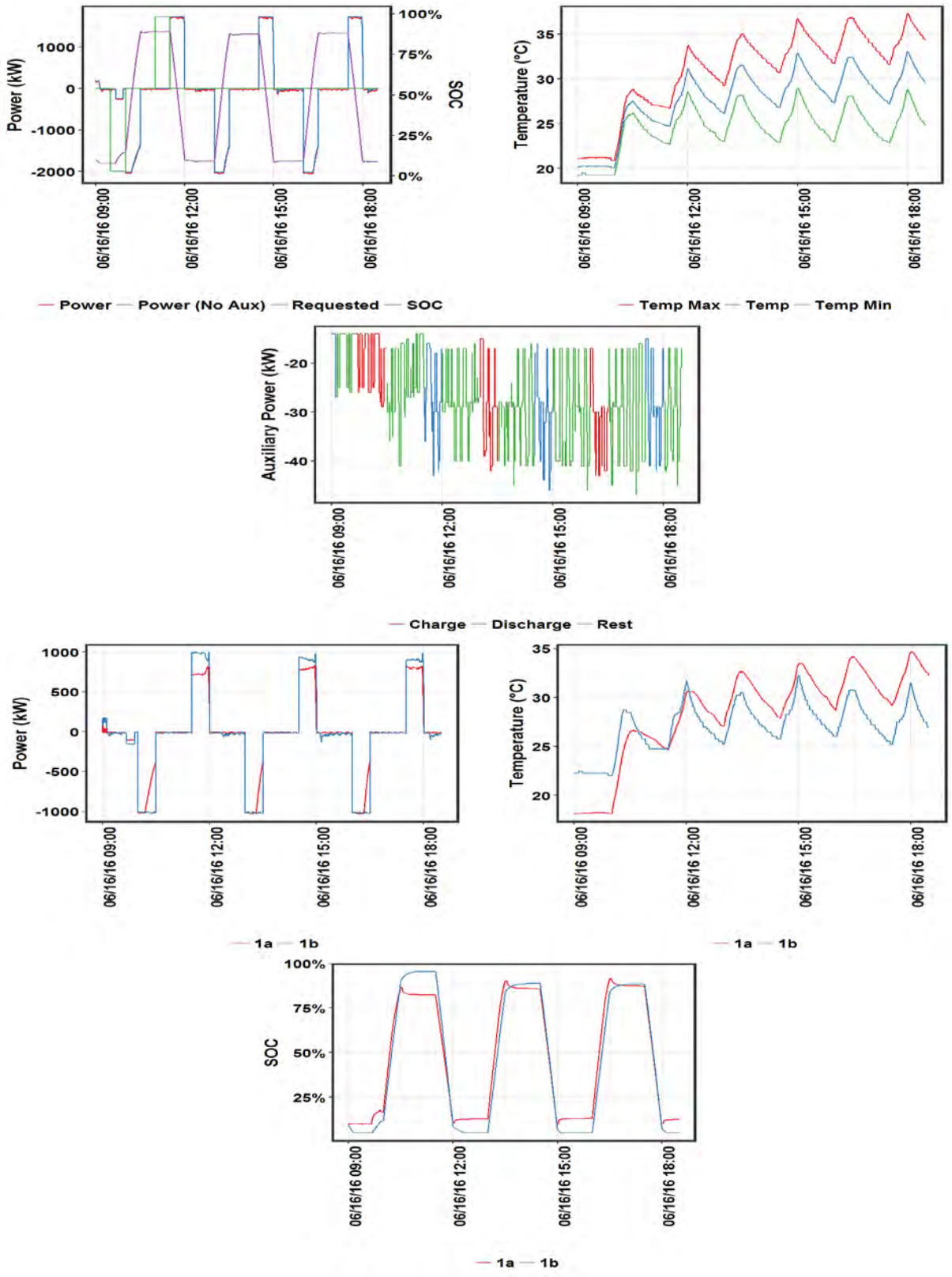

Figure 2.6. Baseline Capacity Test at 2000 kW Charge and Discharge, (Top 3) BESS, (Bottom 3) 1a and b.

The DC current flow through 1a and 1b during rest after charge and discharge was measured in an attempt to explain the SOC behavior after charge and discharge (Table 2.4). The current flow through 1a is positive (discharge), while the current flow through 1b during rest is negligible after charge, and slightly negative after discharge. The magnitude of current flow through 1a during rest is about three times that through 1b.

Table 2.4. Current through 1a and 1b during Rest after Charge and Discharge during Baseline Capacity Tests

Average Discharge Power (kW)	Average Power During Rest After Charge for 1a (kW)	Average Power During Rest after Discharge for 1a (kW)	Average Power During Rest after Charge for 1b (kW)	Average Power During Rest after Discharge for 1b (kW)
C/4	1.7	4.5	0.5	-0.7
C/2	1.9	3.5	0.5	-1.9
C	1.0	3.1	0.0	0.0
2C	0.3	3.5	0.0	-2.8

To explain the SOC relaxation behavior of 1a and 1b during rest, Table 2.5 summarizes the SOC trend, status of PCS switching, average current during rest, calculated change in SOC and actual SOC. For 1a, there is discharge current during rest after charge in the C/2 to 2C range, with no switching of the PCS. However, the calculated decrease in SOC from the discharge current is more than an order of magnitude lower than the actual decrease in SOC. During rest after discharge, there is PCS switching, with the accompanying discharge current being about 2 to 10 times higher than during rest after charge, with a calculated SOC drop of 0.6 to 0.8 percent. However, the SOC remained flat (C/4 to C/2 rate) and increased by 1 percent (C to 2C rate). Hence, the actual SOC change during rest does not correlate with current flow or status of PCS switching for 1a.

Note that the PCS mode for 1b is the same as for 1a – not switching after charge and switching after discharge. For 1b, the current flow during rest after charge is about 0.2 to 0.3 times that of 1a (Table 2.6). The calculated SOC change of -0.08 percent is close to the actual SOC change of 0 percent for the C/4 to C/2 rate tests. For C to 2C rate, the SOC increases by 3 percent and 6 percent respectively, while there is no current flow through 1b during rest after charge. For rest after discharge, the SOC is flat for C/4 and C/2 rates, while there is a small charge current, with a calculated SOC change of 0.1 and 0.3 percent respectively. At the C and 2C rates, the SOC decrease is 6 percent and 4 percent respectively, with no current flow at C rate and a 2.8A charge current at 2C rate, with a calculated SOC increase of 0 percent and 0.45 percent respectively. Hence, the actual SOC change as reported does not correlate with PCS switching status and the current flow through the DC battery for 1b.

Table 2.5. Change in SOC during Rest, PCS Switching State, DC Current Flow and Calculated Change for 1a

	Rest after Charge					Rest after Discharge				
Rate	SOC Trend	PCS Switch -ing Status	Current During Rest (A)	Δ SOC (%)	Actual Δ SOC (%)	SOC Trend	PCS Switch -ing Status	Current during Rest (A)	Δ SOC (%)	Actual Δ SOC (%)
C/4	Decrease	No	1.7	-0.28	-8.0	Flat	Yes	4.5	-0.77	0.0
C/2	Decrease	No	1.9	-0.33	-8.0	Flat	Yes	3.5	-0.60	0.0
C	Decrease	No	1.0	-0.18	-3.0	Increase	Yes	3.1	-0.53	1.0
2C	Decrease	No	0.3	-0.05	-2.5	Increase	Yes	3.5	-0.59	1.0

Table 2.6. ΔSOC during Rest, PCS Switching State, DC Current Flow and Calculated Δ for 1b

	Rest after Charge					Rest after Discharge				
Rate	SOC Trend	PCS Switch -ing Status	Current during Rest (A)	Δ SOC	Actual Δ SOC	SOC Trend	PCS Switch -ing Status	Current during Rest (A)	Δ SOC	Actual Δ SOC
C/4	Flat	No	0.5	-0.08	0.0	Flat	Yes	-0.7	0.10	0.0
C/2	Flat	No	0.5	-0.08	0.0	Flat	Yes	-1.9	0.30	0.0
C	Increase	No	0.0	0.00	3.0	Decrease	Yes	0.0	0.00	-6.0
2C	Increase	No	0.0	0.00	6.0	Decrease	Yes	-2.8	0.45	-4.0

2.2 Internal Resistance Test

The internal resistance of a battery can be measured by various methods. One way is to pulse the battery at high rate and measure the change in voltage ΔV after a fixed duration. Depending on the duration, the ΔV would be different, resulting in different reported internal resistances. At high durations, the ΔSOC would be high, resulting in high reported internal resistance, part of which is due to the change in SOC. As shown in Figure 2.7 of Schweiger et al. 2010, as the ΔSOC increases, the measured internal resistance increases linearly.

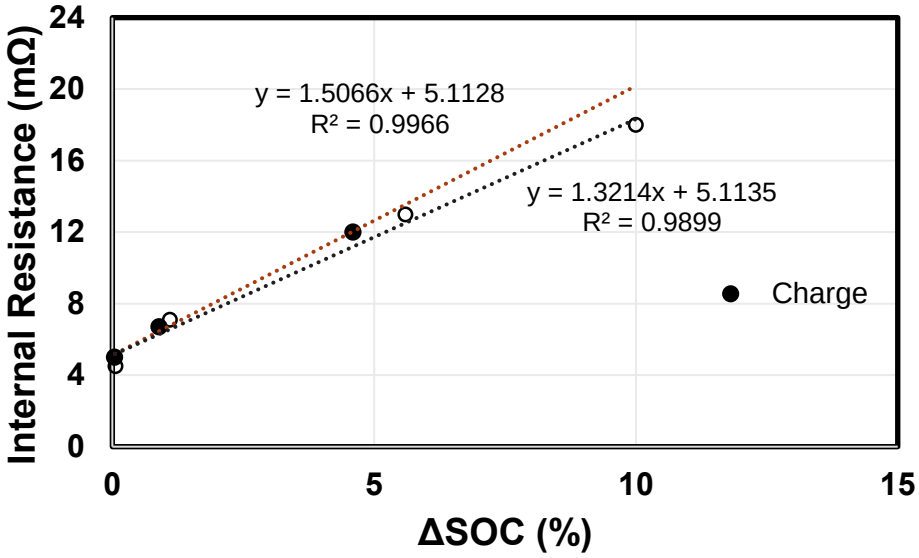

Figure 2.7. Internal Resistance of a 1.8 Ah Li-ion cell as a Function of Change in SOC during Charge or Discharge Pulse (Schweiger 2010)

The internal resistance was reported in accordance with the provisions in Section 7.2 of test plan report (Balducci 2017) and as shown in Table 2.7. This test is done as part of baseline testing, and as Reference Performance Tests (RPT) after use case testing. Results are shown for 10-s and 20-s 2C rate pulses, which correspond to a 0.5 percent and 1 percent ΔSOC respectively. For a 10-s pulse or 0.5 percent ΔSOC, the 1b internal resistance is 20 percent higher than 1a during charge at 8 percent SOC, and about 90 percent of 1a internal resistance for discharge at 85 and 40 percent SOC. For a 20-s pulse or 1 percent ΔSOC, 1b charge resistance is only 7 percent higher than 1a, while 1b discharge resistance is 85 percent of 1a. Considering more power flows through 1b than 1a at 2C rate, the ΔSOC for 1b is higher than 1a for a fixed pulse duration even after accounting for its higher energy capacity. In spite of that, 1b discharge resistance is lower than 1a. Hence comparing the measured internal resistance at 20s for 1a and 1b helps partially explain the lower temperature rise for 1b at high power levels.

Table 2.7. Internal Resistance of the ESS for Discharge at 85 and 45% SOC and Charge at 8% SOC

	Internal Resistance Charge (mΩ) (10s/20s)			Internal Resistance Discharge (mΩ) (10s/20s)		
SOC (%)	1a	1b	BESS	1a	1b	BESS
85	NA	NA	NA	17.2/21. 9	16.6/18.5	8.4/10.0
42	NA	NA	NA	18.8/23.1	16.7/19.9	8.9/10.8
8	22.3/27.3	27.0/29.0	12.3/14.1	NA	NA	NA

2.3 Peak Shaving Duty-Cycle Results

In this section, the peak shaving duty-cycle RTE values are reported with tests differing with respect to discharge power and discharge duration based on the data collected in accordance with the provisions in Section 8.2.3 of the test plan report (Balducci 2017). As shown in Table 2.8, the RTE (including rest and auxiliary load) increases with discharge power from 68.5 to 76.5 percent. Excluding auxiliary consumption, the RTE still increases with discharge power, but to a lesser extent, from 82.3 to 87.1 percent. This is in line with the observation from baseline capacity tests that the lowest RTE rate is achieved at the 1C rate of 1,000 kW.

The corresponding results for 1a and 1b are shown in Table 2.9 and Table 2.10, respectively. Across all power levels, the discharge power for 1a is lower than for 1b, due to its lower starting SOC during discharge, as seen in baseline capacity tests. This results in much lower RTE than for 1b, with the gap increasing at lower discharge power levels. When auxiliary load is excluded, the gap reduces; however, 1b RTE is still higher than 1a by 3 to 5 percent. Figure 2.8 shows the power, SOC, temperature, and auxiliary consumption for the peak shaving test.

Table 2.8. Peak Shaving Duty Cycle Results

Start Date	Duration (h)	Mean Temp. (°C)	Charge Energy (kWh)	Discharge Energy (kWh)	RTE (%)	Charge Energy No Rest (kWh)	RTE No Rest (%)	Charge Energy No Aux (kWh)	Discharge Energy No Aux (kWh)	RTE No Aux (%)	Average Charge Power (kW)	Average Discharge Power (kW)
2016/06/24	8.5	21.4	1130	775	68.5	1104	70.2	1031	849	82.3	277	214
2016/06/24	7.0	22.2	1149	840	73.1	1111	75.6	1033	882	85.4	280	441
2016/06/25	6.0	22.7	1147	877	76.5	1111	79.0	1032	899	87.1	280	895

Table 2.9. Peak Shaving Duty Cycle Results for MESA-1a

Start Date	Duration (h)	Mean Temp. (°C)	Charge Energy (kWh)	Discharge Energy (kWh)	RTE (%)	Charge Energy No Rest (kWh)	RTE No Rest (%)	Charge Energy No Aux (kWh)	Discharge Energy No Aux (kWh)	RTE No Aux (%)	Average Charge Power (kW)	Average Discharge Power (kW)
2016/06/24	8.5	20.2	564	343	60.7	548	62.3	482	381	79.1	131	96
2016/06/24	7.0	21.5	567	377	66.5	549	68.6	484	397	82.1	131	201
2016/06/25	6.0	22.0	523	388	74.2	507	76.5	462	397	86.0	130	408

Table 2.10. Peak Shaving Duty Cycle Results for MESA-1b

Start Date	Duration (h)	Mean Temp. (°C)	Charge Energy (kWh)	Discharge Energy (kWh)	RTE (%)	Charge Energy No Rest (kWh)	RTE No Rest (%)	Charge Energy No Aux (kWh)	Discharge Energy No Aux (kWh)	RTE No Aux (%)	Average Charge Power (kW)	Average Discharge Power (kW)
2016/06/24	8.5	22.6	600	433	72.1	586	73.9	551	467	84.8	153	120
2016/06/24	7.0	22.8	619	466	75.3	591	78.8	554	487	88.0	155	262
2016/06/25	6.0	23.5	628	490	78.1	605	81.0	564	501	88.9	156	500

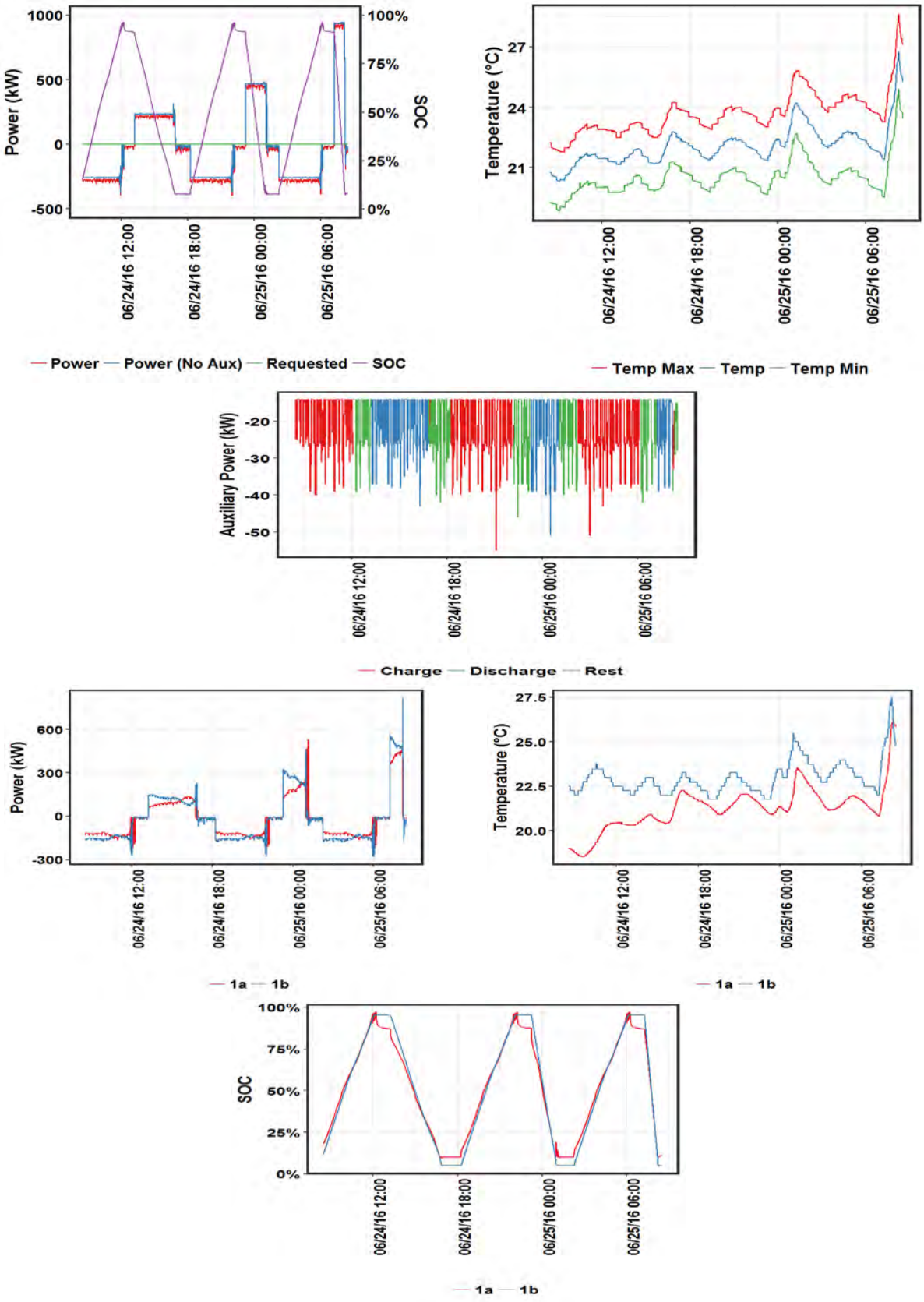

Figure 2.8. Peak Shaving Tests C/4 Rate Charge, C/4, C/2 and C Rate Discharge

2.4 Use Case 1: Energy Arbitrage

2.4.1 Duty Cycle Summary

The energy arbitrage duty cycle was modeled using PNNL's Battery Storage Evaluation Tool (BSET) by maximizing ESS revenue for a one-week period using historic Mid-Columbia (Mid-C) wholesale energy price data.

2.4.2 Test Results

As shown in Table 2.11 and Figure 2.9, Figure 2.10, Figure 2.11, and Figure 2.12, energy arbitrage runs were conducted during Cycle 1 at an average charge power of 665 to 690 kW and discharge power of 475 to 585 kW. The RTE ranged from 53 to 68 percent. While Run 2 on 9/17/2016 had a higher discharge power of 570 kW compared to 475 kW for Run 1, the RTE for Run 2 was slightly lower at 53.4 percent versus 54.6 percent for Run 1. This result was due to some parasitic charge at the PCS level, and a slightly higher rest period as a percent of test time. The RTE for Run 3 at 67.9 percent was much higher, even though the charge and discharge power levels were about the same as for Run 2. As expected, the RTE without rest is nearly the same for all three runs. Excluding auxiliary consumption, the RTE increases as expected for Runs 1 and 3. However, the RTE drops for Run 2 to 70.5 percent (81.1 percent without rest). For this Run, there is some parasitic charge at the PCS level, at an average power of 27 kW compared to lower average charge power levels of 16 kW at the PCS level for the other runs. This leads to a nearly 20 percent higher charge energy excluding auxiliary loads for this run compared to exclusion of rest periods. Note that the percentage of rest for Run 2 is not much different than for the other runs, at 86 percent versus 85 percent. It appears the PCS was placed in a switching mode during rest for Run 2, which consumes power. The temperature of the BESS ranged from 18°C to 26 °C for all the runs. There were steep rises associated with power flow, followed by steady drops during rest.

For Cycle 2, the average charge power ranged from 900 to 940 kW, while average discharge power was within 3 kW of 790 kW. As expected, the RTE (with and without rest) was significantly higher than Cycle 1, at ~ 77 percent due to lower auxiliary consumption as a percentage of total power. The RTE without auxiliary load was also about 1.5 percentage points higher than under Cycle 1 at 90 percent, which is in line with our observation from capacity tests that minimum energy losses are achieved near 1,000 kW for this BESS. The upper limit of the temperature range, at 29 to 30 °C, was about 3 to 4 °C higher than post Cycle 1, thus contributing to higher RTE. For the second run of Cycle 2, the charge input energy was extremely low, probably due to an error in measurement. The charge and energy and the high RTE for this run are shown in *italics*.

Table 2.11. Energy Arbitrage Cycle 1 Test Results

Start Date	Duration (h)	Mean Temp. (°C)	Charge Energy (kWh)	Disch. Energy (kWh)	RTE (%)	Charge Energy No Rest (kWh)	RTE No Rest (%)	Charge Energy No Aux (kWh)	Disch. Energy No Aux (kWh)	RTE No Aux (%)	Avg. Charge Power (kW)	Avg. Disch. Power (kW)	Avg. Aux Power During Charge (kW)	Avg. Aux Power During Charge (kW)
Cycle 1														
2016/08/13	128.0	22.4	5966	3256	54.6	3932	82.8	3856	3392	88.0	666	477	-17.1	-22.0
2016/09/17	59.0	21.1	3633	1938	53.4	2391	81.1	2832	1996	70.5	668	568	-18.9	-16.8
2016/10/1	53.0	22.0	3455	2344	67.9	2771	84.6	2711	2404	88.7	689	586	-15.2	-15.0
Cycle 2														
2017/01/28	12.3	22.2	1994	1576	79.0	1847	85.3	1815	1607	88.5	916	788	-15.4	-15.4
2017/01/29	11.3	23.9	*1933*	2360	*122.1*	*1812*	*130.3*	*1774*	2408	*135.7*	902	787	-18.4	-15.8
2017/01/13	71.0	21.0	7888	6375	80.8	7241	88.0	7157	6464	90.3	911	792	-11.5	-10.9
2017/01/20	47.0	22.3	5192	3959	76.3	4583	86.4	4495	4039	89.9	923	787	-17.6	-16.4
2017/01/29	13.0	22.9	1121	820	73.1	941	87.1	923	835	90.5	941	789	-18.0	-14.8
2017/02/04	35.0	22.3	4105	3148	76.7	3640	86.5	3569	3215	90.1	911	787	-17.7	-16.7

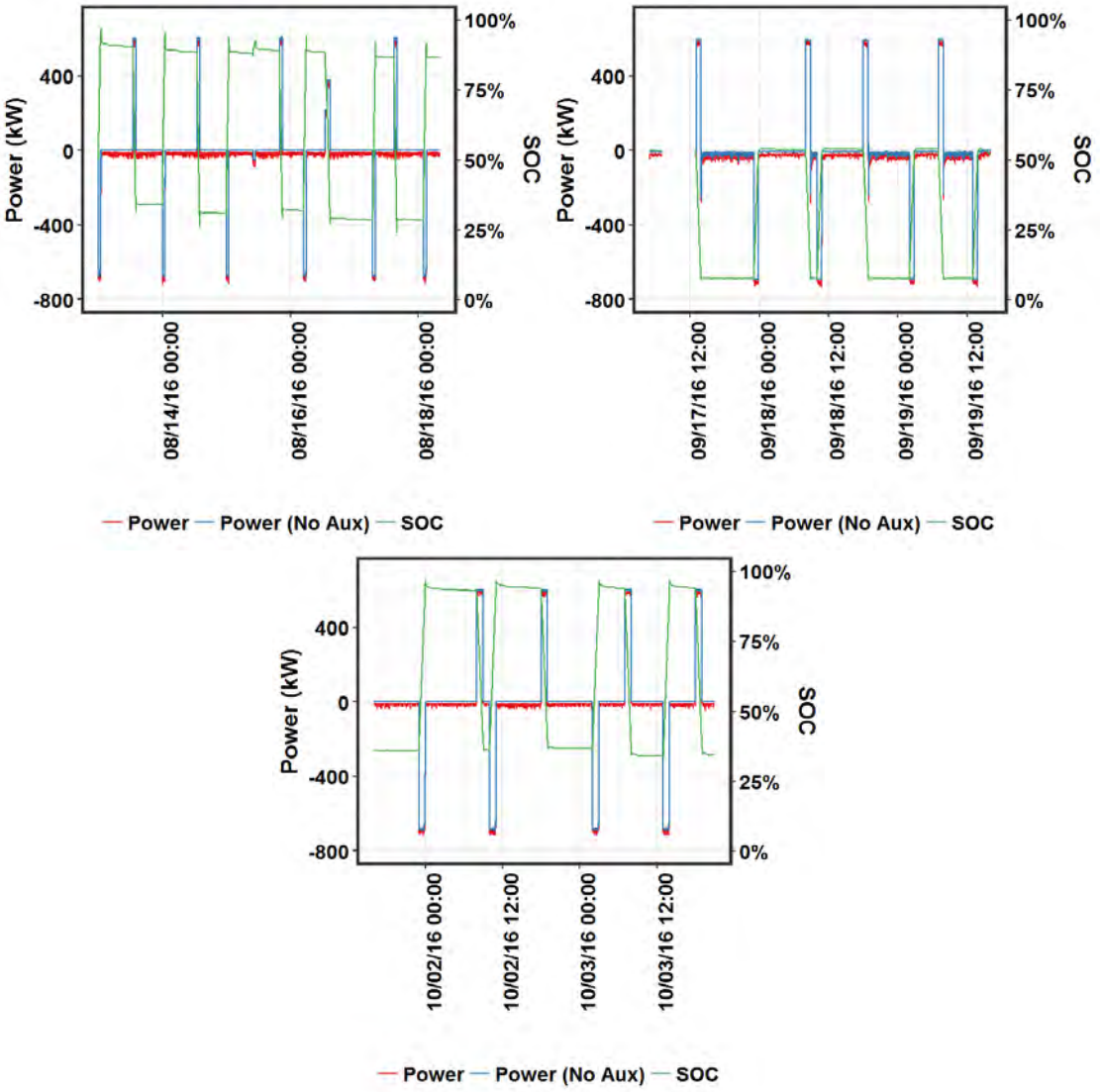

Figure 2.9. Energy Arbitrage Runs for Cycle 1, Power and SOC as a Function of Time

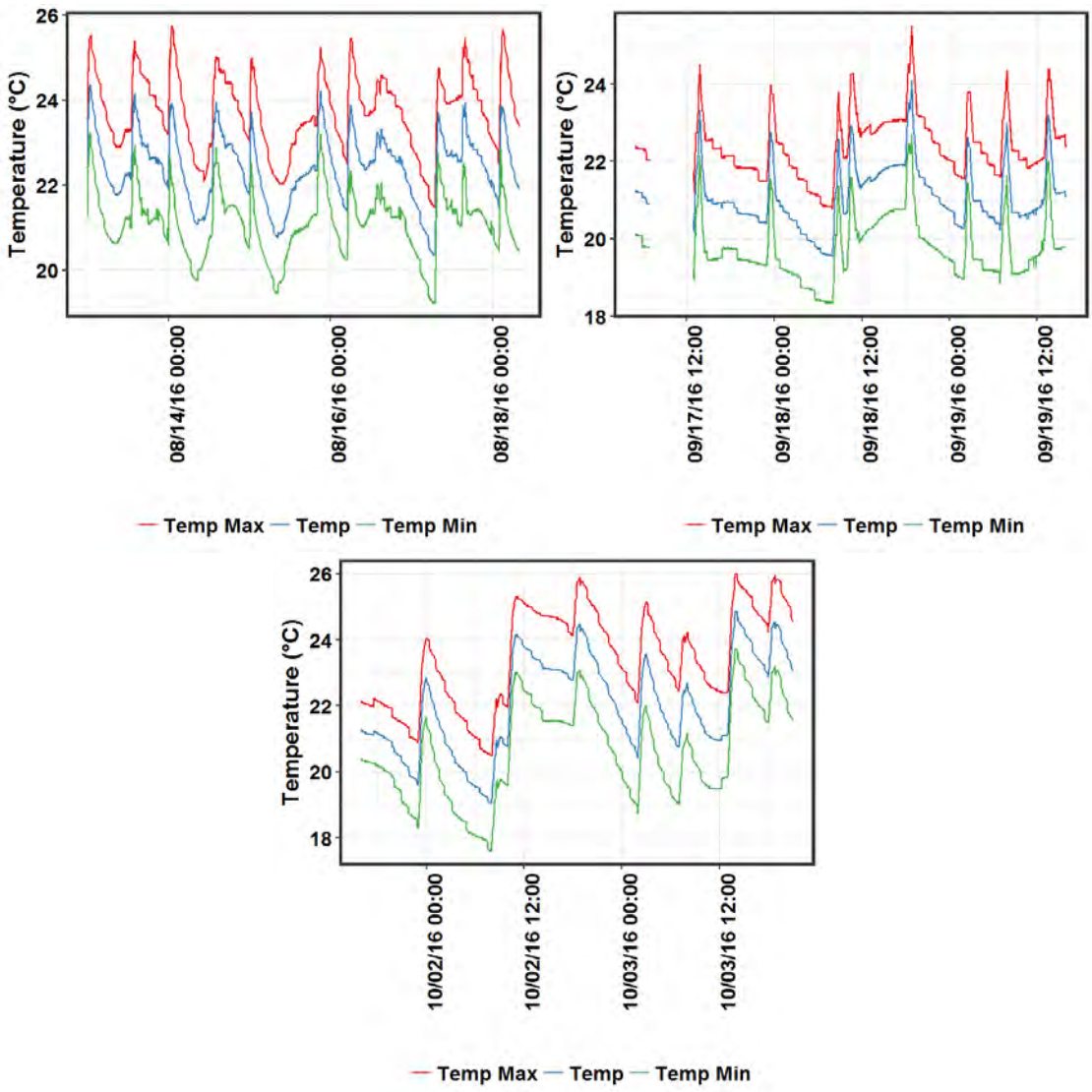

Figure 2.10. Energy Arbitrage Runs for Cycle 1, Temperature as a Function of Time

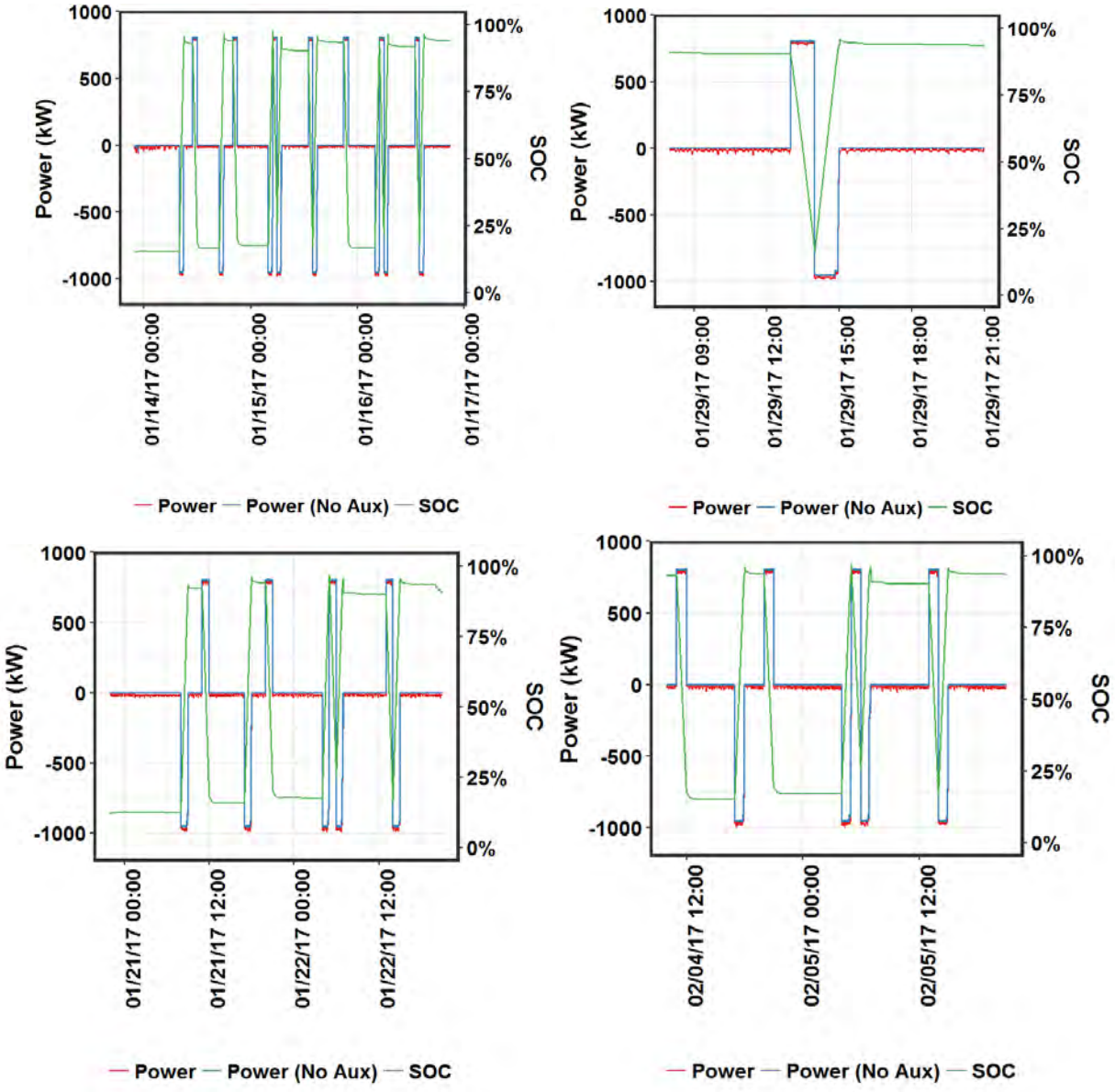

Figure 2.11. Energy Arbitrage Runs, Cycle 2, Power and SOC as a Function of Time

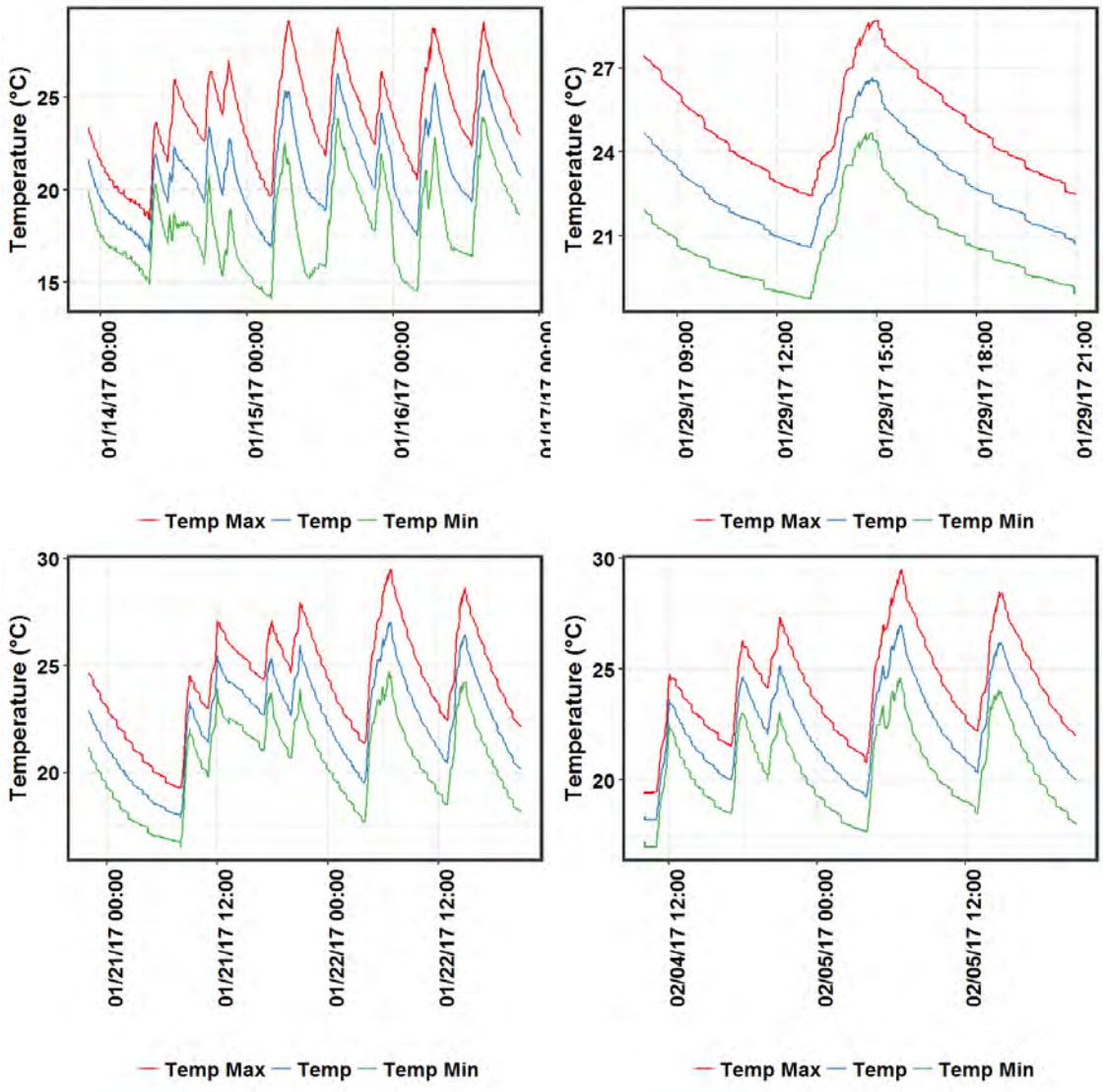

Figure 2.12. Energy Arbitrage, Cycle 2, Temperature as a Function of Time

2.5 Use Case 1: System Capacity

2.5.1 Duty Cycle Summary

The capacity duty cycle was developed as a seven-day schedule of charging/discharging power with discharge periods varying from 1-4 during peak hours and charging adequately to maintain SOC.

2.5.2 Test Results

System capacity test results are shown in Table 2.12, Figure 2.13, and Figure 2.14. For Cycle 1, Run 1 has an average charge power of 465 kW and average discharge power of 315 kW, while Run 2 numbers are 220 kW and 185 kW respectively. However, since the auxiliary consumption for Run 2 is about 65 percent of Run 1 consumption, Run 2 RTE, at 61.2 percent, is only 1.5 percent lower than Run 1 RTE. Due to the long rest period, the gap increases when the rest period is excluded. The gap also increases when auxiliary consumption is excluded, with RTE of 85.5 percent and 81.2 percent for Runs 1 and 2, respectively.

For Cycle 2, charge power ranged from 440 to 515 kW, while discharge power ranged from 160 to 305 kW. The rest time for Run 2 was the highest as a percentage of test duration, hence it had the lowest RTE, even though Run 3 charge and discharge power levels were the lowest. As expected, once the rest period was excluded, Run 1 and Run 2 RTE were nearly the same at 79.4 and 78.9 percent respectively, in line with the fact that Run 1 had higher discharge power. Run 3, with discharge power just greater than 50 percent of Run 1 discharge power, had the lowest RTE at 75.6 percent. Excluding auxiliary consumption, Runs 1 and 3 had nearly the same RTE at 85 to 86 percent, while Run 2 RTE, at 75 percent, was even lower than the RTE with rest excluded. Comparison of charge power at the PCS during rest shows that for Run 2, the charge power, at an average of 25 kW, is higher than the average of 18 kW for Runs 1 and 3. Once again, for Run 2, the PCS appears to have been in the switching mode during rest, which consumes power. Hence it is very important that the BESS control system ensures the PCS is placed in the intended mode.

Table 2.12. System Capacity Test Results Cycle 1

Start Date	Dura-tion (h)	Mean Temp. (°C)	Charge Energy (kWh)	Disch. Energy (kWh)	RTE (%)	Charge Energy No Rest (kWh)	RTE No Rest (%)	Charge Energy No Aux (kWh)	Disch. Energy No Aux (kWh)	RTE No Aux (%)	Avg. Charge Power (kW)	Avg. Disch. Power (kW)	Avg. Aux Power During Charge (kW)	Avg. Aux Power During Disch. (kW)
Cycle 1														
2016/08/01	84.0	21.6	7733	4848	62.7	6329	76.6	6105	5222	85.5	466	313	-24.4	-24.1
2016/08/09	72.0	22.1	5173	3166	61.2	4501	70.3	4200	3410	81.2	220	185	-15.5	-18.1
Cycle 2														
2017/02/10	46.0	19.7	2960	1840	62.1	2316	79.4	2251	1935	85.9	486	307	-17.4	-15.9
2017/02/17	70.0	19.8	4383	2358	53.8	2986	78.9	3345	2507	75.0	516	266	-16.2	-16.8
2017/02/24	46.0	19.7	3224	1999	62.0	2643	75.6	2529	2151	85.1	441	161	-19.1	-17.2

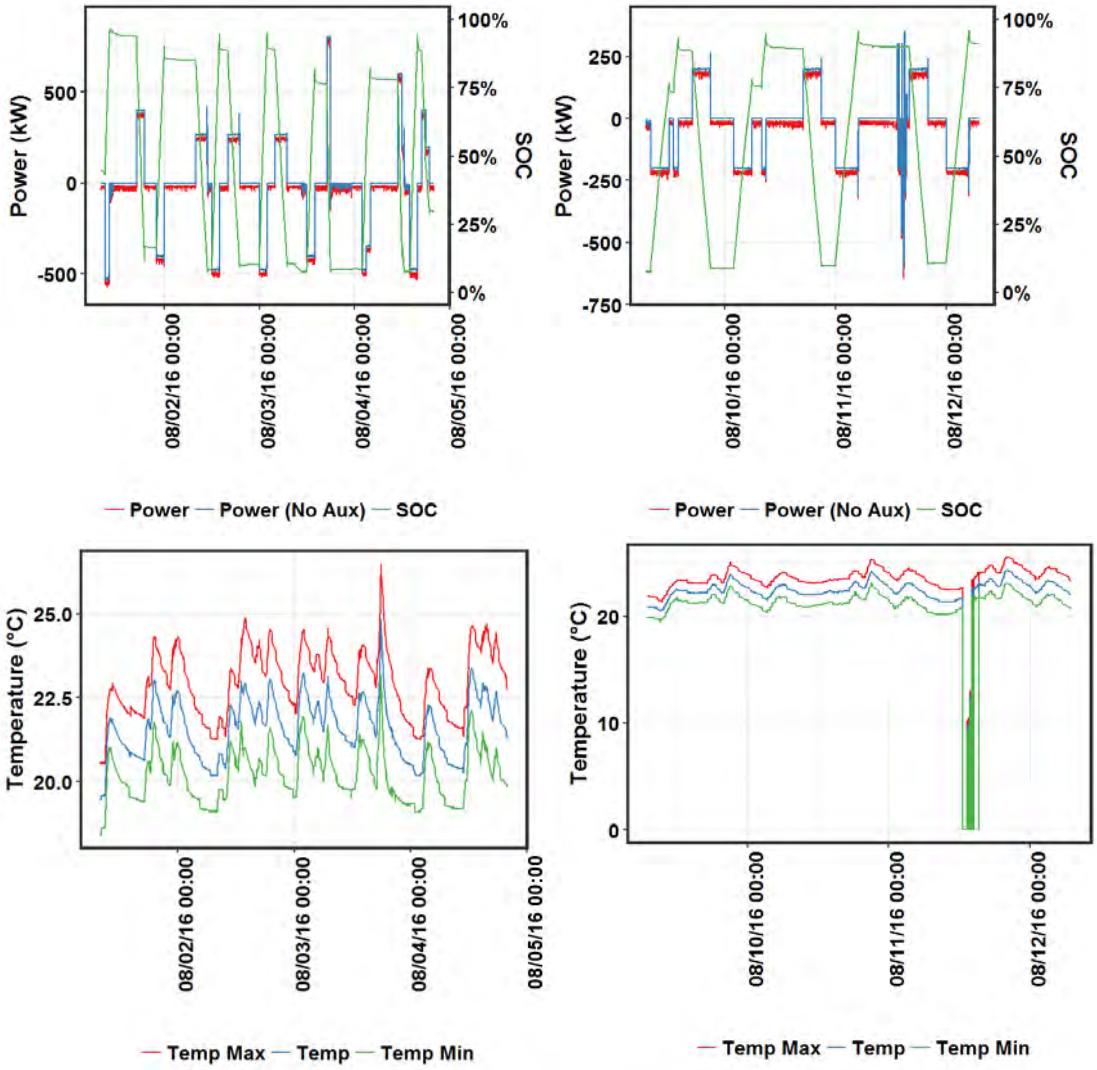

Figure 2.13. System Capacity Tests, Cycle 1

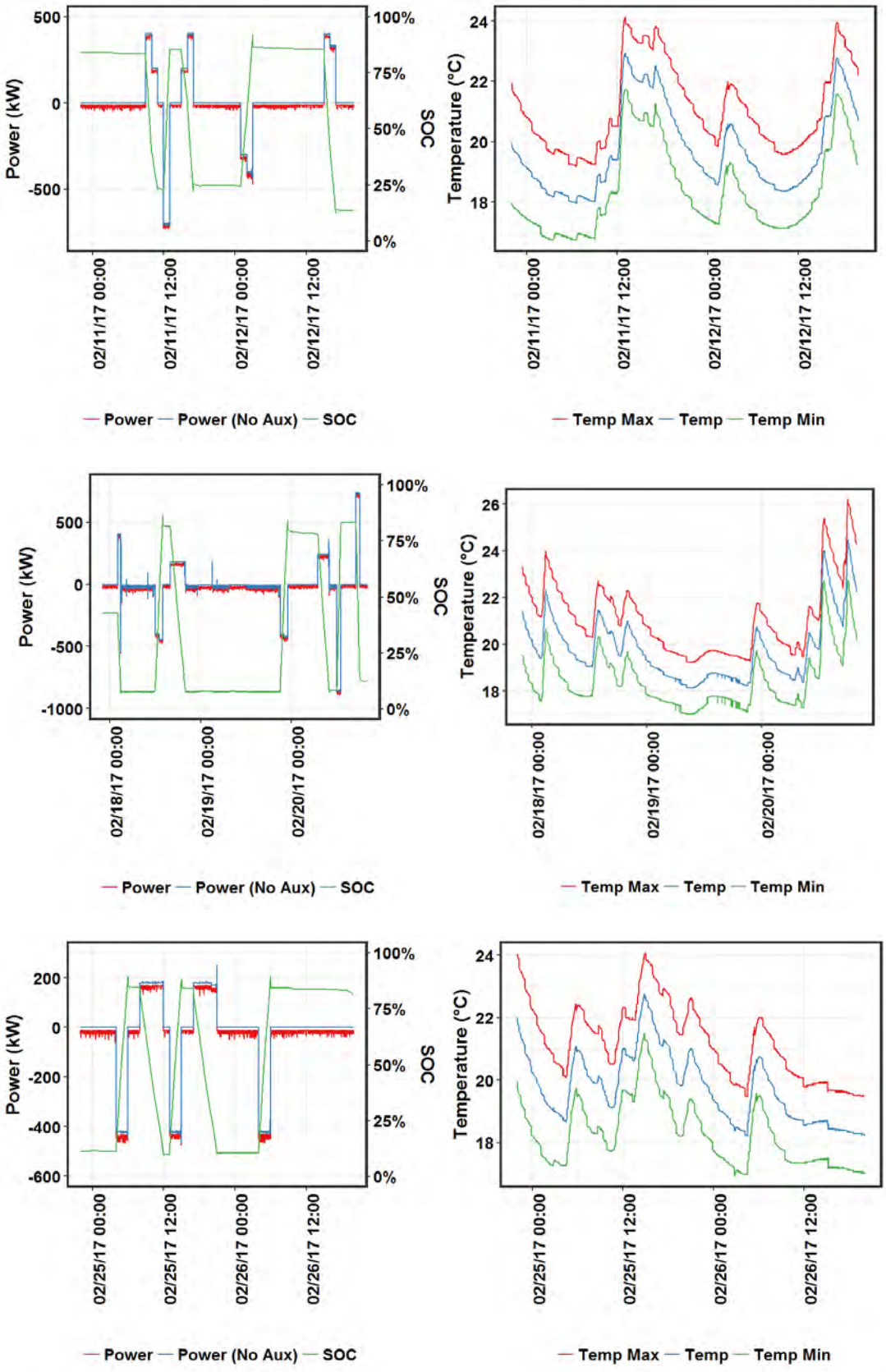

Figure 2.14. System Capacity Tests, Cycle 2

2.6 Use Case 3: Volt/Var

2.6.1 Duty Cycle Summary

This use case test was conducted by deploying the BESS inverters to correct the power factor (PF) at a specific location in the feeder to unity.

2.6.2 Test Results

For Volt/var testing, the BESS was set in the power factor correction mode, with the PF at the Hardeson Bank set to 1. The requested amount of var from the BESS and the actual PF at the point of interest were not available.

Cycle 1 was done in October and November of 2016, and the requested vars were close to 2,000 kvar. Cycle 2, done in March-April of 2017, had negligible var requirements, indicating that during spring, the Bank PF was well within the deadband around 1.

For both Cycle 1 and Cycle 2, it was observed that for some runs, the BESS was subjected to a charge signal in addition to the var request to keep PF = 1. This happened when the BESS SOC was at its lower limit of 7.5 percent. The BESS was also subject to some discharges – three events occurring at 2:30 PM, with SOC at 80 percent, once at 5 AM with SOC at 30 percent. It is not clear why this is happening. It is possible SnoPUD decided to use the BESS discharge capabilities when there was some need, especially when the var requested was being easily met. Hence for some runs, the BESS appears to be placed in Watt limiting mode. Since the BESS is always accepting charge to power the auxiliary, some real power is always flowing through the BESS.

From the acceptance test, it is clear that the BESS vars follows the signal well. MESA-1a supplied or consumed an average of 358 kvar when requested reactive power was 375 kvar (1energy systems 2015) to maintain a power factor (PF) of 0.8, with the average power factor 0.8125. This corresponded to a difference of 4.5 percent from the requested vars. To maintain a PF of 1 at the Hardeson bank with reactive power over 1,400 kvar, maximum vars of 1,000 kvar was requested from the battery, which was able to provide only 925 kvar, a deviation of 7.5 percent from the requested vars. For the 0.8 PF test, MESA-1b tracked the requested vars of 375 kvar within 0.6 percent. (1energy systems, 2016) Note that for the MESA-1b PF =1 test, the requested vars was less than the battery apparent power rating of 1,000 kVA. At the start of the test, the vars in the bank was 800 kvar, while the battery provided 730 kvar, a tracking error of 9 percent. In this test, the BESS vars varied, and always remained less than 600 kvar, except at the start. It can be concluded that the overall BESS tracking error is less than 10 percent for vars.

Hence, it can be assumed that the vars delivered closely follow the vars requested.

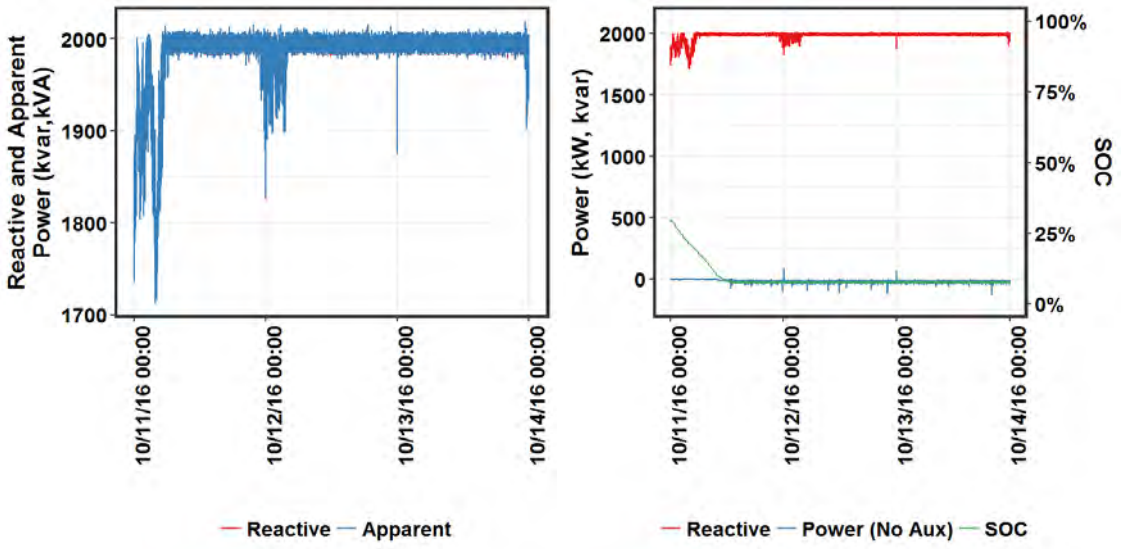

Figure 2.15. Power Factor Correction Mode, Cycle 1 (left) Reactive Power and total kVA, (right) Real and Reacive Power, SOC

For run 1, Cycle 1, the SOC reached < 10 percent from an initial SOC of 30 percent within 11 hours, which is a high rate of self-discharge for the BESS (Figure 2.15). The BESS received charge at power levels < 50 kW, with two discharge spikes of 50 to 75 kW. During these spikes, the reactive power drops. However, the power drop sometimes is more than needed to suport real power, as seen from the plots of apparent power. For Run 1 of Cycle 1, during the initial drop in SOC from 30 percent to 10 percent in 11 hours, there was no real power flow. For the first 6 hours, the requested vars and apparent power is lower than 2,000 kvar and 2,000 kVA, respectively. *This indicates that the requested var is less than the BESS rated apparent power*. At the start of October 12 2016, there is a a spike in discharge power to 85 kW. This is accompanied by a steep drop in apparent power to ~ 1825 kVA, indicating the DERO optimizer may be dropping requested var more than the calculated available vars. For the next 3 hours, the vars flow is less than rated apparent power, and is in the 1,900 to 1,980 kvar range for the most part. At the start of October 13, 2016, there is a spike in discharge power to 50 kW, accompanied by a decrease in vars and drop in apparent power to 1870 kVA (from close to 2000 kVA), again, indicating the DERO optimizer may be dropping var request more than the calculated available vars, in order to ensure the rated power of the BESS is not exceeded. This drop in apparent power was present for all occasions when discharge spikes were present, and did not occur when charge spikes were present. This appears to indicate that the required vars is lower when the BESS is discharging.

However, as seen in Figure 2.16, for Run 2 of Cycle 1, when the BESS SOC drops from 20 percent to 8 percent SOC in 6 hours due to a 250 kW discharge starting 11/1/2016, there is no decrease in kvar, thus indicating the drop in kvar and kVA duing the first 6 hours of Run 1 was simply related to grid needs, and not tied to BESS discharge. The first 6 hours of Run 2, with negligible real power flow, have reactive power less than 2,000 kvar, again indicating the requested vars was less than 2,000 kvar. During the 750 kW and 900 kW charge starting at 5 AM and 8 AM respectively on 11/10/16, the apparent power was < 2000 kVA. For the rest of the period, including the two discharges, the apparent power was at 2,000 kVA. This shows that even when discharge was occuring at 250 kW, the BESS is commanded to output 2,000 kVA. Hence, it is not clear why during some charge and discharge periods, the apparent power is lower than 2,000 kVA (or the var output is lower than the available vars). Without knowing the DERO algorithm, no definitive conclusion can be drawn; it appears that there are some periods when requested vars is < 2000 kvar, even though the BESS can support this vars (with no real power flow). For Run 2 of Cycle 1, at ~ 4 AM, the BESS is charged at 750 kW from 12 percent SOC to get it ready for a

7 AM discharge of 250 kW, and then recharged at 8 AM to get it ready for a 9 AM discharge at 250 kW. From the total kVA curve (left), when total kVA is 2000 kVA, the BESS is asked to provide its max var capability. Note that when the BESS is charging at 750 kW or at 1000 kW, the total kVA is < 2000 kVA. During other times, the total kVA is 2000, including the two discharges at 250 kW. Hence, at times, mostly during high power charge, the DERO optimizer appears to be setting aside some headspace for the BESS to provide the required real power and hence does not use the full var capability of the BESS.

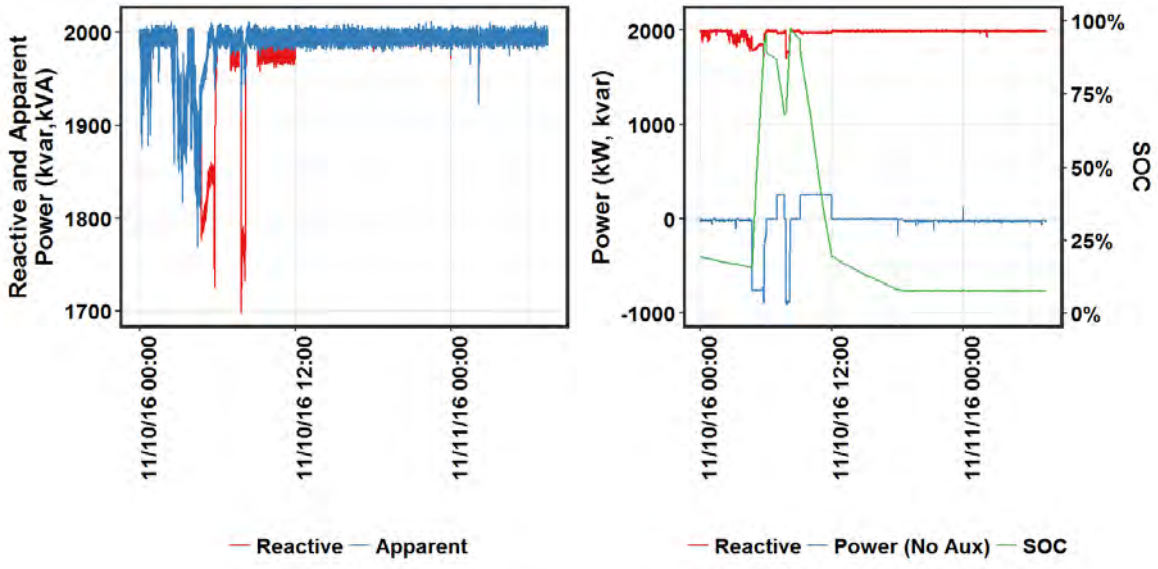

Figure 2.16. Power Factor Correction Mode, Run 2, Cycle 1 (left) Reactive Power and Total kVA, (right) Real and Reacive Power, SOC

Figure 2.17 shows that Run 3 of Cycle 1 starts on 11/19/2016 at 8 AM. There was no active power exchanged. The var output was lower than 2000 kvar for most of this test. This appears to indicate that the requested vars were less than 2000 kvar. Note that small spikes of less than 25 kW of real power correspond to > 1999 kvar available, which appears to indicate that requested vars is close to the rated capacity of the BESS.

The SOC drops from 50 percent to 10 percent during the approximately 8 hours preceding the start of this test, even though no real power flows during this time. The BESS appears to be providing very low vars, as verified by the reactive power being visible during this period in the figure on the left. With the PCS in switching mode, the rate of decrease of SOC is much higher than when the BESS is at rest. However, this steep decrease in SOC is surprising, considering the expected duration for this 40 percent SOC decrease is around 24 hours (Figure 2.20).

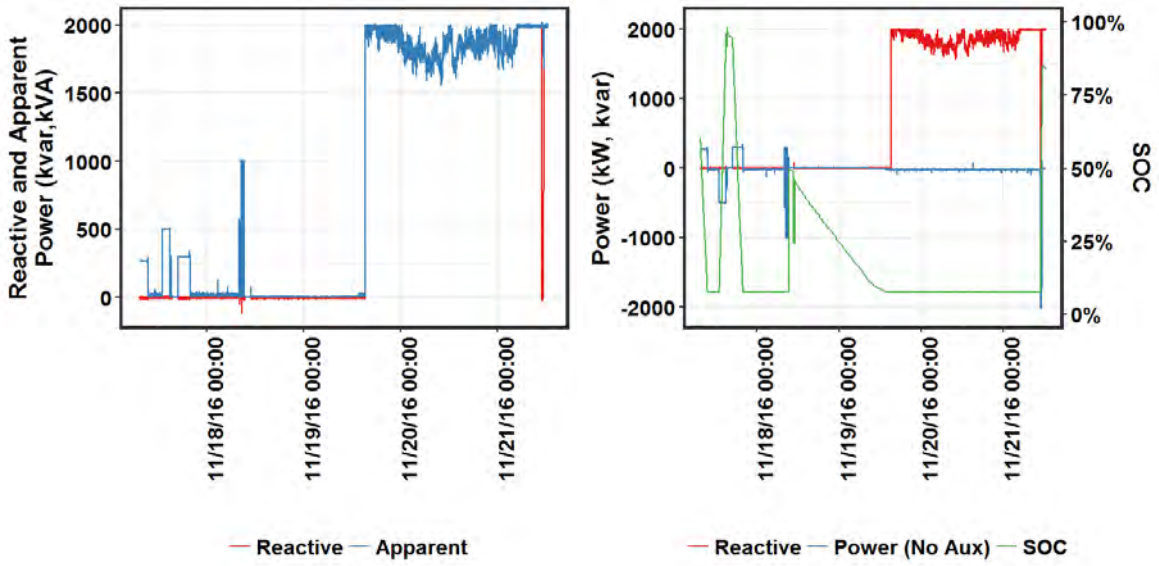

Figure 2.17. Power Factor Correction Mode, Run 3, Cycle 1 (left) Reactive Power and Total kVA, (right) Real and Reacive Power, SOC. The duty cycle starts 8 AM 11/19/16.

Run 1 for Cycle 2 has only two short time periods when vars are being provided by the BESS, 1,300 kvar at the test beginning, and 2,000 kvar ~ 4 AM on 3/13/17, both less than an hour in duration (Figure 2.18). Again, the BESS SOC decreased from 87 percent to 12 percent in 2 days following the 1,300 kvar, which is an extremely fast self-discharge rate. As seen from the figure on the left, the reactive power is clearly visible, indicating the PCS is in switching mode The BESS was recharged at this stage, followed by a discharge and a charge, during which no reactive power flows.

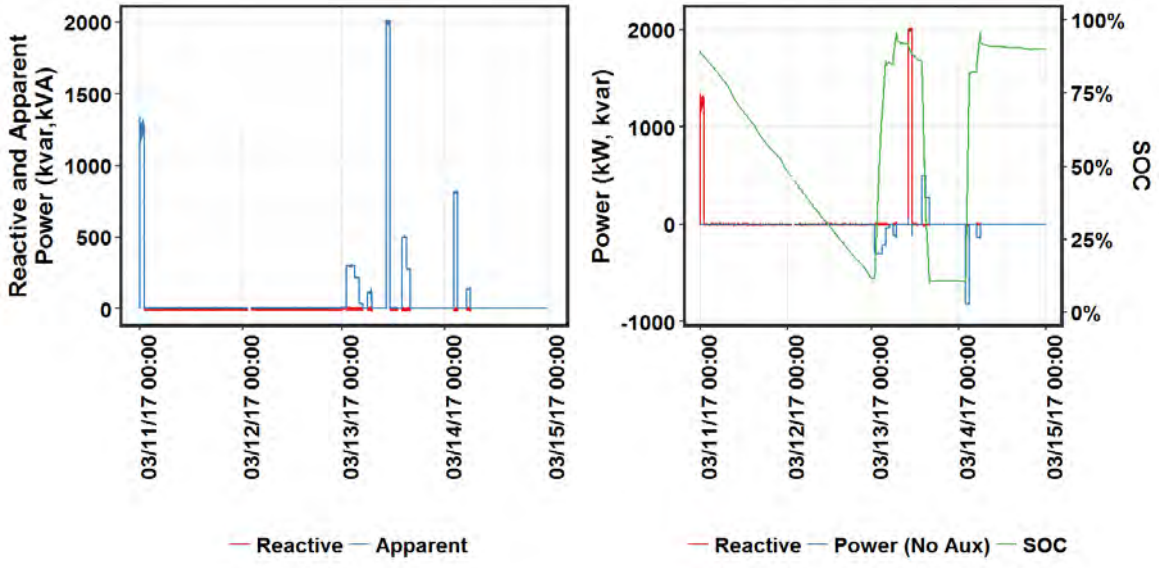

Figure 2.18. Power Factor Correction Mode, Run 1, Cycle 2 (left) Reactive Power and total kVA, (right) Real and Reacive Power, SOC. Reactive power not being requested when real power flows.

Run 2 for Cycle 2 has no vars flowing that is significant (Figure 2.19). During the first hour, with the BESS discharging, as expected, the rate of SOC change is high. Following the discharge, the BESS is at

rest, with the PCS not switching. The rate of SOC decrease is extremely low as expected. At the start of 4/2/17 00:00 hours, the PCS is in switching mode, possiibly because the DERO has placed the BESS in PF correction mode. The SOC drops from 80 percent to 35 percent in 25 hours. The rest of the test has some discharges and charges, some rest periods, and some periods when PCS is in switching mode with no real power flow. The rate of decrease of SOC when the PCS is in switching mode with no real power flow is much higher than when the BESS is at rest. For about 3 hours starting 4/3/17 at 5 AM and for the last 8 hours, DERO appears to have removed the BESS from PF correction mode. During this period, the rate of SOC change was much lower. For this test, the vars requested appears to be extremely low, indicating the PF at the bank was well within the deadband around 1.

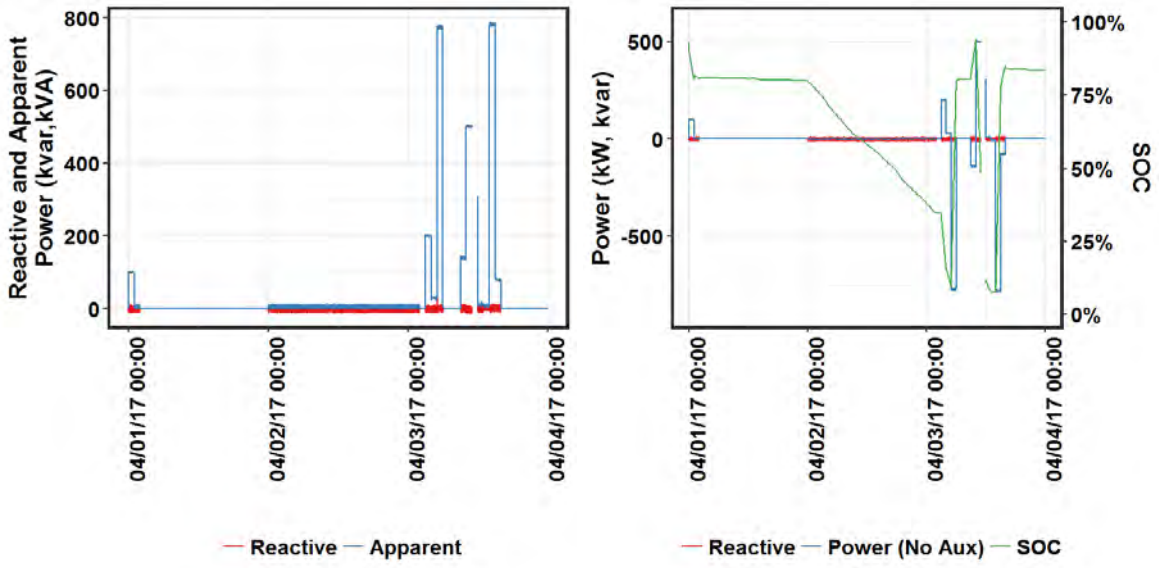

Figure 2.19. Power Factor Correction Mode, Run 2, Cycle 2 (left) Reactive Power and Total kVA, (right) Real and Reacive Power, SOC. Negligible reactive power flow.

Figure 2.20 shows SOC as a function of time during volt-var tests when 1) BESS is in PF correction mode, 2) BESS is not in PF correction mode, during the volt-var runs. The rate of SOC change when the BESS is in PF corection mode is -1.62 percent/hour, while during Rest, it is -0.063 percent/hour. Since most of the data points in the PF mode fall in a straight line, the rate of decrease of SOC does not depend on the magnitude of var. This finding is in line with the fact that during some runs, the SOC dropped much fatser than expected without any real power flow at the beginning of the project. At the time, it was assumed that when the PCS switches, this brings down the SOC. Subsequent to that, we found that during rest after charge, the PCS was not in switched mode, while during rest after discharge, the PCS was in switched mode. At C/4 and C/2 rates, SOC for 1a dropped by 5 to 7 percent during rest after charge, even though there was no switching of PCS, while 1b SOC was constant. For higher C rates, the drop in SOC for 1a was lower, while 1b SOC increased during rest after charge. During rest after discharge, with PCS switching, 1a SOC was flat for C/4 and C/2 rates, while it increased very slightly (< 1 percent) during rest after dischaare for C and 2C rates. 1b SOC was flat after discharge at the C/4 and C/2 rates, while it increased after C and 2C rate discharge. While this may appear confusing, it actualy makes sense once we ignore the fluctuation sin SOC minutes after charge or discharge is stpped. These fluctuations account at most for 6 percent SOC, with most in the range of 1 to 4 percent. Hence, over a longer pwriod (of > 3 h), the rate of charnge of SOC depends on the PCS switching status.

For all use cases involving power flow, it was observed that when the SOC at the end of discharge was > than the lower threshold, the PCS was not placed in switching mode, while the PCS was in switching

mode with the SOC at the end of discharge at or near the lower threshold (Figure 2.21). After every charge, the PCS is not in switching mode as seen by reactive power being 0. When the SOC at the end of discharge is > 13 percent, the PCS is not in switching mode (0 reactive power). With the SOC around 9 percent, the PCS is in switching mode. This shows that during optimization of battery performance, acre should be exercised to keep the SOC about 5 percent above the lower threshold of 7.5 percent.

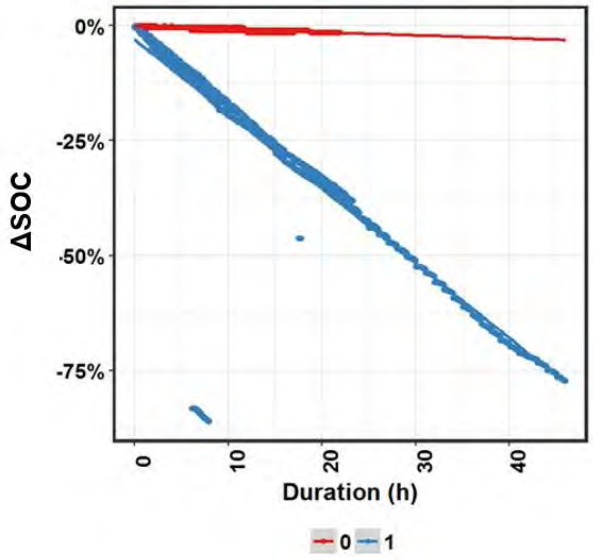

Figure 2.20. Rate of Change of SOC for Volt-Var Runs with BESS in PF Mode (1), and during Rest (0)

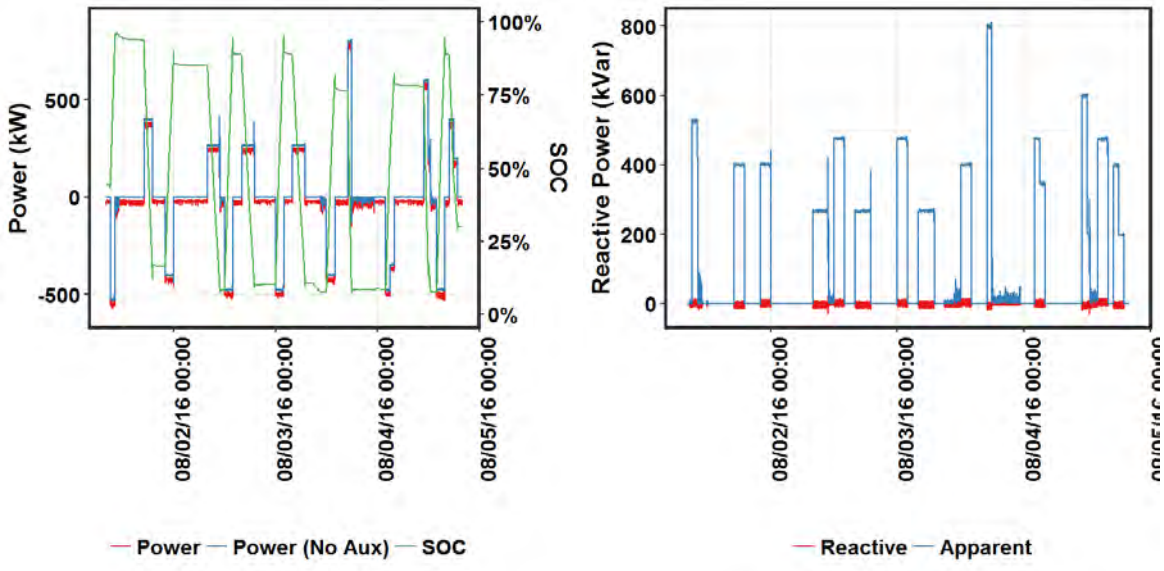

Figure 2.21. PCS Switching State as a Function of SOC Level after Discharge (left) Real Power, (right) Apparent and Reactive Power

2.7 Use Case 3: Load Shaping

2.7.1 Duty Cycle Summary

The load shaping duty cycle for SnoPUD was developed using BSET by minimizing the cost of balancing the SnoPUD system. Effectively, the BESS can be used to avoid balancing payments to BPA. If the cost of using the battery to address deviations between scheduled and actual loads are lower than the costs of balancing payments to BPA to do it, BSET would simulate the inflows and outflows of power necessary to minimize costs to SnoPUD. The resulting duty cycle was used as the basis of the use case test results reported here. A one-month balancing duty cycle using December 2015 data was developed. However, the actual test was conducted for slightly over a week.

2.7.2 Test Results

Load shaping test results are shown in Table 2.13 and in Figure 2.22, Figure 2.23, Figure 2.24, and Figure 2.25. The RTE ranges from 56.9 to 69.8 percent. This wide range is due to the fact that the charge and discharge power levels have a wide range. For Cycle 1, average charge power was 380 kW, while average discharge power was 178 kW, with a 57 percent RTE. For Cycle 2, the RTE was in a very tight range of 69.2 to 69.8 percent. The percentage time at rest was about the same for all runs in Cycles 1 and 2 (75 to 78 percent). For Cycle 1, the lower power level is the main reason for the low RTE of 56.9 percent. Looking at the charge and discharge energy excluding auxiliary load, the charge and discharge energy levels are reasonably matched. The average power levels (charge + discharge) are 279 kW, 595 kW, 502 kW, and 534 kW for Cycle 1, and Runs 1-3 of Cycle 2, respectively. As expected, the RTE tracks the average power levels, with lower RTE at lower average power. Since rest times are a high percent of total duration, excluding rest improves RTE for all runs, especially for Cycle 1, for which auxiliary consumption during rest forms a significant percent of total charge energy. Removing auxiliary consumption further reduces the gap, with RTE for cycle 1 at 82.9 percent, while for Cycle 2, it ranges from 84.8 to 87.1 percent. As expected, the RTE for Cycle 2 is higher when average power level is higher, due to temperature effects. Note that Cycle 1 is performed in winter, which further contributes to its lower RTE.

For run 1, Cycle 1, the BESS operates in the 17 °C to 27.5 °C range. The difference between Tmax and Tmin is around 2.5 °C, which corresponds to a tight range. Considering the low auxiliary average power, there does not appear to be any active heating in this temperature range (cooling probably will not kick in till temperature is higher than the upper end of this range). The same observation applies to all Runs in Cycle 2.

The RTE was lower for Cycle 1, due to lower charge and discharge power. The RTE without rest were similar for Cycle 1 and Run 3 of Cycle 2, which had similar discharge power levels. Run 1 of Cycle 2, with discharge power level of 685 kW, had the highest RTE when rest was excluded, at 85.1 percent. The RTE without auxiliary load was in a tight range of 83 to 87 percent for both cycles, with higher RTEs for higher power levels, in line with our findings that 1000 kW is the sweet spot. Note that the average auxiliary consumption was similar for both Cycles 1 and 2, since they were performed with the low ambient temperature in October and December.

Table 2.13. Load Shaping Test Results

Start Date	Dura-tion. (h)	% Time at Rest	Mean Temp. (°C)	Charge Energy (kWh)	Disch. Energy (kWh)	RTE (%)	Charge Energy No Rest (kWh)	RTE No Rest (%)	Charge Energy No Aux (kWh)	Disch. Energy No Aux (kWh)	RTE No Aux (%)	Avg. Charge power (kW)	Avg. Disch. Power (kW)	Avg. Aux Power During Charge (kW)	Avg. Aux Power During Disch. (kW)
Cycle 1															
2016/10/04	166.0	77	20.4	7488	4261	56.9	5300	78.0	5563	4612	82.9	380	178	-15.6	-14.6
Cycle 2															
2016/12/16	56.0	78	20.2	4999	3458	69.2	4059	85.1	4069	3543	87.1	504	686	-17.0	-16.8
2016/12/23	79.0	76	20.1	7464	5201	69.7	6318	81.3	6414	5439	84.8	698	306	-16.3	-15.6
2016/12/30	70.0	75	20.3	6606	4612	69.8	5852	76.9	5730	4896	85.4	817	250	-15.9	-15.4

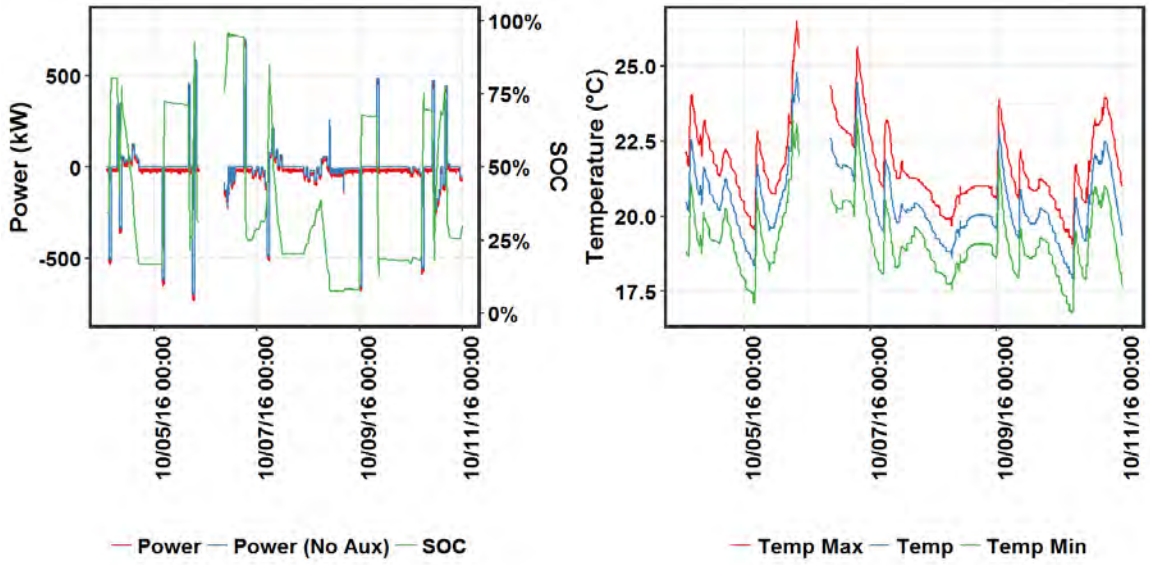

Figure 2.22. Load Shaping Results, Cycle 1. BESS Operates in the 17 °C to 27.5 °C Range

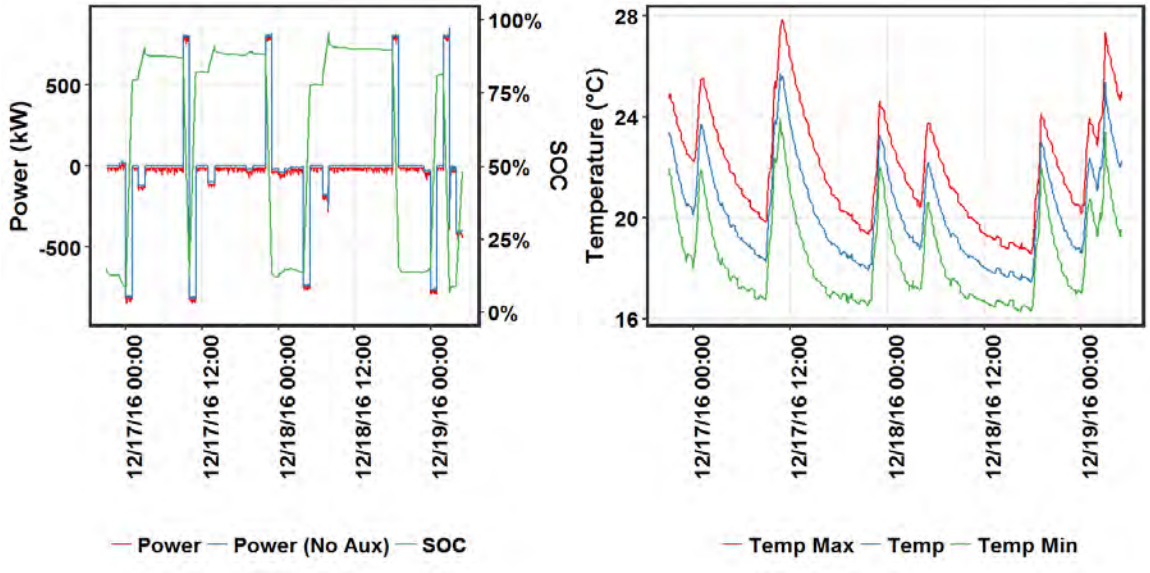

Figure 2.23. Load Shaping Results, Cycle 2. BESS Operates in the 17 °C to 28°C Range

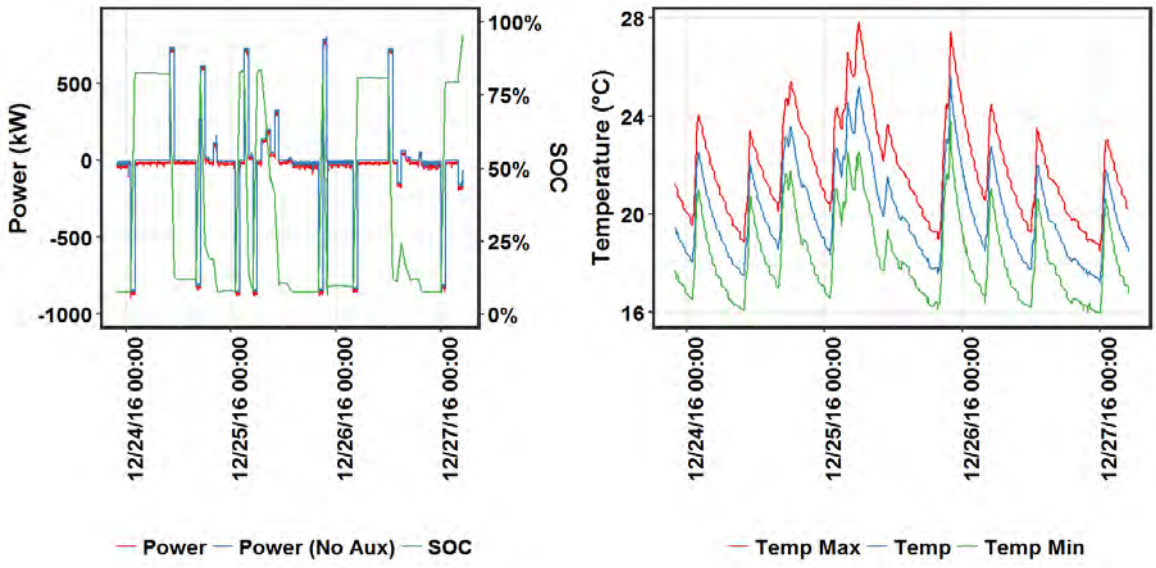

Figure 2.24. Load Shaping Results, Cycle 2. BESS operates in the 16 °C to 28 °C range.

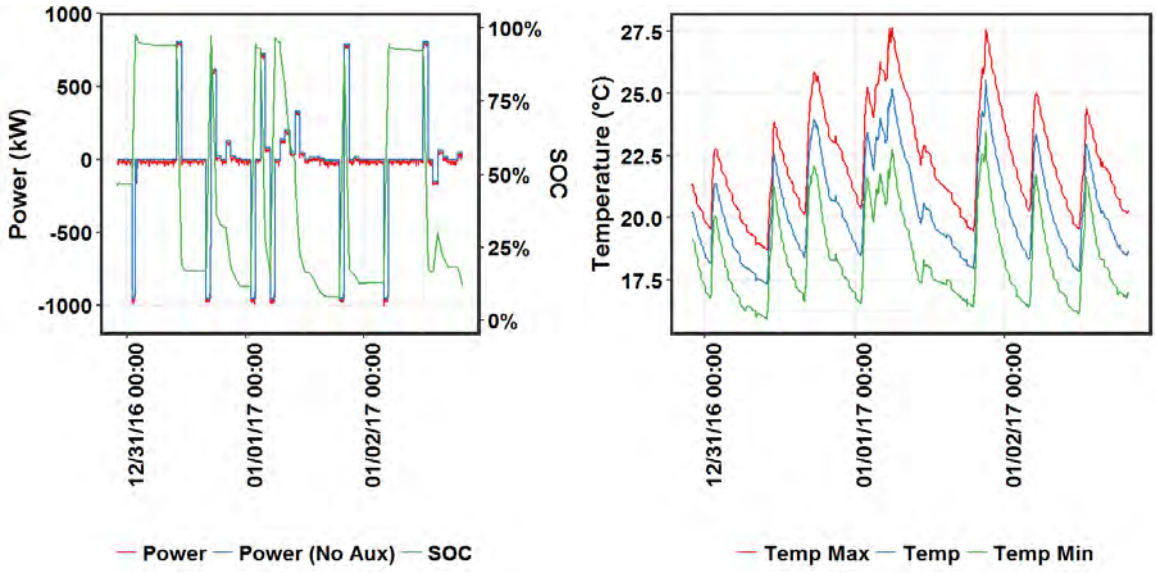

Figure 2.25. Load Shaping Results, Cycle 2. BESS operates in the 16 °C to 27.5 °C range.

2.8 Capacity Stability Test after Cycle 1 and Cycle 2

Table 2.14 and Table 2.15 show the reference performance capacity test results after Cycle 1 and Cycle 2. Figure 2.26, Figure 2.27, Figure 2.28, and Figure 2.29 show the power, SOC, temperature and auxiliary consumption for the BESS and power, temperature and SOC for MESA-1a and 1b. Figure 2.30, Figure 2.31, Figure 2.32, and Figure 2.33 show similar results for post Cycle 2 capacity tests. The general observations remain the same as for baseline capacity tests before cycling. The RTE increases with increasing power, especially when rest and auxiliary losses are included. For post Cycle 1, RTE tops off at 500 kW, since this test is done in winter, while for post Cycle 2 RTE peaks at 1,000 kW. As expected, removing auxiliary losses reduces the gap between RTEs at various power levels. The numbers in italics for energy and RTE excluding rest correspond to missing data.

Table 2.14. Capacity Stability after Cycle 1

Start Date	Dura-tion (h)	Mean Temp. (°C)	Charge Energy (kWh)	Discharge Energy (kWh)	RTE (%)	Charge Energy No Rest (kWh)	RTE No Rest (%)	Charge Energy No Aux (kWh)	Discharge Energy No Aux (kWh)	RTE No Aux (%)	Average Charge Power (kW)	Average Discharge Power (kW)
2016/11/22	10.7	21.1	1229	859	69.9	1167	73.6	1124	918	81.6	269	214
2016/11/23	11.4	20.0	1358	960	70.7	1290	74.4	1244	1027	82.6	268	213
2016/11/23	10.8	19.5	1309	922	70.4	1251	73.6	1195	990	82.8	269	212
Mean	11.0	20.2	1298	914	70.4	1236	73.9	1188	978	82.3	269	213
Cumulative	31.1	20.2	3538	2489	70.3	3366	73.9	3234	2667	82.5	269	213
2016/11/24	7.5	22.0	1540	1283	83.3	1483	86.5	1458	1325	90.9	514	429
2016/11/24	6.6	22.6	1043	832	79.7	989	84.1	976	859	88.1	497	425
Mean	7.1	22.3	1292	1057	81.5	1236	85.3	1217	1092	89.5	506	427
Cumulative	13.3	22.3	2119	1690	79.8	2007	84.2	1981	1746	88.1	505	427
2016/11/23*	5.1	22.2	1622	1374	84.7	1565	87.8	1559	1394	89.4	950	964
2016/11/23	4.7	26.1	1773	1485	83.8	1741	85.3	1714	1516	88.5	1018	873
2016/11/23	5.6	26.4	1062	885	83.4	1007	87.9	991	902	91.0	1007	874
Mean	5.1	24.9	971	834	85.9	962	86.8	947	849	89.6	1017	910
Cumulative	13.6	25.3	2905	2504	86.2	2877	87.0	2833	2547	89.9	1018	908
2016/11/21	2.9	28.7	1034	856	82.8	994	86.2	981	866	88.3	1570	1713
2016/11/21	3.0	30.1	1020	857	84.0	977	87.7	967	867	89.7	1880	1714
2016/11/21	3.1	30.4	1023	855	83.5	976	87.6	969	864	89.2	1896	1710
Mean	3.0	29.7	1026	856	83.5	982	87.1	972	866	89.1	1782	1712
Cumulative	9.0	29.7	3068	2568	83.7	2937	87.4	2907	2597	89.3	1782	1712

*Start SOC 42%

Table 2.15. Capacity Stability after Cycle 2

Start Date	Dura-tion (h)	Mean Temp. (°C)	Charge Energy (kWh)	Discharge Energy (kWh)	RTE (%)	Charge Energy No Rest (kWh)	RTE No Rest (%)	Charge Energy No Aux (kWh)	Discharge Energy No Aux (kWh)	RTE No Aux (%)	Average Charge Power (kW)	Average Discharge Power (kW)
2017/05/11	8.9	22.2	1122	772	68.8	1068	72.3	1040	824	79.2	267	214
2017/05/11	10.9	21.0	1125	768	68.3	1039	73.9	1013	824	81.3	267	213
2017/05/12	10.9	21.9	1122	771	68.7	1038	74.2	1015	824	81.2	266	213
Mean	10.2	21.7	1123	770	68.6	1049	73.5	1023	824	80.6	267	214
Cumulative	28.9	21.7	3316	2311	69.7	3145	73.5	3042	2473	81.3	267	214
2017/05/16	5.9	22.9	1063	851	80.0	1020	83.4	1004	880	87.7	512	427
2017/05/16	5.9	24.7	1072	856	79.8	1028	83.2	1004	888	88.4	509	428
2017/05/16	5.9	24.7	1055	858	81.4	1017	84.4	996	891	89.4	510	426
Mean	5.9	24.1	1064	855	80.4	1022	83.7	1001	886	88.5	510	427
Cumulative	17.9	24.1	3166	2547	80.5	3035	83.9	2977	2639	88.6	510	427
2017/05/15	3.9	24.5	1041	876	84.2	1005	87.2	996	892	89.5	1005	872
2017/05/15	3.9	26.2	1040	888	85.5	1008	88.2	991	906	91.4	1008	872
2017/05/16	3.9	26.5	1026	872	85.0	995	87.6	977	887	90.8	990	872
Mean	3.9	25.7	1035	879	84.9	1003	87.7	988	895	90.6	1001	872
Cumulative	11.9	25.7	3105	2635	84.9	3003	87.7	2960	2683	90.6	1001	872
2017/04/04	2.9	27.4	1015	828	81.6	964	85.9	962	839	87.2	1672	1657
2017/04/05	2.9	29.6	1026	849	82.8	973	87.3	969	860	88.8	1740	1695
2017/04/05	2.9	30.0	1023	850	83.0	971	87.5	966	860	89.0	1762	1699
Mean	2.9	29.0	1021	842	82.5	969	86.9	966	853	88.3	1725	1683
Cumulative	8.9	29.0	3064	2525	82.4	2904	87.0	2894	2557	88.3	1725	1683

The C/4 rate results for Cycle 1, shown in Figure 2.26, shows similar behavior as seen in baseline capacity tests for MESA-1a during rest at the end of charge – SOC drops steeply from 95 percent to 86 percent, while the 1b SOC is stable at 95 percent. The SOC at the end of discharge is stable for both 1a and 1b. The starting discharge power for 1a is only 55 percent of starting power for 1b, possibly because the starting SOC is lower. MESA-1a discharge ends at 10 percent SOC, while MESA-1b discharge ends at 5 percent SOC. The starting charge power for 1a is 70 percent of 1b charge power – possibly because the starting SOC is higher. There was no tapering of power during charge or discharge, with 1a power increasing over time, and 1b power decreasing. MESA-1a temperature drops throughout this test, while 1b temperature remains constant, possible due to lower power levels for 1a combined with its higher starting temperature and the season being winter for post Cycle 1 capacity tests. There are spikes at the end of charge and discharge. The upper SOC for both 1a and 1b was at 95 percent at the end of charge, while the lower SOC limit for 1a was 10 percent, and for 1b 5 percent.

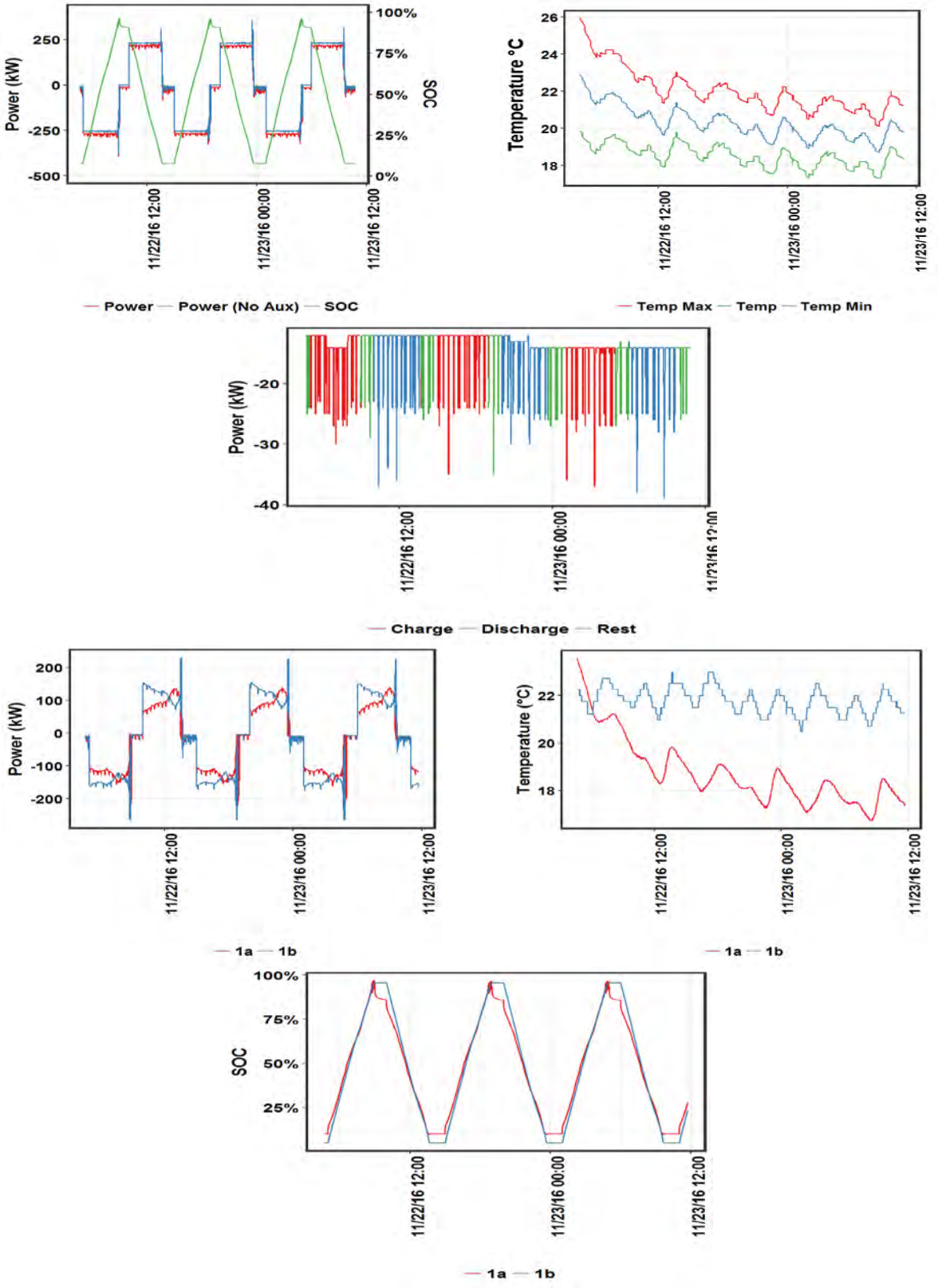

Figure 2.26. Power, SOC, Temperature and Auxiliary Consumption for Capacity Tests Post Cycle 1 at C/4 Rate; (top 3) BESS, (bottom 3) MESA-1a and 1b

The C/2 rate results for Cycle 1, shown in Figure 2.27, shows the same behavior for MESA11a at the end of charge – the SOC drops steeply from 95 percent to 86 percent, while the 1b SOC is stable at 95 percent. The SOC at the end of discharge increases slightly for 1a, while it is stable for 1b. The starting discharge power for 1a is 45 percent of 1b, while the starting charge power for 1a is 60 to 80 percent of 1b. The SOC range is the same as for the C/4 rate– 10 to 85 percent for 1a and 5 to 95 percent for 1b. The ΔT for both 1a and 1b is nearly the same at the C/2 rate, with a slight increase for both. There are spikes at the end of charge and discharge, which predominantly appears to be caused by 1b after discharge, and by both 1a and 1b after charge. The upper SOC for both 1a and 1b was at 95 percent at the end of charge, while the lower SOC limit for 1a was 10 percent, and for 1b 5 percent. There was no tapering of power during charge or discharge. As seen for the baseline capacity test at C/2 rate, the 1a power flow extended slightly past 1b at the end of charge and discharge, with resultant small spikes in SOC.

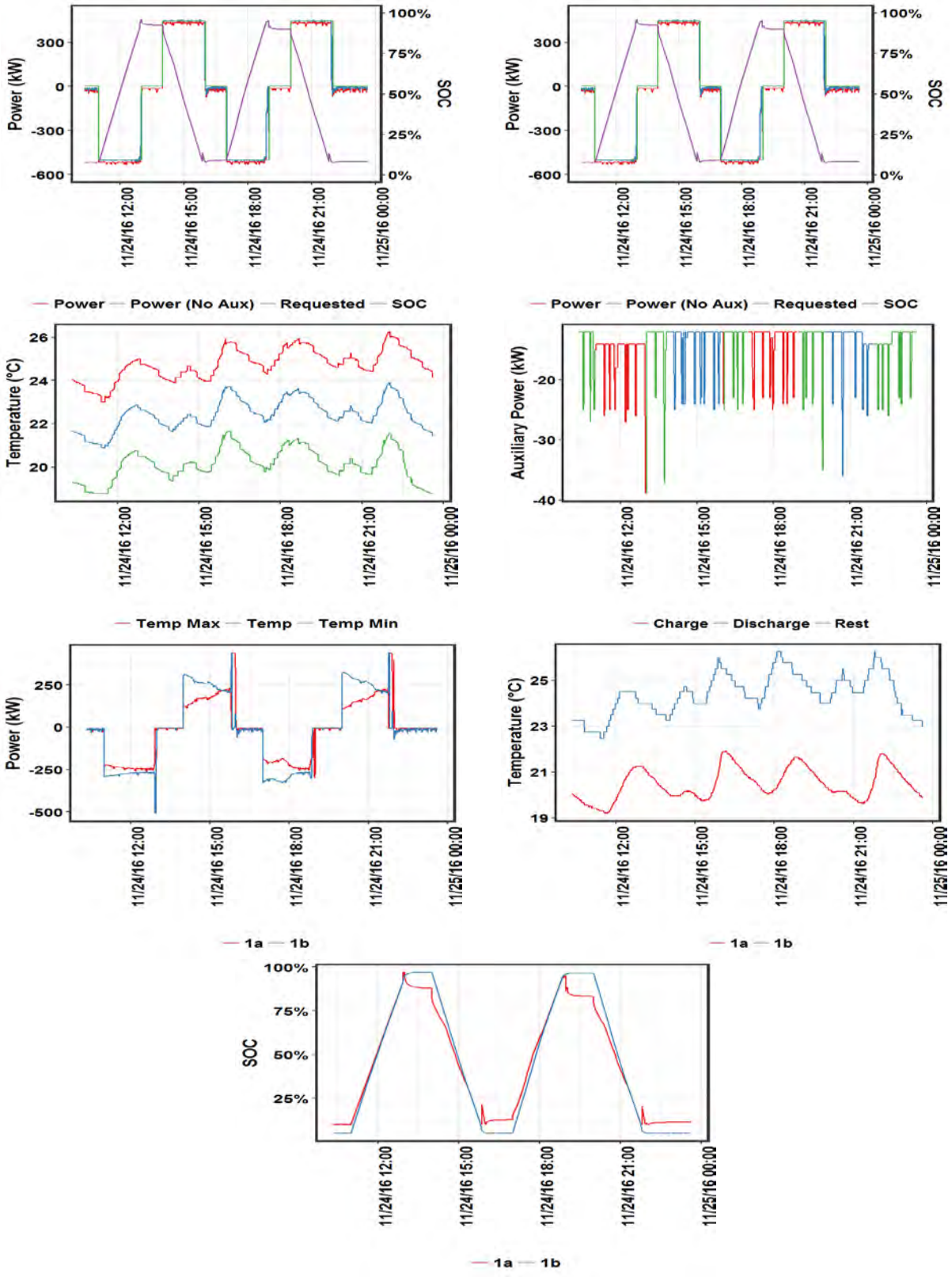

Figure 2.27. Power, SOC, Temperature and Auxiliary Consumption for Capacity Tests Post Cycle 1 at C/2 Rate; (top) BESS, (bottom) MESA-1a and 1b

Just as observed in the baseline tests, there is a less steep SOC drop for MESA-1a after charge at 1C, and a very slight increase in SOC after discharge at 1C (Figure 2.28). MESA-1b shows the same behavior at 1C rate as for baseline – there is an increase in SOC after charge and decrease in SOC after discharge (only for Cycles 2 and 3, SOC constant after discharge for Cycle 1). For discharge, starting SOC for 1a lower, so lower initial power. Discharge power increases with time for 1a. For Cycles 2 and 3, the 1a starting SOC is higher – hence lower starting power for 1a. Charge power increases until the SOC reaches ~ 85 percent, accompanied by a sharp drop in power, with 1b picking up the slack. For Cycle 1, the 1a starting SOC is lower, hence 1a has a higher starting charge power. The ΔT for both 1a and 1b is nearly the same. There are spikes at the end of charge and discharge, which predominantly appears to be caused by 1b. The upper SOC for 1a and 1b was at 90 and 95 percent, respectively, at the end of charge, while the lower SOC limit for 1a was 10 percent and 5 percent for 1b.

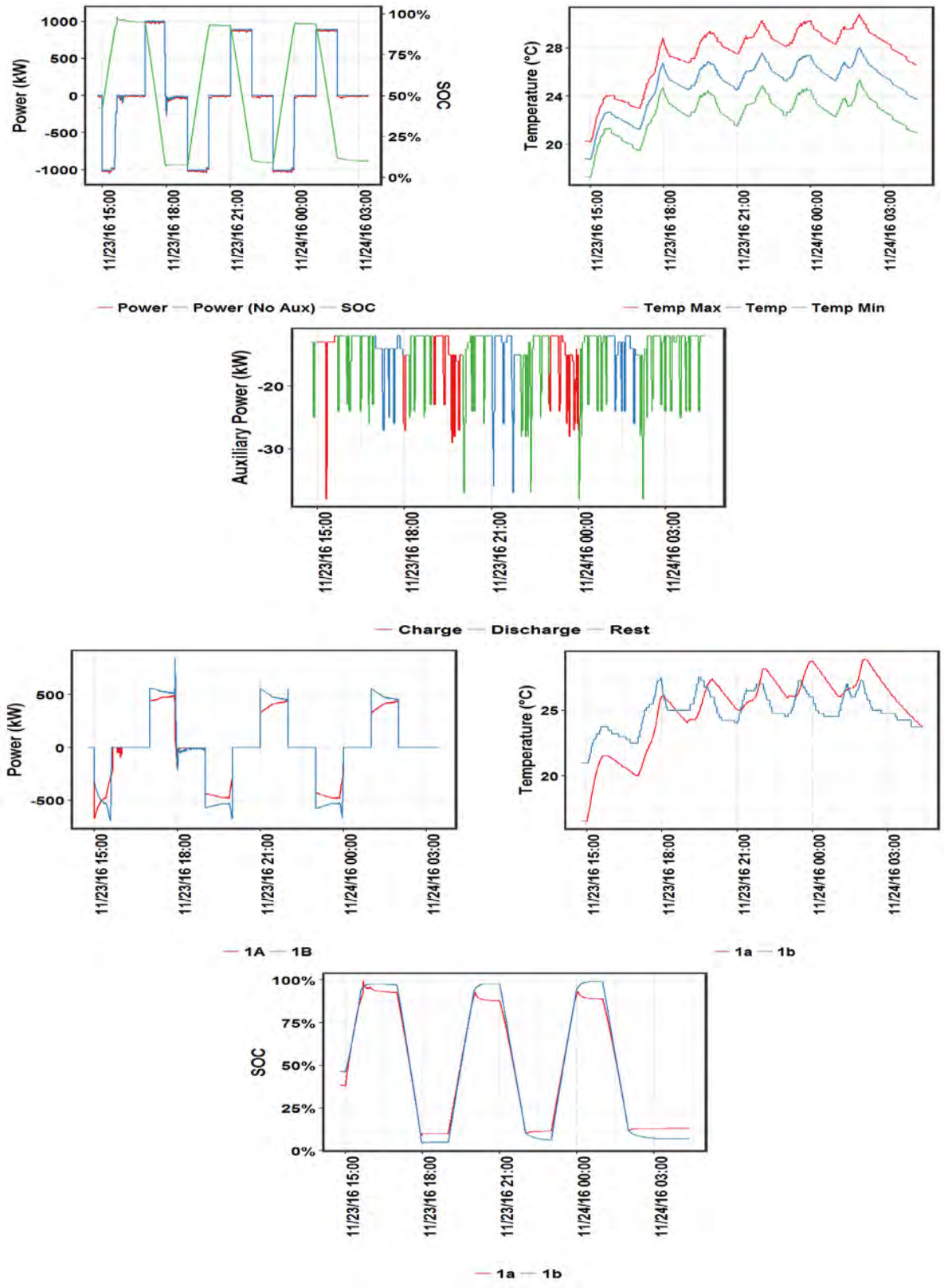

Figure 2.28. Power, SOC, Temperature and Auxiliary Consumption for Capacity Tests Post Cycle 1 at C Rate; (top) BESS, (bottom) MESA-11a and 1b

Results for 2C rate are shown in Figure 2.29. The BESS temperature increases with time, with auxiliary power during discharge being slightly higher. The power flow distribution between MESA-1a and 1b during charge and discharge follows the trend seen in baseline capacity test at 2C rate. During charge, both batteries support 1,000 kW initially, with 1a charge power tapering to 0.3C towards the end of charge. During discharge, 1a supports lower discharge power, which increases with time, while 1b discharge power starts at 1,000 kW and decreases with time. The MESA-1a SOC decreases after charge during rest, and increases very slightly after discharge, while 1b SOC increases by 2 to 4 percent after charge and decreases significantly by 5 to 9 percent after discharge. There is taper during charge related to 1a, while the discharge power remains stable. The change in temperature for 1a is 7 °C, while the 1b change in temperature is 0 °C. The upper SOC for 1a and 1b was at 90 and 95 percent, respectively, at the end of charge, while the lower SOC limit for 1a was 10 percent, and for 1b 5 percent. There are no spikes at the end of charge or discharge; during charge, 1b power is at 1,000 kW, hence it has no room to increase. During discharge, 1a power increases with time, hence there is no need for 1b to take up the required power. For the last cycle, 1a power does taper, and 1b picks up the slack during discharge.

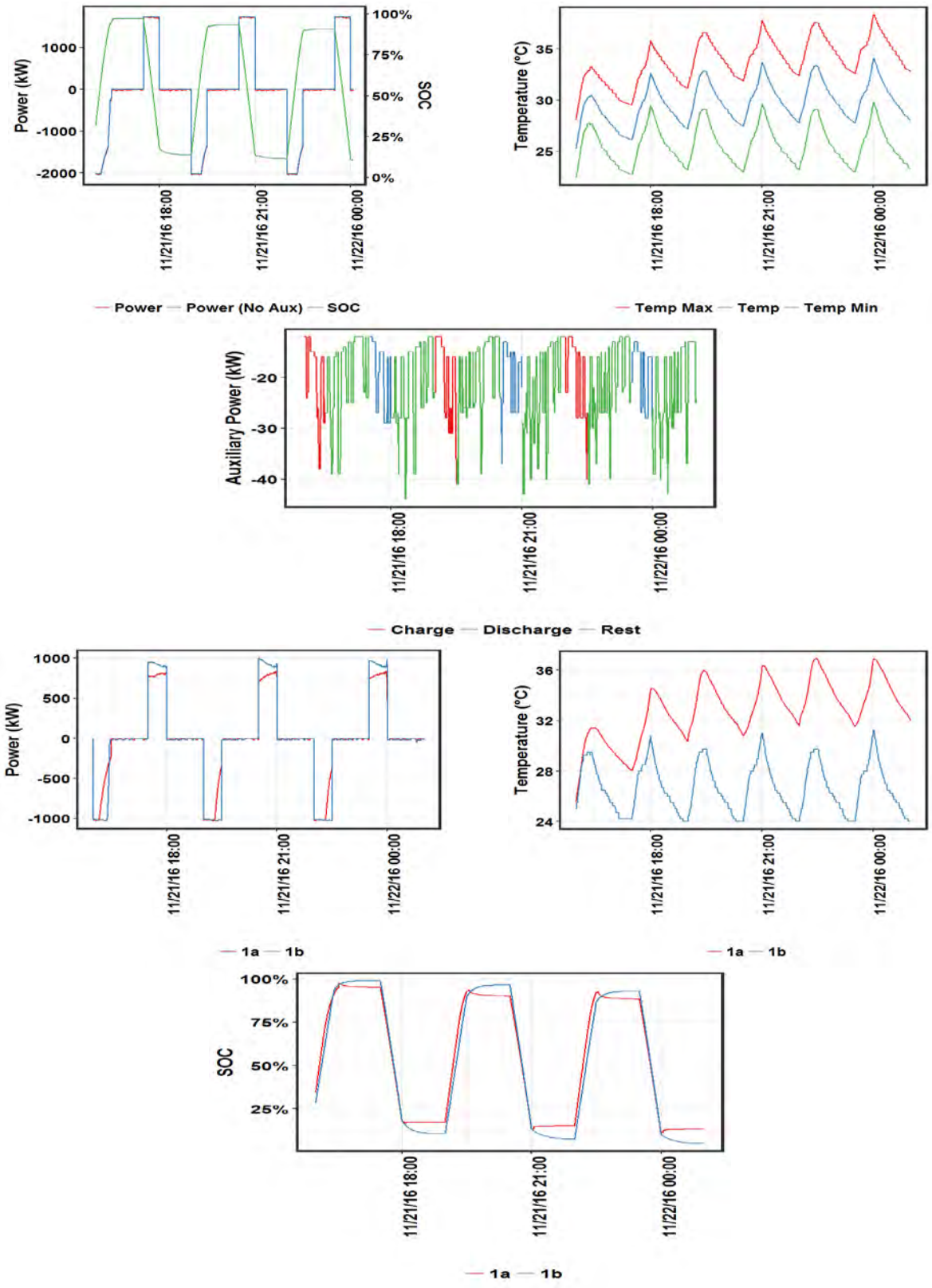

Figure 2.29. Power, SOC, Temperature and Auxiliary Consumption for Capacity Tests Post Cycle 1 at 2C Rate; (top) BESS, (bottom) 1a and 1b

Figure 2.30 shows results for C/4 rate cycling for post Cycle 2. For MESA-1a, the same behavior as for C/4 rate baseline and post Cycle 1 of 1a at the end of charge was observed, with the SOC dropping steeply from 95 percent to 86 percent. The 1b SOC is stable at 95 percent. The starting discharge power for 1a is only 55 percent of starting power for 1b, possibly because 1a starting SOC is lower. MESA-1a ends at 10 percent SOC, while 1b ends at 5 percent SOC. The starting charge power for 1a is 70 percent of 1b charge power, since its starting SOC is higher. The change in temperature for both 1a and 1b was nearly the same. There are spikes at the end of charge and discharge, which predominantly appears to be caused by 1b. The upper SOC for both 1a and 1b was at 95 percent at the end of charge, while the lower SOC limit for 1a was 10 percent, and for 1b 5 percent. There was no tapering of power during charge and discharge.

Similar to Table 2.5 and Table 2.6, the SOC change during rest for 1a and 1b did not correlate with the PCS switching state and the DC current flow through the batteries (data for Post Cycle 1 not shown).

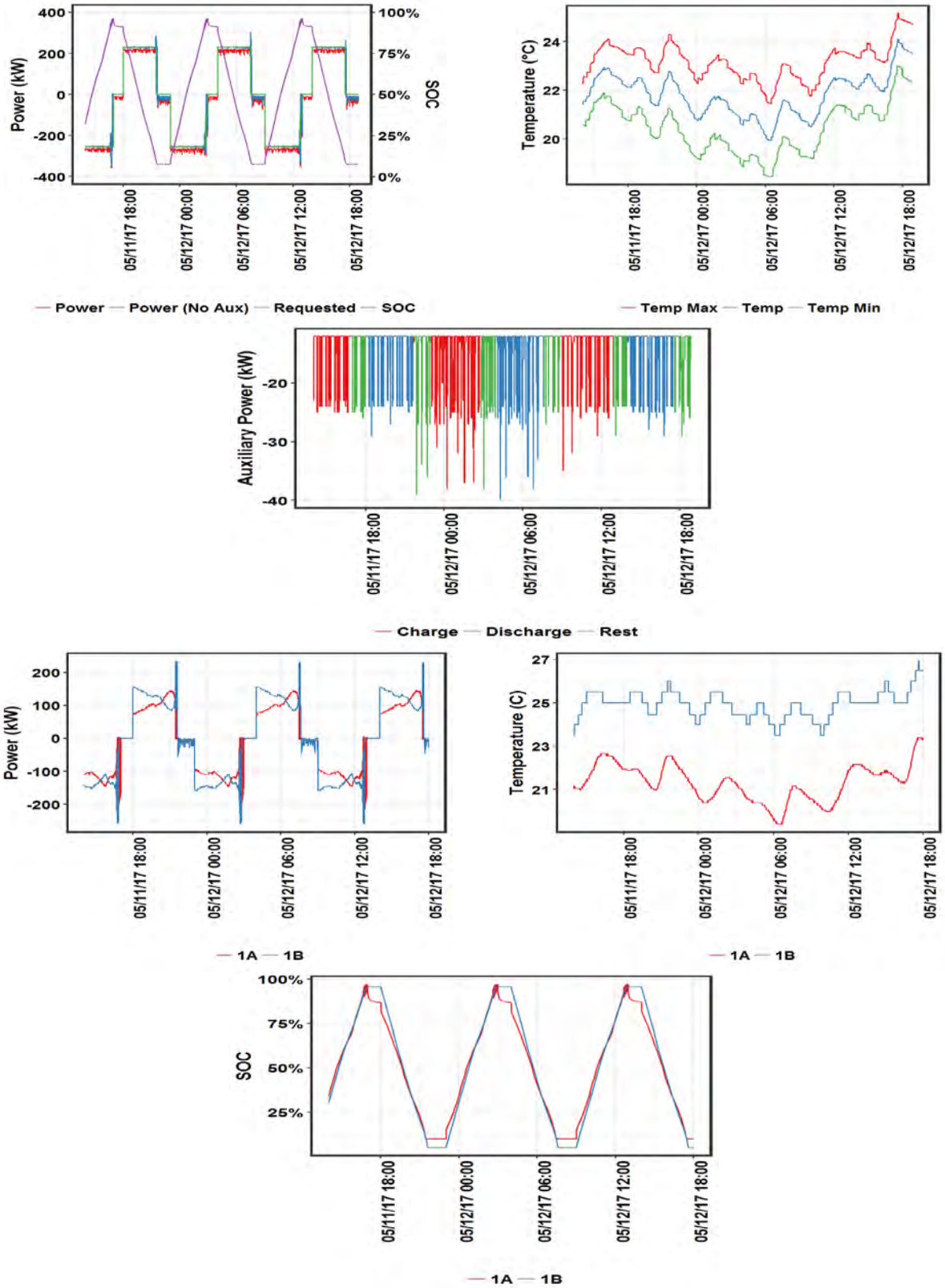

Figure 2.30. Power, SOC, Temperature and Auxiliary Consumption for Capacity Tests Post Cycle 2 at C/4 Rate; (top) BESS, (bottom) MESA-11a and 1b

Figure 2.31 shows results for C/2 rate cycling for post Cycle 2. The starting charge power for MESA-1a is 70 percent of 1b due to its higher starting SOC of 10 percent vs 5 percent for 1b. The SOC at the start of charge is 85 percent for MESA-1a and 95 percent for 1b, resulting in nearly double the starting discharge power for 1b. The change in temperature for both 1a and 1b was nearly the same. The MESA-1a SOC drops at the end of charge from 95 percent to 87 percent, as seen earlier, while the SOC is stable after discharge to 10 percent SOC. For 1b, SOC after charge and discharge is stable at 95 percent and 5 percent, respectively. There are spikes at the end of charge and discharge, which predominantly appears to be caused by 1b after charge, and by both 1a and 1b after discharge. This was the same behavior observed for C/2 rate post Cycle 1. The upper SOC for both 1a and 1b was at 95 percent at the end of charge, while the lower SOC limit for 1a was 10 percent, and for 1b 5 percent. There was no tapering of power during charge or discharge.

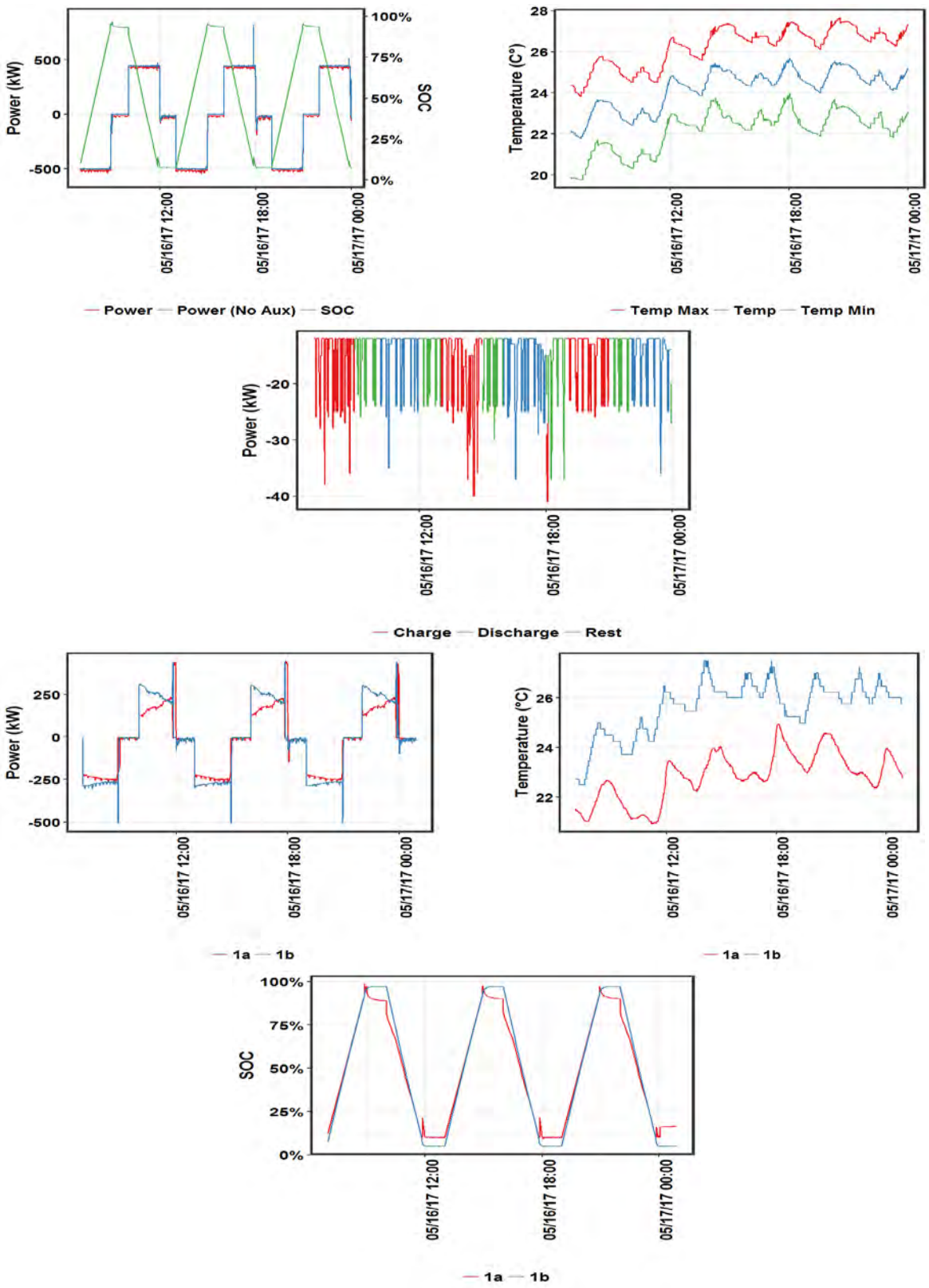

Figure 2.31. Power, SOC, Temperature and Auxiliary Consumption for Capacity Tests Post Cycle 2 at C/2 Rate; (top) BESS, (bottom) MESA-1a and 1b

Just as for the baseline and post Cycle 1 tests, there is a less steep SOC drop for MESA-1a after charge at the 1C rate (Figure 2.32). The end SOC after charge is 90 percent, as opposed to 95 percent for the C/2 and C/4 rates). This appears to indicate that the MESA-1a BMS adjusts charge power such that for charging at < C/2, the reported SOC is 95 percent, while for charging at > 1C rate, the charge power is adjusted to ensure the end SOC does not exceed 90 percent. There is a very slight increase in MESA-1a SOC after discharge at 1C. MESA-1b shows the same behavior as for baseline and post Cycle 1 tests – increase in SOC after charge and decrease in SOC after discharge. The SOC after charge increases to 100 percent during rest, which is cause for concern if real. The SOC at the end of discharge keeps decreasing from 10 percent to 5 percent for 1b, similar to the observation for baseline and post cycle 1C rate tests.

For discharge, the starting SOC for 1a is lower, hence it supports lower initial power. Discharge power increases with time for MESA-1a. At the start of charge, 1a SOC is higher, hence it supports a lower starting power. The charge power for 1a increases until the SOC reaches ~ 85 percent, accompanied by a sharp drop in power, with 1b picking up the slack. In spite of the lower average power through 1a, the change in temperature for 1a is greater than that for 1b, due to a combination of higher internal resistance and thermal management. There are spikes at the end of charge, which is be caused by 1b. The upper SOC for MESA-1a and 1b was at 90 and 95 percent, respectively, at the end of charge, while the lower SOC limit for 1a was 10 percent, and for 1b 5 percent. There is no taper of power for both charge and discharge.

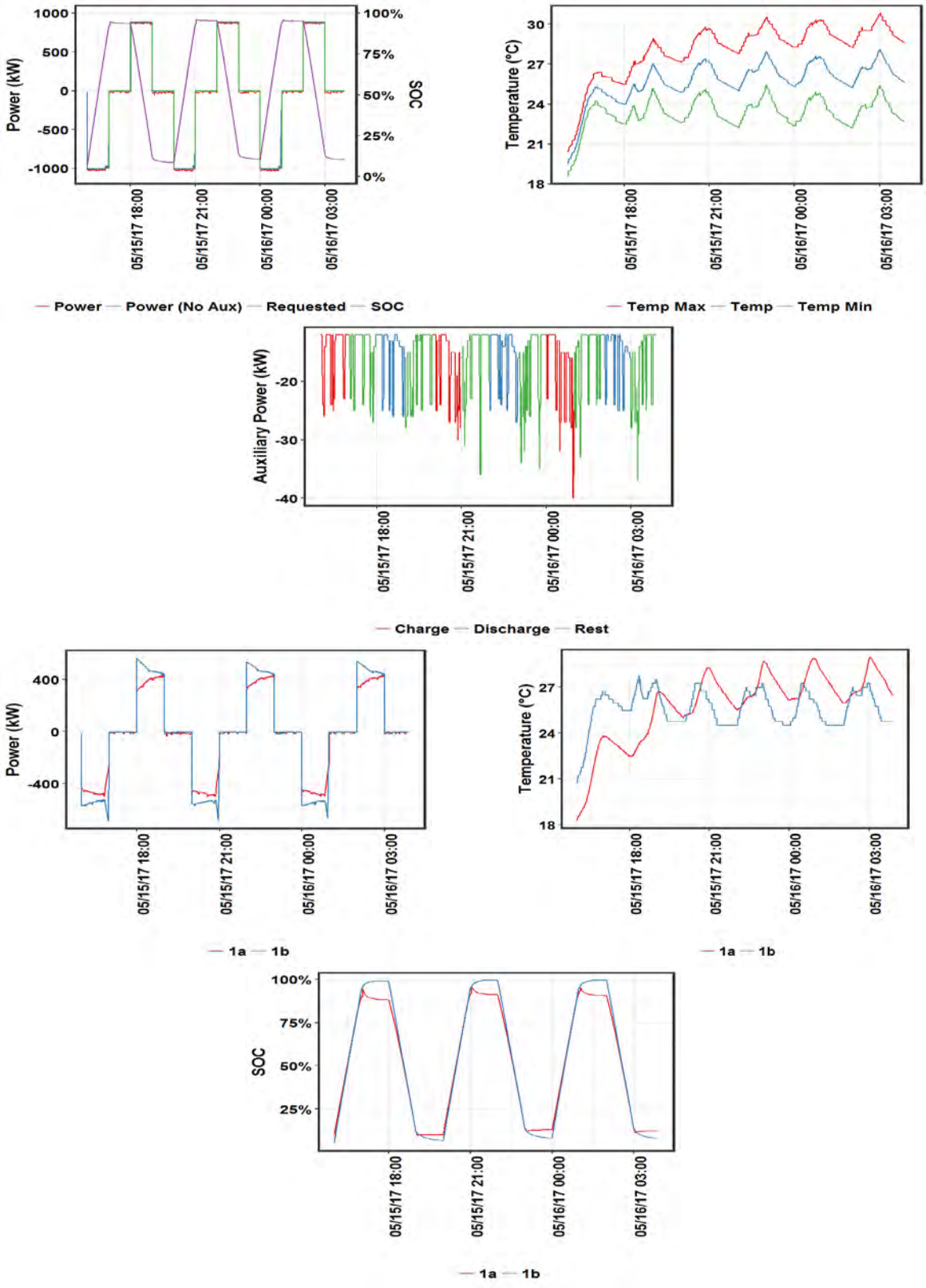

Figure 2.32. Power, SOC, Temperature and Auxiliary Consumption for Capacity Tests Post Cycle 2 at C Rate; (top) BESS, (bottom) MESA-1a and 1b

The same behavior of SOC for MESA-1a and 1b was observed as in baseline test and post Cycle 1 at the 2C rate (Figure 2.33), with slight differences for 1b. These differences include the 1b SOC after charge increases from 87 to 90 percent, after discharge increased in Cycle 1 from 4 to 5 percent, and decreased in Cycle 2 from 7 to 5 percent. The SOC for MESA-1a after discharge stabilizes at 10 percent SOC, and hence increases slightly after discharge. This appears to indicate that the SOC for the battery systems are controlled at the target values during rest by some internal charging or discharging. Further analysis indicated that the SOC behavior during rest for 1a and 1b cannot be easily predicted since it is not clear how the BMS for each battery is programmed.

At the 2C rate, the starting power for both 1a and 1b is the same. This is probably because 1b cannot accept > 1,000 kW charge. Hence, 1a has to pick up the rest. MESA-1a power starts tapering at ~ 55 percent SOC, similar to the baseline and post Cycle 1 test for 2C rate. This is simply due to the differences in BMS for the two systems. MESA-1a temperature increases much more than 1b, in spite of lower average discharge and charge power, due to higher internal resistance and differences in thermal management. During discharge, since the power is less than rated power for the system, starting discharge power for 1a is less than for 1b, since starting SOC for 1b is lower. Discharge power for 1a increases slightly with time, as the 1b SOC decreases. There is taper during charge related to 1a, while the discharge power remains stable. The change in temperature for 1a is 12 °C, while the 1b change in temperature is 2 °C. The upper SOC for 1a and 1b was at 90 and 95 percent, respectively, at the end of charge, while the lower SOC limit for 1a was 10 percent, and for 1b 5 percent.

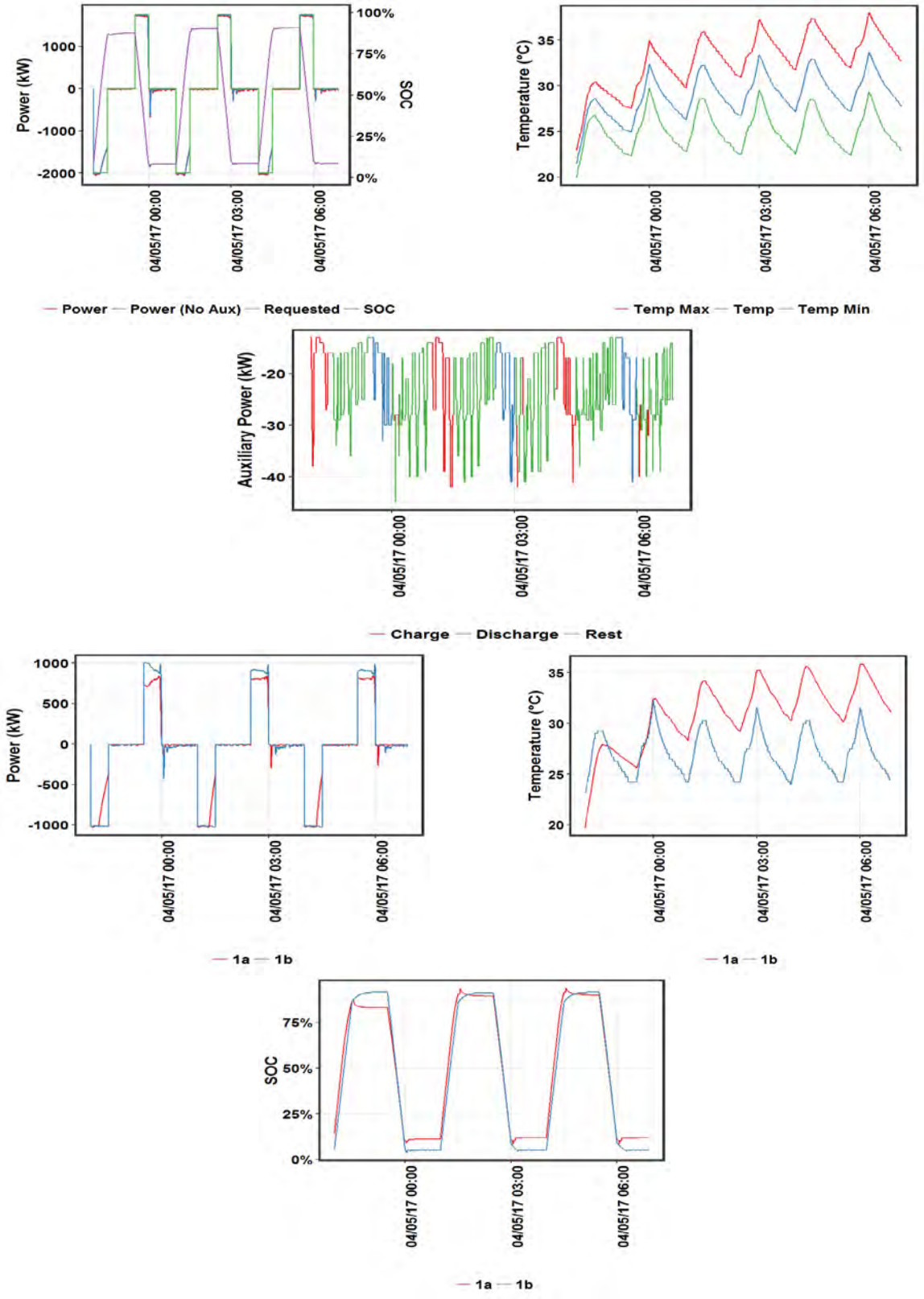

Figure 2.33. Power, SOC, Temperature and Auxiliary Consumption for Capacity Tests Post Cycle 2 at 2C Rate; (top) BESS, (bottom) MESA-1a and 1b

Similar to Table 2.5 and Table 2.6, the SOC change during rest for 1a and 1b did not correlate with the PCS switching state and the DC current flow through the batteries. The average DC current during rest after charge and discharge for the baseline, post Cycle 1 and post Cycle 2 tests is plotted for 1a and 1b in Figure 2.34. Mesa 1a has a discharge current during rest after charge for baseline test and for C/4-C/2 rate tests for post Cycle 2, and a small charge current for post Cycle 1. For rest after discharge, 1a has a discharge current for all tests except C/2 rate for post Cycle 1. The discharge current is higher in magnitude compared to rest after charge. Since 1a SOC decreases during rest after charge and is essentially flat after discharge, the SOC changes are not correlated with the direction and magnitude of DC current during rest. For 1b, the DC current after charge is a very small discharge current, accompanied by a flat SOC profile in the C/4 to C/2 range and a rising SOC profile in the C to 2C range. For rest after charge, a DC charge current flows through 1b, accompanied by a flat profile in the C/4 to C/2 range and a decreasing profile in the C to 2C rate.

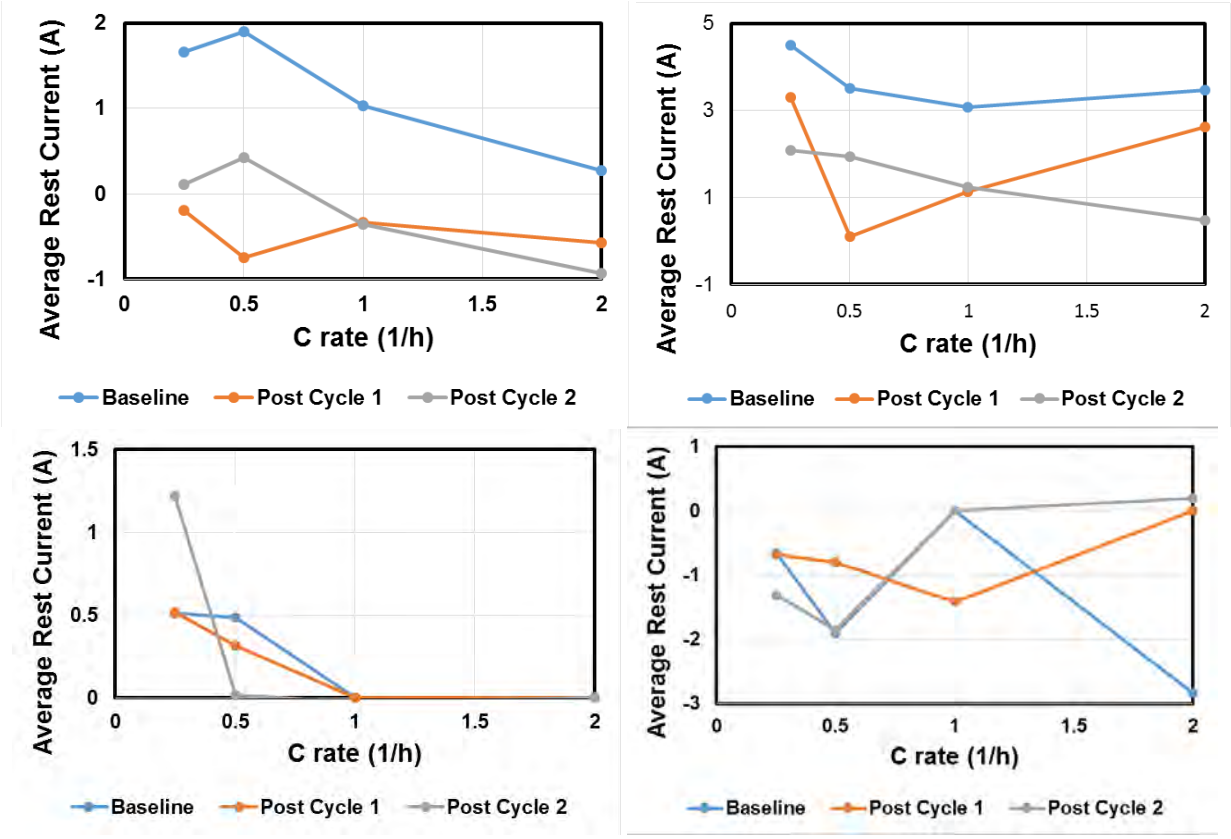

Figure 2.34. Average DC Current during Rest (left) after Charge; (right) after Discharge; (top) 1a, (bottom) 1b

Li-ion cell open circuit voltage (OCV) has a negative temperature coefficient. After charge or discharge, as the cell cools, the OCV goes up, and this is reflected in the SOC if SOC measurement is based on OCV. Hence, we expect to see an increase in SOC during rest after charge or discharge, especially at high rates. However, the natural relaxation of the open circuit voltage to lower values after charge and higher values after discharge is expected to override the temperature effect. Hence, we expect to see the SOC decrease during rest after charge and increase after discharge. MESA-1a SOC increases slightly after discharge and decreases after charge, while the MESA-1b SOC increases after charge and decreases after discharge indicates that the SOC measurement algorithm for these batteries is different. The MESA-1a SOC drop after charge is greatest for C/4 and C/2 rates. Battery SOC also reaches high levels at these rates, whereas at the 2C rate, the SOC tops out at ~ 85 percent, leaving less room to drop. It is possible

that for 1a, during operation, the SOC is calculated by coulombic counting. This is consistent with the fact that the end SOC after charge increases with decreasing C rate.

At the end of charge, as the OCV relaxes, the BMS incorporates a correction for the SOC based on the OCV, possibly without applying a temperature adjustment. For C/4 and C/2 rate charge and the first cycle of C rate charge, the end SOC was 95 percent. For the first cycle of 1C rate charge, the starting SOC for 1a was lower, with a higher initial charge power. As charge proceeds, the 1a power decreases to C/4 rate, resulting in similar behavior as C4 rate charge. For the 2C rate, the end SOC for 1a was lower at ~ 85 percent. During rest, the OCV drops rapidly. However, since the end SOC after high rate charge was low, this rapid decline in OCV does not result in a rapid decline in SOC. On the other hand, for low rate charge, the decline in OCV truly reflects the decline in SOC, since end SOC after charge was 95 percent. For MESA-1b, at low rates, the SOC is stable. This is because at low rates, the coulombic counting is probably more accurate, and the battery reported SOC is the correct SOC. At high rates, the SOC increases with time during rest after charge to its target SOC of 95 percent. It does not seem plausible that the BMS undercounts the charge Ah during charge at 1C and 2C. It is possible that there is some power exchange between 1a and 1b at the end of charge to bring their SOCs to their respective targets of 90 percent and 95 percent. Similarly, at the end of 1C and 2C rate discharge, MESA-1b SOC decreases during rest and ends at its target 5 percent SOC. The MESA-1a SOC increases slightly and ends at its 10 percent target SOC. Again, there may be power exchange between 1a and 1b to enable each to reach its target SOC.

Note that for all capacity tests, the PCS was in switched mode after discharge as seen from the reactive power flow during rest after discharge for the BESS and for both 1a and 1b, whereas during rest after charge, the PCS for the BESS and both 1a and 1b are not in switched mode (Figure 2.35). This could be a reason for SOC to continue to drop for 1b after high C rate discharge. No definitive conclusions can be drawn from the available information on why the SOC relaxes in certain ways during rest after charge or discharge at various rates for 1a and 1b. Note that the reactive power flow for 1a and 1b was always in the 5 to 20 kvar range, regardless of whether BESS is in the charge, rest (after discharge)or discharge mode, while the reactive power was 0 during rest after charge. While it is also possible that there could be DC discharge power flow from 1b to get the SOC to the 5 percent target level, this does not appear to be the case from Figure 2.34.

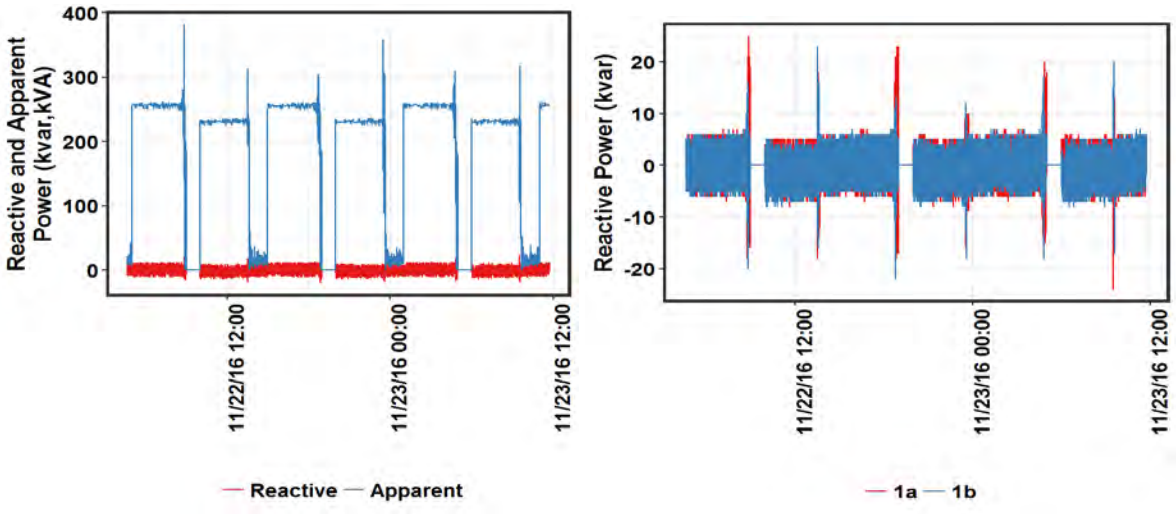

Figure 2.35. Reactive and Reactive Power Flow during C/4 rate Post Cycle 1 Capacity Test for BESS (left), Reactive Power Flow for MESA-1a and 1b (right)

Table 2.16. Comparison of Baseline Tests and Post Cycle 1 and 2 Tests

Type	Disch. Power (kW)	Charge Energy No Rest (kWh)	Charge Energy (kWh))	Disch. Energy (kWh)	Charge Energy No Aux (kWh)	Disch. Energy No Aux (kWh	RTE (%)	Cum. RTE (%)	RTE No Rest (%)	Cum. RTE No Rest (%)	RTE No Aux (%)	Cum. RTE No Aux (%)	Aux Charge Power (kW)	Aux Disch. Power (kW)
Baseline	230	1088	1142	739	1018	843	66.9	66.2	*73.6*	70.2	82.5	87.8	20.7	21.0
Baseline	445	1026	1089	786	1000	880	77.0	77.7	86.0	81.9	88.5	92.9	21.2	20.3
Baseline	885	1008	1051	829	984	895	83.0	82.9	*86.3*	86.5	90.9	90.8	23.5	22.4
Baseline	1750	966	1021	799	962	837	80.7	81.9	83.0	86.7	88.5	89.0	25.8	27.1
Post Cycle 1	230	1058	1105	781	1013	838	71	71	74	74	83	83	15.2	15.3
Post Cycle 1	445	1007	1057	847	992	876	80	80	84	84	88	88	15.0	14.2
Post Cycle 1	885	1027	1074	896	1017	912	83	83	87	87	90	90	15.9	15.4
Post Cycle 1	1750	982	1026	856	972	856	83.5	83.7	81	87.4	89.1	89.3	20.0	19.5
Post Cycle 2	230	1049	1123	770	1023	824	68.6	69.7	73.5	73.5	80.6	81.3	14.8	14.9
Post Cycle 2	445	1022	1064	855	1001	886	80.4	80.5	83.7	83.9	88.5	88.6	16.3	15.3
Post Cycle 2	885	1003	1035	879	988	895	84.9	84.9	87.7	87.7	90.6	90.6	16.5	15.1
Post Cycle 2	1750	969	1021	842	966	853	82.5	82.4	86.9	87	88.3	88.3	20.8	21.0

* High charge energy due to inclusion of small portion of next charge cycle. RTE accounts for this using estimated discharge energy to initial SOC.

Table 2.16, Table 2.17, and Figure 2.45 compare baseline capacity with post Cycle 1 and 2 capacity test results. For the post cycling run, RTE increased at the C/4 rate for both post Cycle 1 and post Cycle 2 (Table 2.16). This can be attributed to auxiliary power playing a greater role at low power; the auxiliary power for post Cycle 1 and post Cycle 2 runs were lower than experienced during baseline testing. In the C/2-2C range, baseline RTE was lowest. When the rest period was excluded, the baseline RTE was similar to post Cycle RTE in the C-2C range. Excluding auxiliary load, the RTE for all three cases were nearly the same across the range of C rates.

At 2C rate, the post Cycle 2 RTE was 5.2 percentage points higher than baseline, possibly indicating the positive conditioning effect of battery use. Once auxiliary losses are excluded, the gap in RTE decreases. Table entries in italics correspond to runs for which the charge power during rest was missing.

Note that the first run for post Cycle 2 at 2C was excluded since the temperature was 3.5 °C lower than for Runs 2-4, with an RTE about 8 percentage points lower. Hence, there are lots of variables such as SOC range, battery temperature, auxiliary load consumption (which may be related to ambient temperature) that affect battery performance.

To extract the degradation or improvement in performance for post Cycle 1 and post Cycle 2, a regression analysis was performed using power, temperature and the type of test (baseline, post Cycle 1, post Cycle 2) as regressors. By including power and temperature as regressors, the effect of the test type (post Cycle 1 or post Cycle 2) was determined (Table 2.18). The corresponding p values are also given. The lower the p value, more reliable the effect, with p values < 0.05 showing high reliability.

The effect of the test type on auxiliary power consumption, for example, is significant, and has high reliability, with a p value < 1.5×10^{-8} for auxiliary power consumption during charge and discharge. Both post Cycle 1 and post Cycle 2 tests have a 6.5 kW lower auxiliary consumption, which affects the RTE. All reliable p values are shown in italics, which shows the effect of ambient temperature on auxiliary power consumption.2. The RTE post Cycle 1 is higher than baseline, mainly due to lower auxiliary power consumption, which results in 12.6 kWh lower charge energy and 3.3 kWh higher discharge energy. When auxiliary consumption is ignored, the charge energy increases by 1.8 kWh, and the discharge energy decreases by 8.7 kWh, resulting in a lower RTE. For post Cycle 2, there is a 25 kWh decrease in charge energy and 7.7 kWh increase in discharge energy, resulting in increase in RTE. When auxiliary load is excluded, the charge energy decrease is 7.9 kWh while discharge energy decrease is 3.6 kWh, resulting in a slight increase in RTE over baseline. Hence, accounting for the cold ambient conditions for post Cycle 1, it appears the BESS has improved slightly during the one year of testing.

Table 2.17. Change in Performance Metrics with Respect to Baseline

	Percent Change*											
Test	Discharge Power (kW)	Charge Energy No Rest (kWh)	Discharge Energy No Rest (kWh)	Charge Energy (kWh)	Discharge Energy (kWh)	Charge Energy No Aux (kWh)	Discharge Energy No Aux (kWh)	RTE (%)	RTE No Rest (%)	RTE No Aux (%)	Aux Chg Power (kW)	Aux Dis Power (kW)
Post Cycle 1	230	-2.89	1.73	-2.89	2.17	-0.86	-0.65	3.83	*3.83*	0.17	-5.50	-5.60
	445	0.30	1.91	0.78	1.97	1.51	0.41	1.05	0.45	-0.95	-6.20	-6.10
	885	0.16	1.36	1.09	0.66	0.96	-0.18	-0.40	0.50	-1.05	-7.50	-7.00
	1750	1.01	-1.54	-1.42	-1.54	1.26	-2.22	-0.10	-2.03	-2.87	-5.80	-7.60
Post Cycle 2	230	-4.68	0.25	-4.68	0.81	-2.15	-2.13	4.13	*4.13*	-0.03	-5.90	-6.10
	445	2.11	2.48	2.11	2.54	3.04	1.27	0.35	-0.65	-1.55	-4.90	-5.00
	885	-0.99	0.02	-0.99	-0.66	-0.21	-1.35	0.30	*0.30*	-0.95	-7.00	-7.30
	1750	-1.80	2.46	-3.54	2.46	-1.58	2.09	5.20	3.77	3.23	-5.00	-6.10

* For auxiliary power, it is simply the change in auxiliary power in kW for charge and discharge.

Table 2.18. Degradation or Improvement in Performance after Cycle 1 and Cycle 2

Variable	Post Cycle 1 Effect	Post Cycle 2 Effect	Post Cycle 1 p Value	Post Cycle 2 p Value
Charge Energy No Rest (kWh)	-9.2	-19.9	1.2E-01	1.1E-03
Discharge Energy No Rest (kWh)	3.3	7.7	6.5E-01	2.9E-01
Charge Energy (kWh)	-12.6	-24.9	3.7E-02	7.4E-05
Discharge Energy (kWh)	3.3	7.7	6.5E-01	2.9E-01
Charge Energy No Aux (kWh)	1.8	-7.9	7.2E-01	1.1E-01
Discharge Energy No Aux (kWh)	-8.7	-3.6	2.4E-01	6.2E-01
RTE	0.013%	0.028%	1.7E-01	4.1E-03
RTE No Rest	0.011%	0.024%	2.7E-01	1.3E-02
RTE No Aux	-0.011%	0.003%	2.6E-01	7.0E-01
Aux Chg Power (kW)	-6.4	-5.6	1.4E-09	*1.5E-08*
Aux Dis Power (kW)	-6.6	-6.1	7.4E-14	*4.4E-13*

Auxiliary consumption was nearly constant up to the 1 C rate, and increased at > 1C rate for both charge and discharge. The auxiliary power for charge and discharge was nearly equal for all C rates up to and including 1C, while at 2C, auxiliary consumption was higher for both charge and discharge. Additionally, for the baseline case, performed during summer 2016, the auxiliary consumption during discharge was greater than that during charge. This indicates that the exothermic reaction during discharge coupled with I^2R ohmic losses during summer at 2C correspond to greater auxiliary consumption during summer. For all C rates, and for both charge and discharge modes, auxiliary consumption was lower for post Cycle 1 and post Cycle 2 due to the cooler weather by 5 to 7 kW. Figure 2.36 shows auxiliary power consumption for charge and discharge for baseline, post Cycle 1 and post Cycle 2 capacity tests. The plots for 1a and 1b are also shown. No significant difference is seen for auxiliary consumption for 1a and 1b. Note that all plots are presented as a function of discharge power, whether the operating mode is charge or discharge. The relationship between charge and discharge power is shown in Figure 2.37.

The charge energy for baseline and post Cycle 1 and Cycle 2 were compared for various power levels in Figure 2.38. The charge energy for post Cycle 2 was the lowest across all power levels and did not depend too much on power level. The charge energy for post Cycle 1 had a similar low dependence on power level, and was higher than post Cycle 2 for all power levels. The baseline charge energy went through a minimum at 1,000 kW. The main difference in the shapes of the baseline vs post cycle charge energy curves is the higher auxiliary consumption contributing to higher baseline charge energy at C/4, leading to a local minimum at 1,000 kW. While for post Cycle 1 and post Cycle 2, the curve is flat to slightly increasing with power, since auxiliary losses at C/4 is a much smaller portion of total charge energy. As power increases, the still lower auxiliary contribution is countered by higher polarization losses.

Once auxiliary consumption was removed, the charge energy increases with increasing power, since higher power is associated with greater polarization. Interestingly, the charge energy appears to have plateaued at 1,000 kW, possible because of higher operating temperature at 2,000kW countering the over-potential associated with higher current. For discharge, the energy with auxiliary consumption peaks at slightly greater than 1C rate, while it peaks at slightly less than 1C rate when auxiliary consumption is excluded. This shows that form an electrochemical efficiency point of view, the sweet spot is slightly less

than 1C, whereas, including auxiliary consumption pushes the maximum to higher power levels where auxiliary consumption is a lower percentage of total power flow.

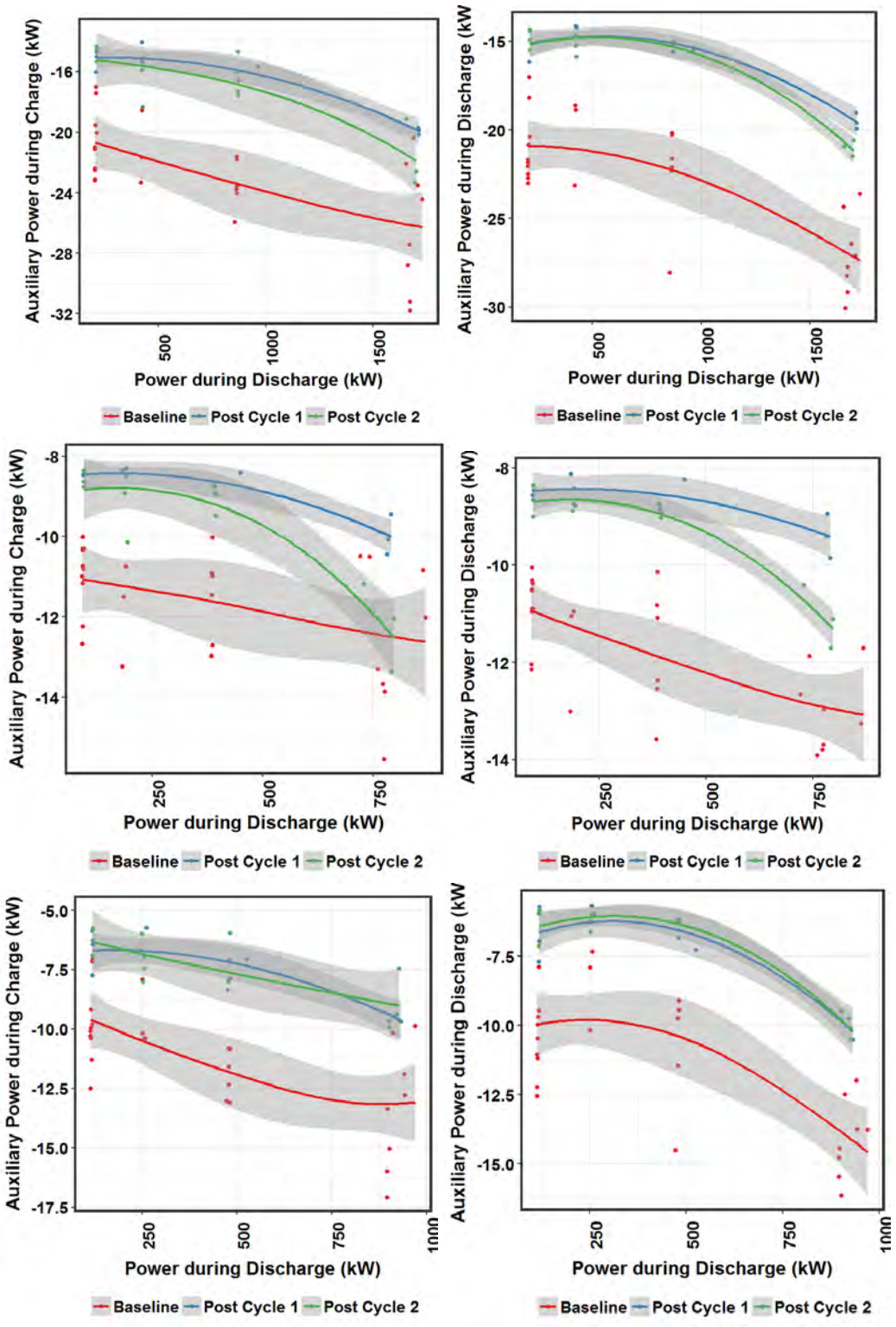

Figure 2.36. Auxiliary Power Consumption during Charge (l) and Discharge (r) for Baseline and Post Use Case Tests; (top) BESS, (middle) 1a, (bottom) 1b

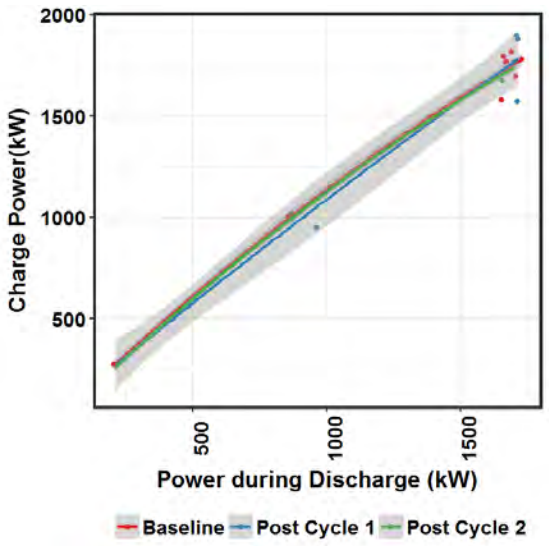

Figure 2.37. Relationship between Charge and Discharge Power Levels for BESS

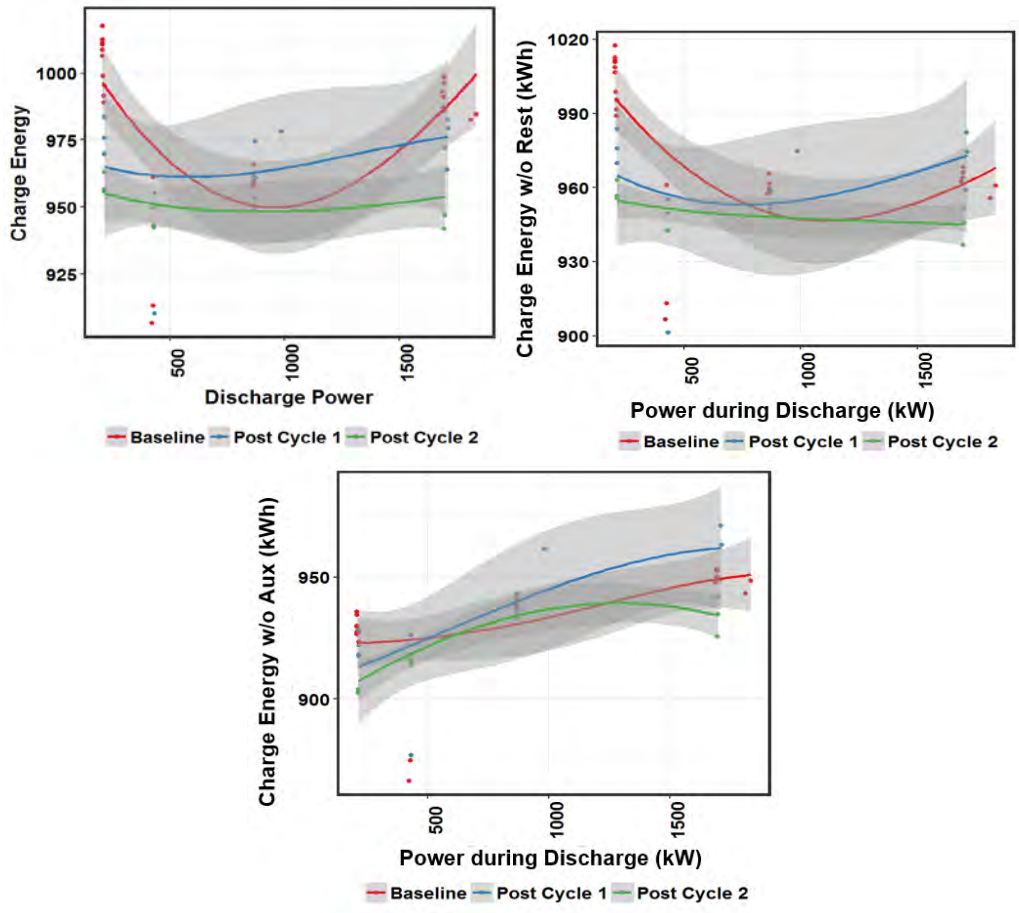

Figure 2.38. Charge Energy at Various Power Levels for Baseline and Post Cycle 1 (left) Includes Rest and Aux, (right) Excludes Rest, (bottom) Excludes Aux

The corresponding plots for 1a and 1b are shown in Figure 2.39 and Figure 2.40 respectively.

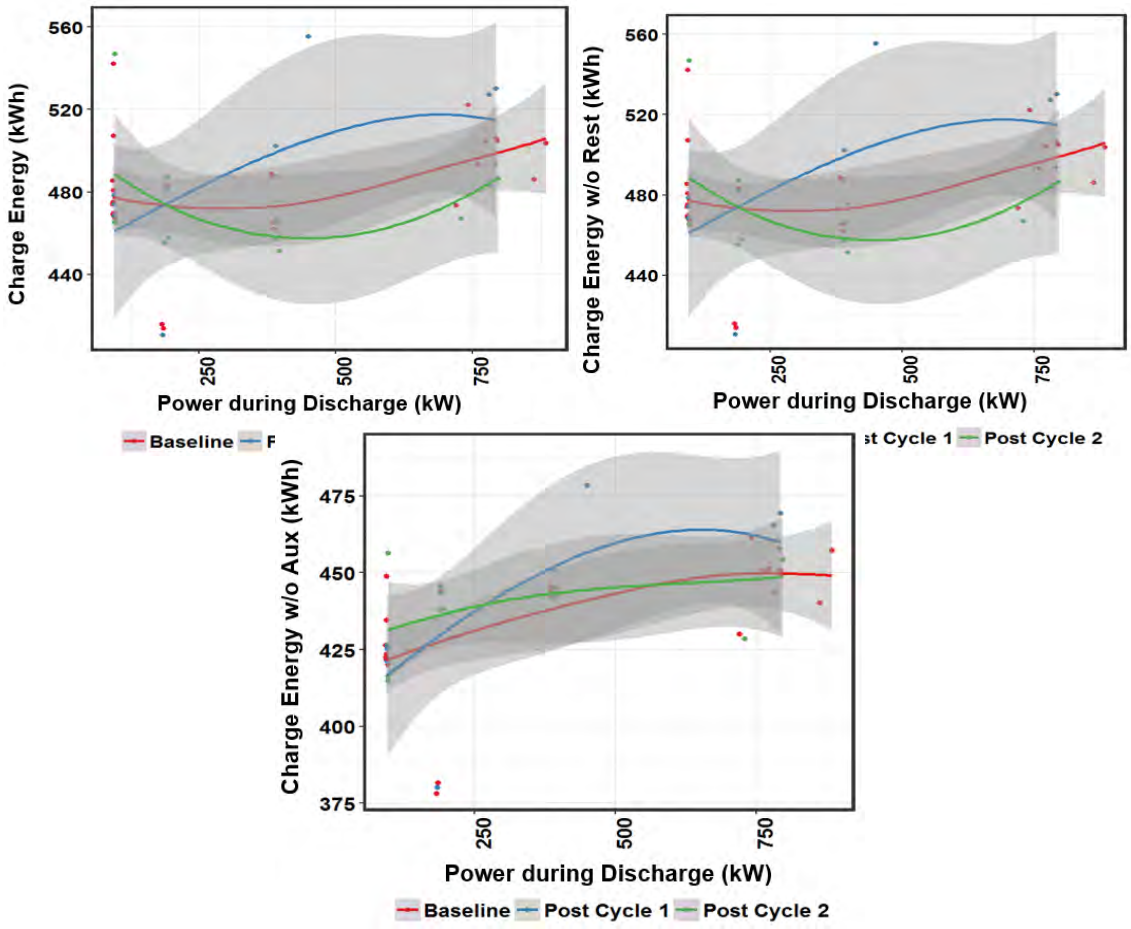

Figure 2.39. Charge Energy at Various Power Levels for MESA-1a Baseline and Post Cycle 1 (left) Includes Rest and Aux, (right) Excludes Rest, (bottom) Excludes Aux

The minimum in charge energy at 1,000 kW for baseline with auxiliary load is due to a combination of steep decrease in charge energy from 225 kW to 600 kW for MESA-1b and a slight increase for the same power range for MESA-1a. When auxiliary load is excluded, the behavior of the BESS appears to be dominated by MESA-1a, with charge energy increasing slightly with power for baseline and post Cycle 2, while for MESA-1b, there is a maximum at 600 kW for baseline and post Cycle 2 tests. For baseline and post Cycle 2, 1a still dominates the BESS charge energy versus power shape, with charge energy increasing with power. This indicates that the higher internal resistancve of 1a dominates charge behavior. The shape of 1a and 1b is nearly the same for post Cycle 1 tests, especially when auxiliary load is excluded, with charge energy increasing with power, possibly due to the cold ambient conditions resulting in high internal resistance.

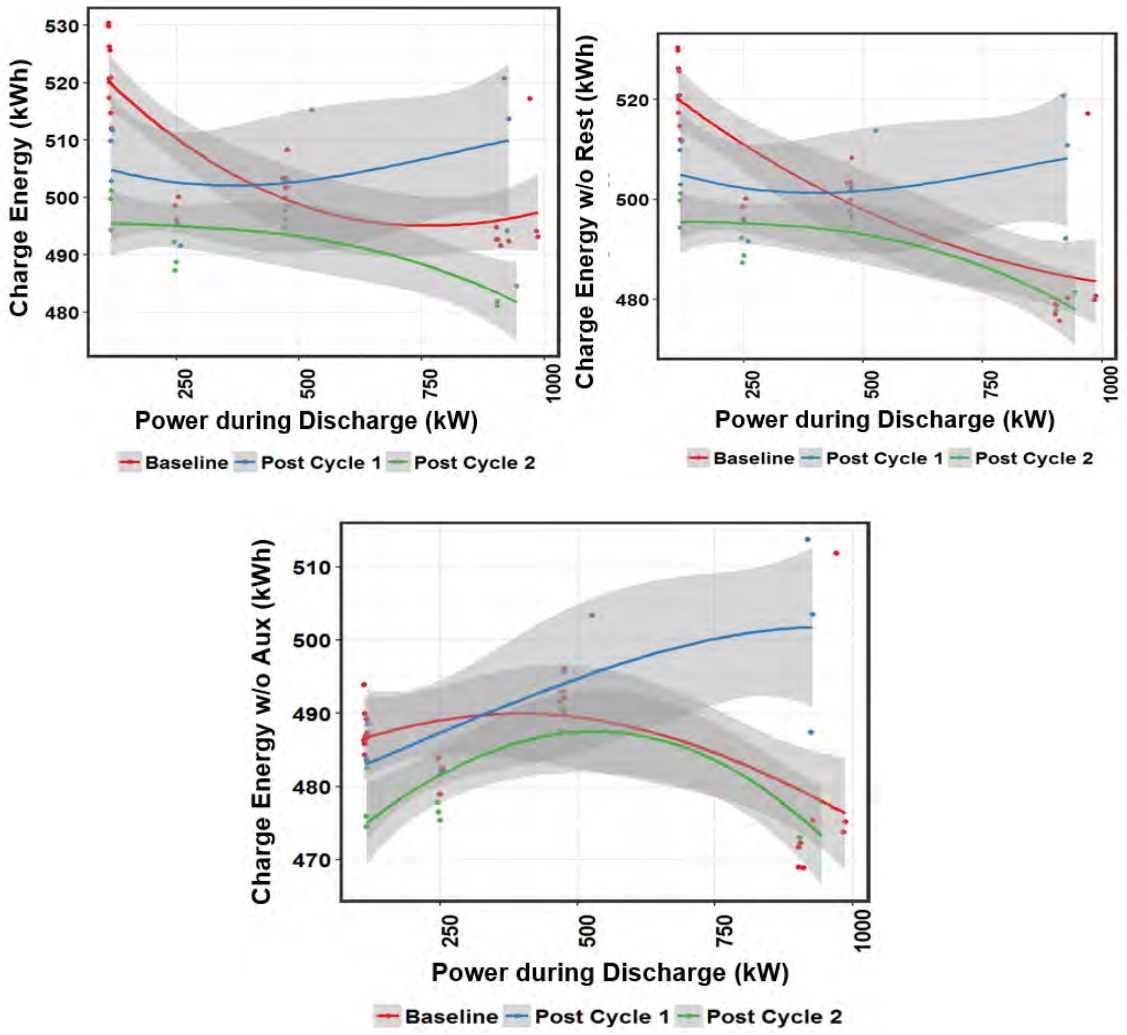

Figure 2.40. Charge Energy at Various Power Levels for MESA-1b Baseline and Post Cycle 1 (left) Includes Rest and Aux, (right) Excludes Rest, (bottom) Excludes Aux

The average temperature for the BESS, 1a, and 1b batteries are provided in Figure 2.41. As expected, the average temperature increases with increasing discharge power, with the temperature for 1a higher than 1b at the 2C rate.

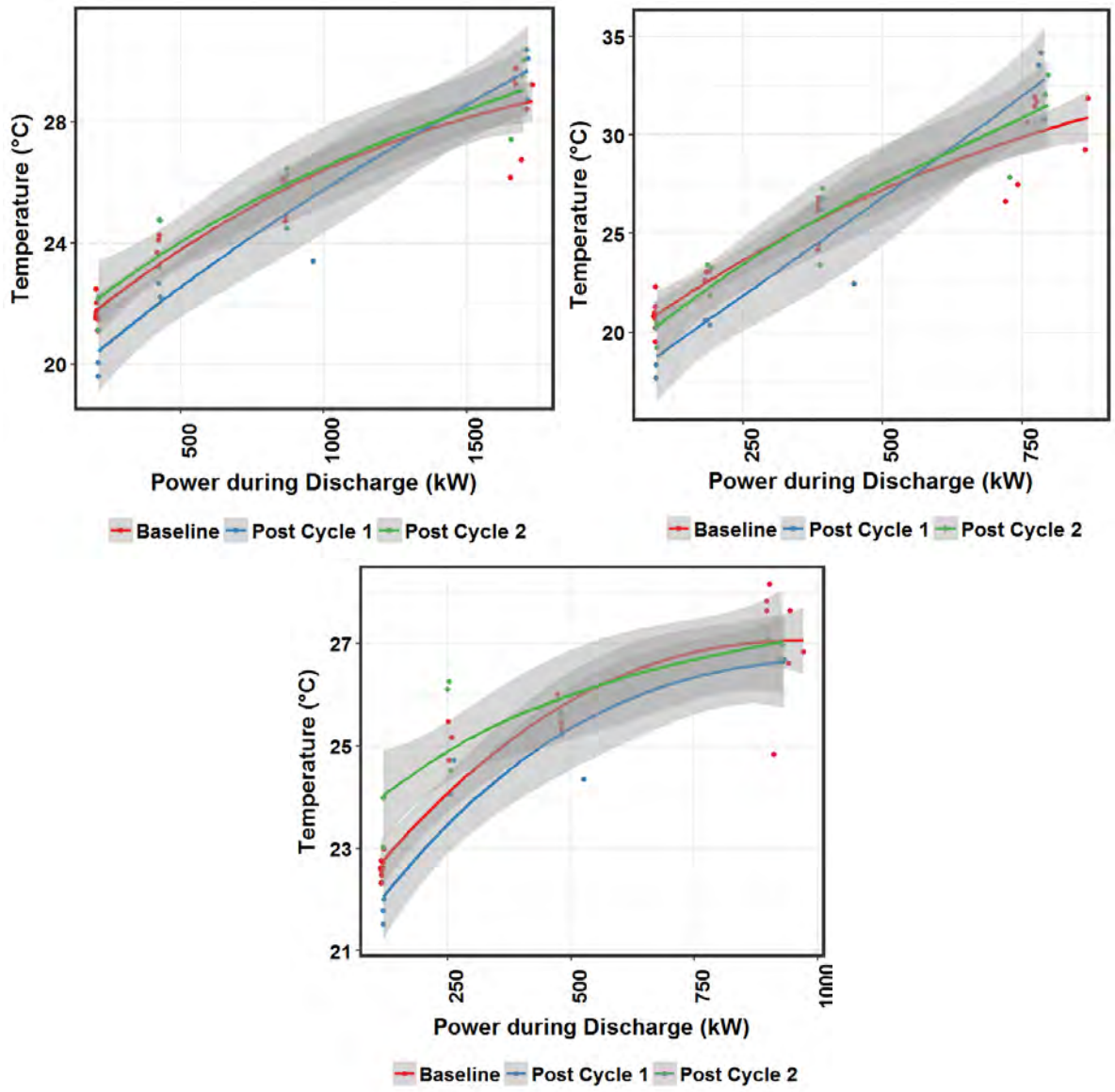

Figure 2.41. Average Temperature for the BESs (top left), 1a (top right) and 1b (bottom) at Various Power Levels

The discharge energy increases with cycling when measured at the grid up to the C rate (Figure 2.42). At 2C rate, post Cycle 1, done in winter, has the lowest discharge energy, while post Cycle 2 has the highest discharge energy. However, when measured at the inverter, excluding auxiliary loads, the discharge energy actually decreases very slightly with cycling up to the C rate. At the C rate and 2C rate, as expected, post Cycle 1 test gives the lowest discharge energy due to low temperature. Post Cycle 2 has the best performance at the 2C rate. This appears to indicate that there is no measurable degradation with cycling for the BESS.

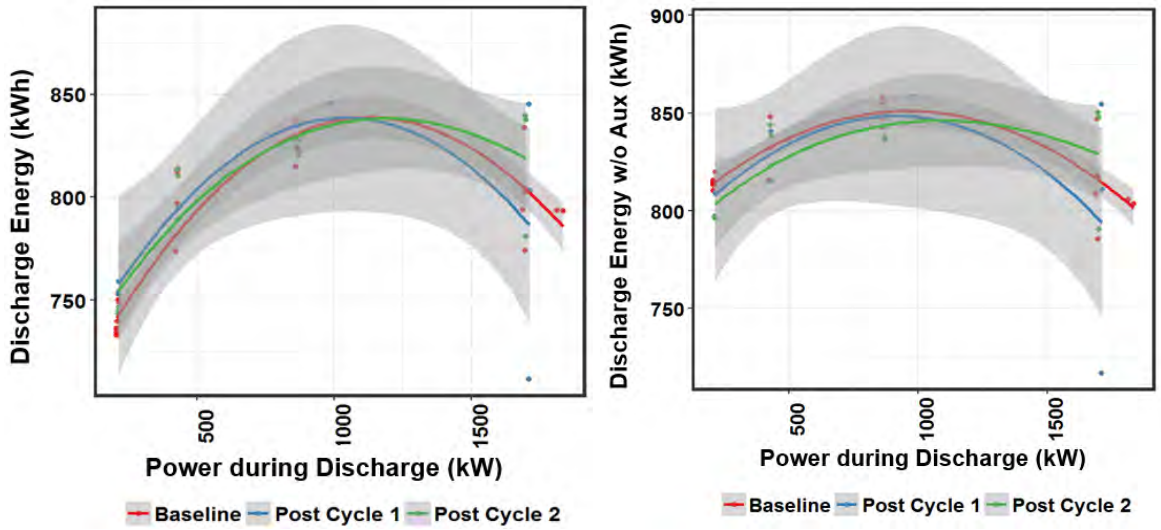

Figure 2.42. Discharge Energy at Various Power Levels for Baseline and Post Cycle 1 Tests (a) Includes Auxiliary Loads, (b) Excludes Auxiliary Loads

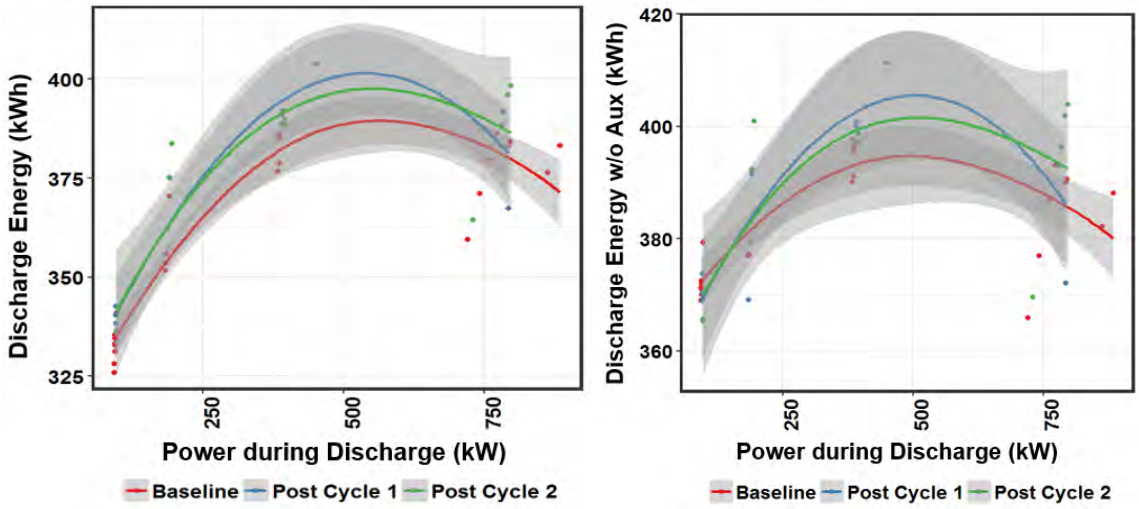

Figure 2.43. Discharge Energy at Various Power Levels for MESA-1a for Baseline and Post Cycle 1 Tests (a) Includes Auxiliary Loads, (b) Excludes Auxiliary Loads

At a fixed power, 1b has a greater average power compared to 1a. This is also reflected in the higher discharge energy for 1b compared to 1a (see Figure 2.43 and Figure 2.44). For example, for post Cycle 2 testing at 2C rate, the energy delivered by 1b is 445 kWh at 910 kW, while 1a delivers 395 kWh at 790 kW. As seen later, for all power ranges, more power flows through 1b than 1a during charge and discharge. Due to the constraint of a minimum of 15 minutes per operation step, the SOC range cannot be tightly controlled. But the SOC range for 1b was typically about 5% wider than that for 1a. It was able to sustain higher power levels at low SOC for discharge and high SOC for charge, probably due to the BMS, as opposed to the 1E-1C controller actions. The discharge energy as a function of discharge power is controlled by 1a, which has a maximum energy at the 1C rate, while 1b energy increases with power. For post Cycle 1 discharge, both 1a and 1b have a maximum at 1C rate, again reflecting the effect of cold ambient conditions (higher internal resistance leads to lower energy content at 2C rate for both 1a and 1b).

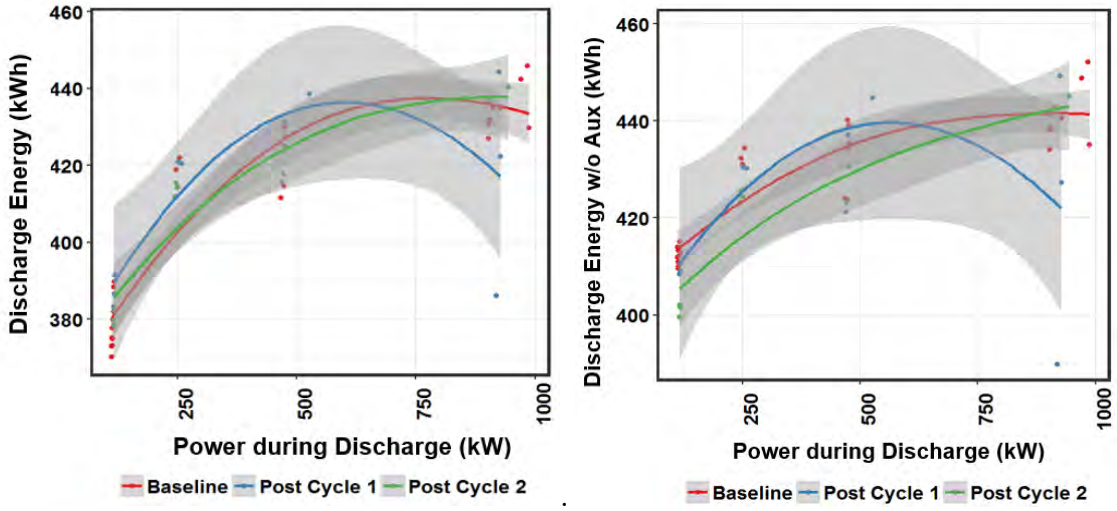

Figure 2.44. Discharge Energy at Various Power Levels for MESA-1b for Baseline and Post Cycle 1 Tests (left) Includes Aux, (right) Excludes Aux

The BESS RTE goes theough a maximum at discharge power of 1,000 kW for the baseline, post Cycle 1 and post Cycle 2 when auxilary load is included (Figure 2.45). The same behavior is seen for 1a. But the RTE increases with power for 1b. When auxiliary load is excluded, the behavior of all 3 (baseline, post Cycle 1 and post Cycle 2) is nearly the same up to 1000 kW. However, the RTE for MESA-1b increases all the way to 2C rate, while BESS and MESA-1a RTE decrease past 1C rate. This indicates that MESA-1b performs better at high rates.

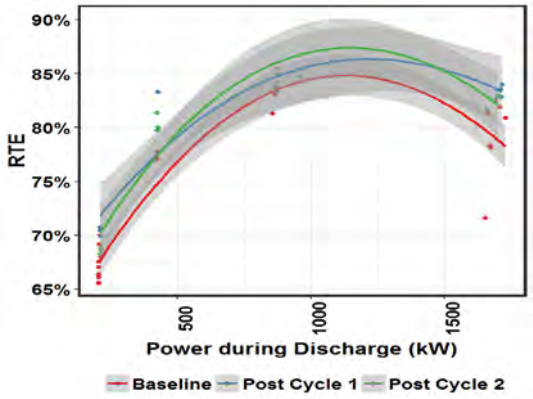
RTE
90%
85%
80%
75%
70%
65%
500
1000
1500
Power during Discharge (kW)
Baseline
Post Cycle 1
Post Cycle 2

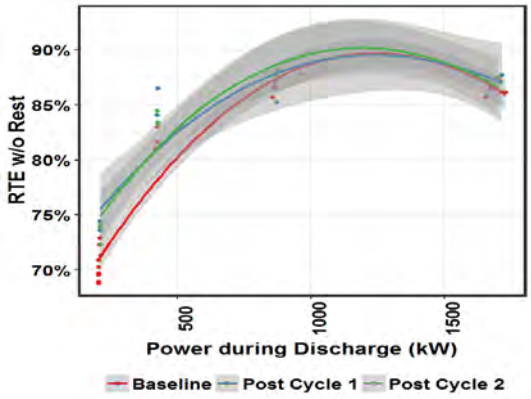
RTE w/o Rest
90%
85%
80%
75%
70%
500
1000
1500
Power during Discharge (kW)
Baseline
Post Cycle 1
Post Cycle 2

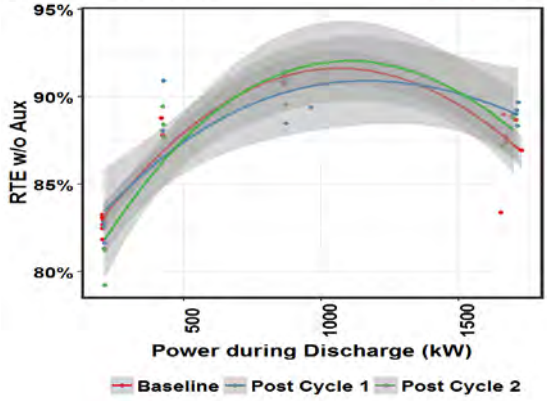
RTE w/o Aux
95%
90%
85%
80%
500
1000
1500
Power during Discharge (kW)
Baseline
Post Cycle 1
Post Cycle 2

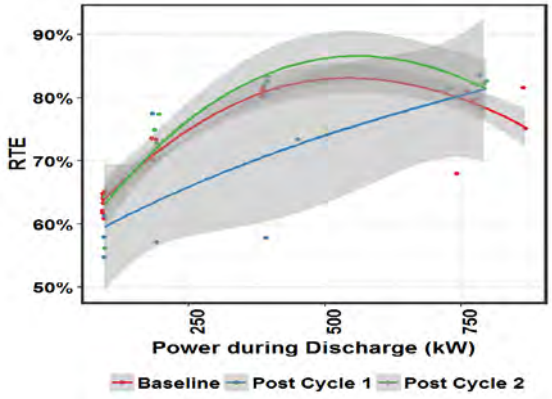
RTE
90%
80%
70%
60%
50%
250
500
750
Power during Discharge (kW)
Baseline
Post Cycle 1
Post Cycle 2

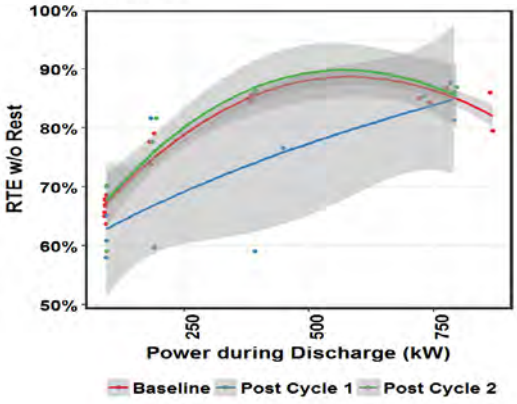
RTE w/o Rest
100%
90%
80%
70%
60%
50%
250
500
750
Power during Discharge (kW)
Baseline
Post Cycle 1
Post Cycle 2

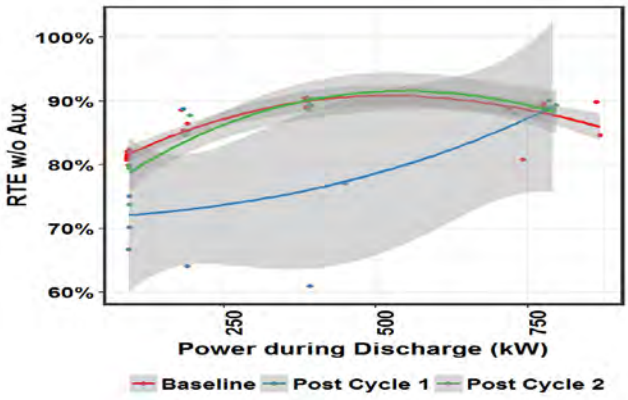
RTE w/o Aux
100%
90%
80%
70%
60%
250
500
750
Power during Discharge (kW)
Baseline
Post Cycle 1
Post Cycle 2

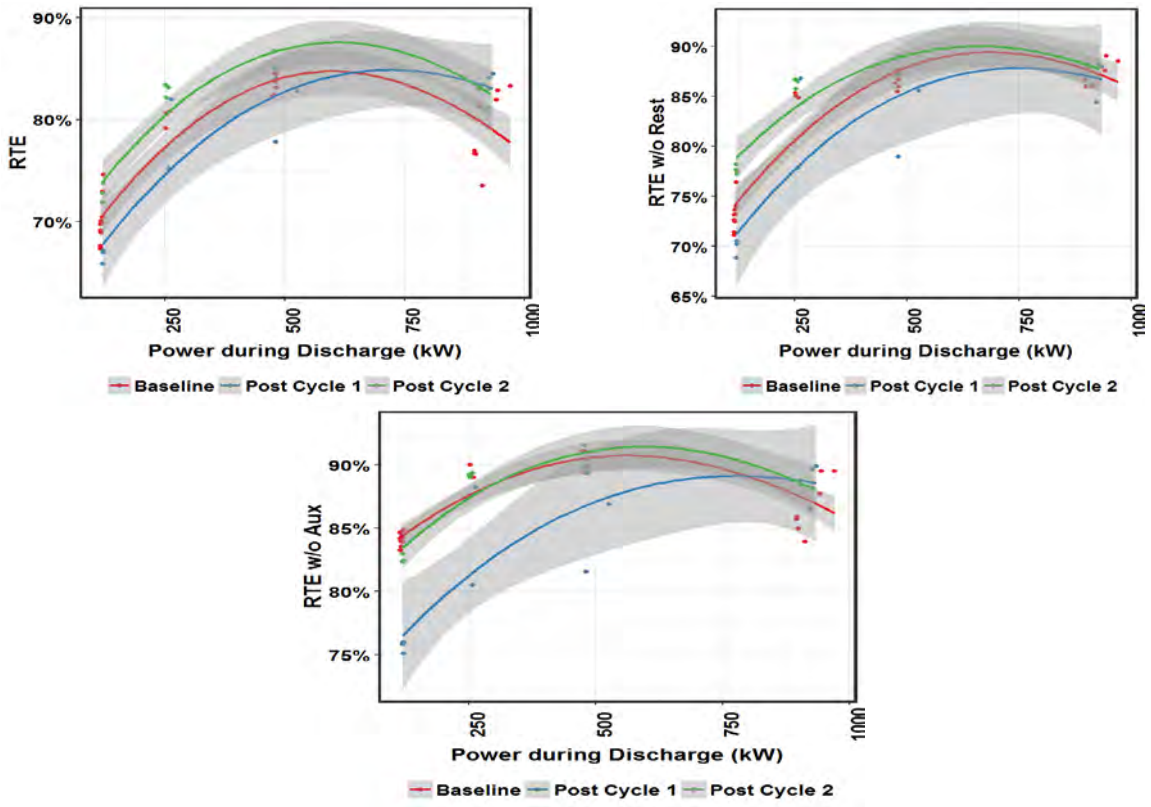

Figure 2.45. RTE at Various Power Levels for Baseline and Post Cycle 1 and Post Cycle 2; (left) includes Auxiliary Loads and Rest (right) Excludes Rest (bottom) Excludes Rest and Auxiliary Loads. Top 3: BESS, Middle 3: MESA-1a, Bottom 3: MESA-1b.

The temperature trend as a function of discharge power and test type is shown in Figure 2.46. While the temperatures are in a tight band and increase with power levels, due to higher ambient temperature for baseline tests, this requires greater auxiliary cooling power. At power levels of C/4 to 1C, the temperature is nearly the same for 1a and 1b. At 2C, 1a has a higher temperature by 2.5 °C. Since we do not have information on how thermal management control strategies differ for 1a and 1b, a definitive conclusion cannot be made on the reasons for this higher temperature for 1a. The auxiliary power flow for 1a and 1b are similar across all power levels. Considering 1a also absorbs and delivers less power, it appears its internal resistance is higher. However, as seen earlier, this is not the case. The higher change in temperature for 1a appears to be due to differences in thermal management.

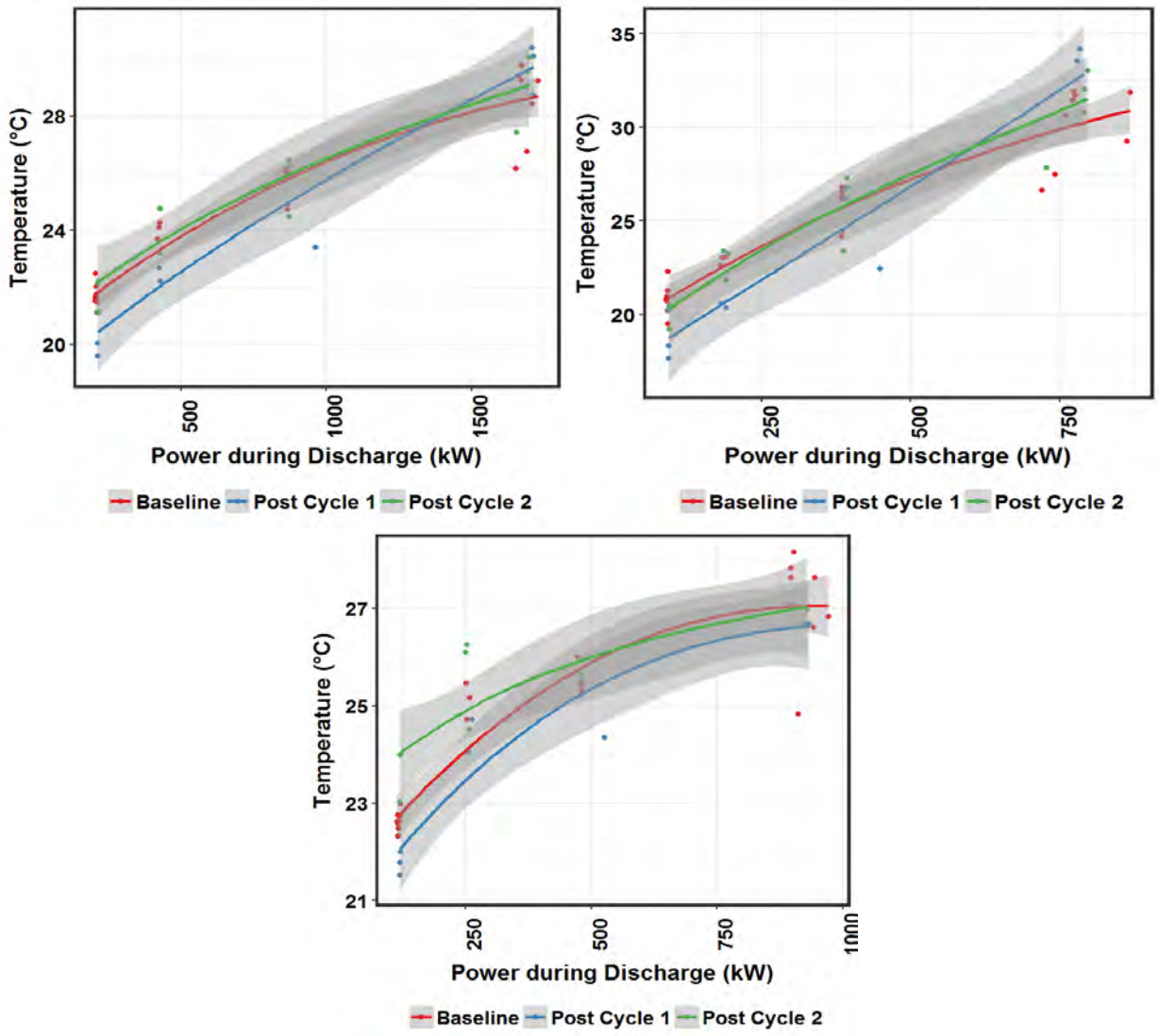

Figure 2.46. Average Temperature as a Function of Power Levels for Baseline and Post Cycle 1 and Post Cycle 2 Tests (left) BESS, (right) MESA-1a, (bottom) MESA-1b

The amount of charge energy and discharge energy per unit change in SOC is shown in Figure 2.47. As expected, the charge energy and discharge energy curves are mirror images of each other. Since RTE increases as charge energy per unit SOC decreases and discharge energy per unit SOC increases, the discharge energy curves look similar to RTE curves. Note that the charge and discharge energy per unit SOC is shown only for the case including auxiliary and rest. 1a accepts charge much better at low power levels for baseline and post Cycle 1. This advantage disappears as power levels increased. The power levels for 1b is greater than 1 a across all power ranges. Hence, we would expect the charge acceptance to be better for 1b at low power, since auxiliary losses are a smaller percentage of total charge power flow. As the batteries get conditioned during operation, the charge acceptance is similar for both 1a and 1b across all power levels as seen in post Cycle 2 results. Across all power levels, 1b provides more energy during discharge per unit change in SOC than 1a. The gap is highest for baseline test, where the difference is in the 6 to 10% range. For BESS and 1a, the discharge energy provided goes through a maximum at C rate, while for 1b, the discharge energy increases slightly with power for baseline and post cycle 2 (both done in warm weather). Only for post Cycle 1, done in cold weather, the discharge energy peaks at the C rate for 1b. The BESS behavior is dominated by 1a, especially during discharge.

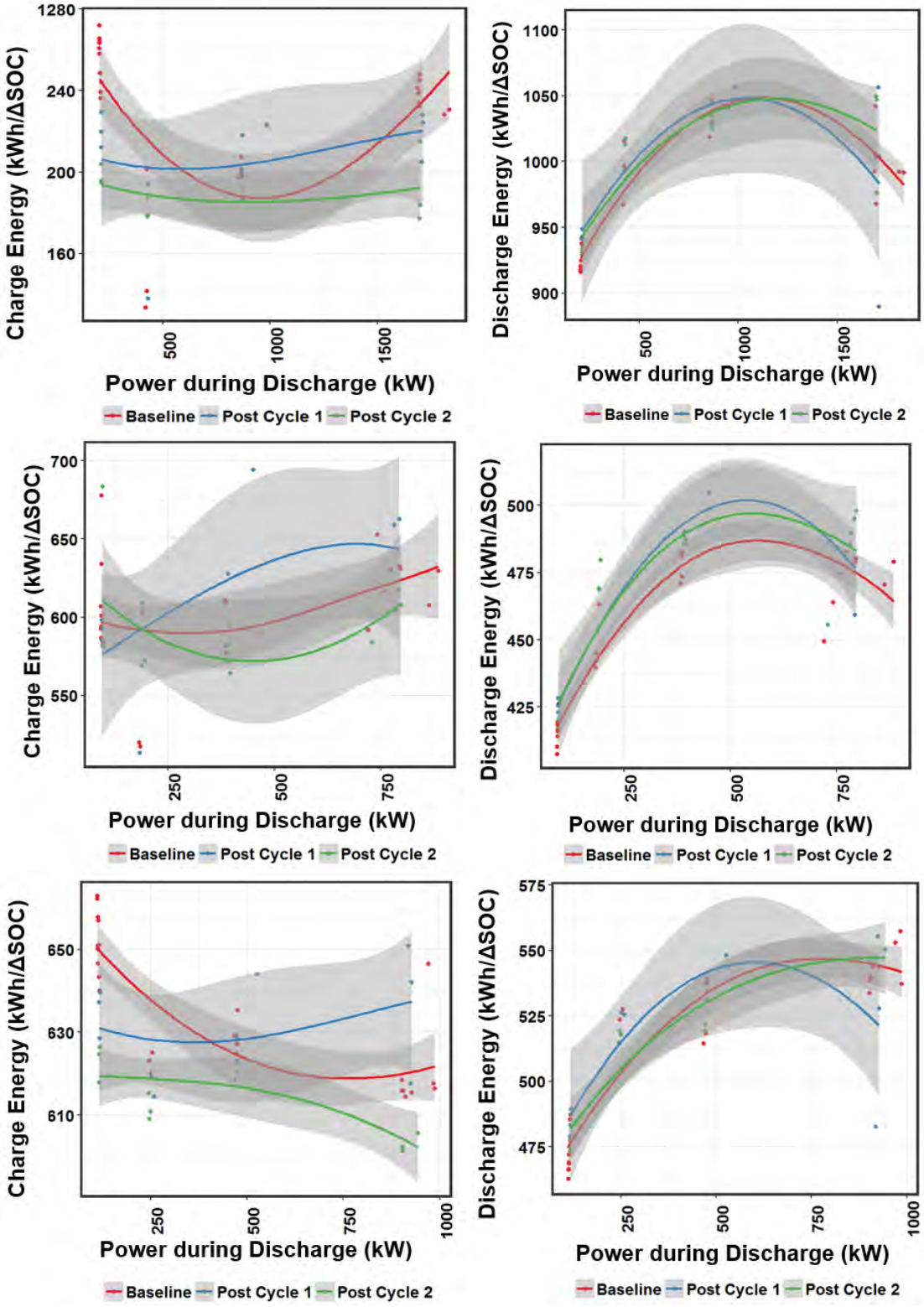

Figure 2.47. Effect of Power and Test Type (Baseline vs Post Cycle 1 or 2) on Charge or Discharge Energy needed per unit SOC, (top) Combined, (middle) MESA-1a, (bottom) MESA-1b

The summary of internal resistance data is shown in Table 2.19, Table 2.20, and Figure 2.48. Since the minimum time step is 15 minutes, it was difficult to obtain resistance at multiple SOCs. The actual data is shown in an expanded scale without a linear fit. The discharge resistances were nearly the same. However, the charge resistance after Cycle 2 at 8 percent SOC was much lower than the value measured during the baseline test, showing the conditioning effect on the battery. Note that post Cycle 1 was done in the winter (November 2016). Hence, its higher values compared to post Cycle 2 is expected. Considering the resistance for post Cycle 1 was nearly equal to the Baseline values, this indicates there is a conditioning effect after Cycle 1. Note that at 8 percent SOC, the internal resistance is for charge, while for 45 and 85 percent SOC, the internal resistance is for discharge. Results are shown for both 10s and 20s pulses, with the charge pulse corresponding to 1,400 kW, and the discharge pulse to 1800 kW.

The different power levels were due to the restriction of commands being executed with a lower limit of 15 minutes for the time step. At 1,400 kW charge, the delta SOC was 0.39 percent after 10 seconds, and 0.79 percent after 20 seconds. For 1,800 kW discharge, the delta SOC was 0.5 percent after 10 seconds, and 1 percent after 20 seconds. The data at 10 seconds is more appropriate, since this corresponds to the lower delta SOC. As discussed earlier, it has been shown that delta SOC should not exceed 0.1 percent for accurate measurement of internal resistance form pulse tests (Schweiger 2010).

As expected, the internal resistance is lower for the 10s measurement. The values for baseline and post Cycle 1 are similar across the SOC ranges investigated. However, for post Cycle 2, the internal resistance for 50 percent SOC discharge was lower by 15 percent. The charge resistance at 8 percent SOC was lower by nearly an order of magnitude for the 10s measurement, and is lower by 25 percent for the 20-s measurement. This appears to indicate that the BESS has been getting conditioned over the nearly one year of testing, and has a lower internal resistance.

The uncertainty bands are quite high as seen in Figure 2.48. However, this is because the forcing function applied was a straight line fit, resulting in an artificially high error band. With three data points, unless the data fall in a straight line, the error bands would be very high. At the other extreme, using a polynomial to fit the data, the error band would be zero, since a polynomial would fit any three data points perfectly. While the error bands have been presented for the sake of transparency, it is suggested that this information is not very useful in this context.

Since several tests have been done at > 1,000 kW, future work would analyze the internal resistance during these cycles to get a more reliable estimate of battery state of health during operation.

Table 2.19. Internal Resistance of the ESS Post Cycle 1

	Internal Resistance Charge (mΩ)			Internal Resistance Discharge (mΩ)		
SOC (%)	1a	1b	BESS	1a	1b	BESS
87	NA	NA	NA	17.1/23.1	15.1/18.9	8.0/10.3
43	NA	NA	NA	18.1/24.9	16.0/18.3	8.5/10.6
8	20.2/27.1	23.9/27.3	11.1/13.6	NA	NA	NA

Table 2.20. Internal Resistance of the ESS Post Cycle 2

	Internal Resistance Charge (mΩ)			Internal Resistance Discharge (mΩ)		
SOC (%)	1a	1b	BESS	1a	1b	BESS
90	NA	NA	NA	16.9/21.4	16.0/19.1	8.2/10.1
40	NA	NA	NA	14.9/21.5	14.6/17.7	7.4/10.1
8	1.8/20.4	16.8/20.3	4.3/10.2	NA	NA	NA

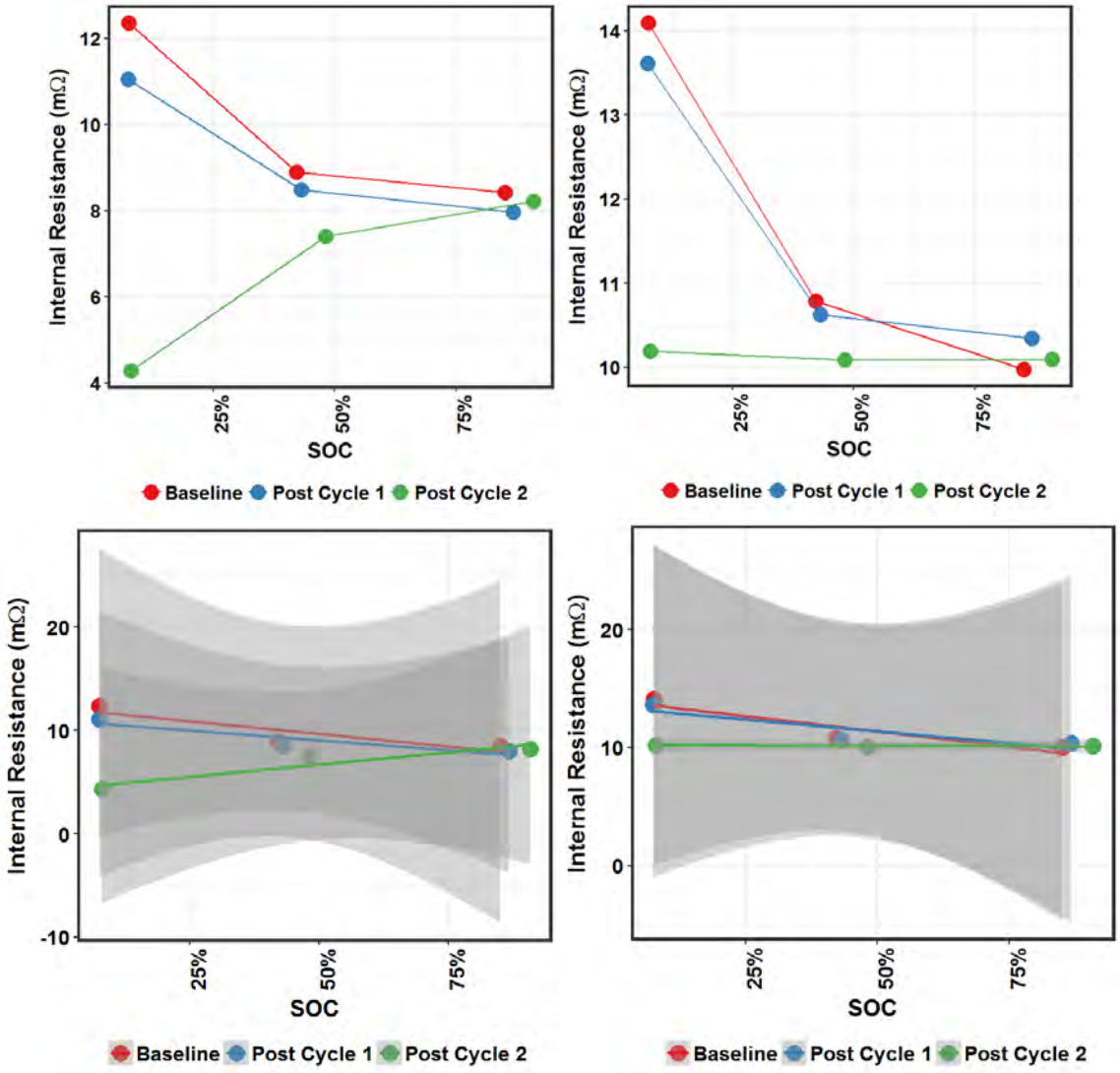

Figure 2.48. Internal Resistance from Pulse Testing of MESA-1 BESS (left) 10s Pulse, (right) 20s Pulse. Data shown with and without uncertainty bands.

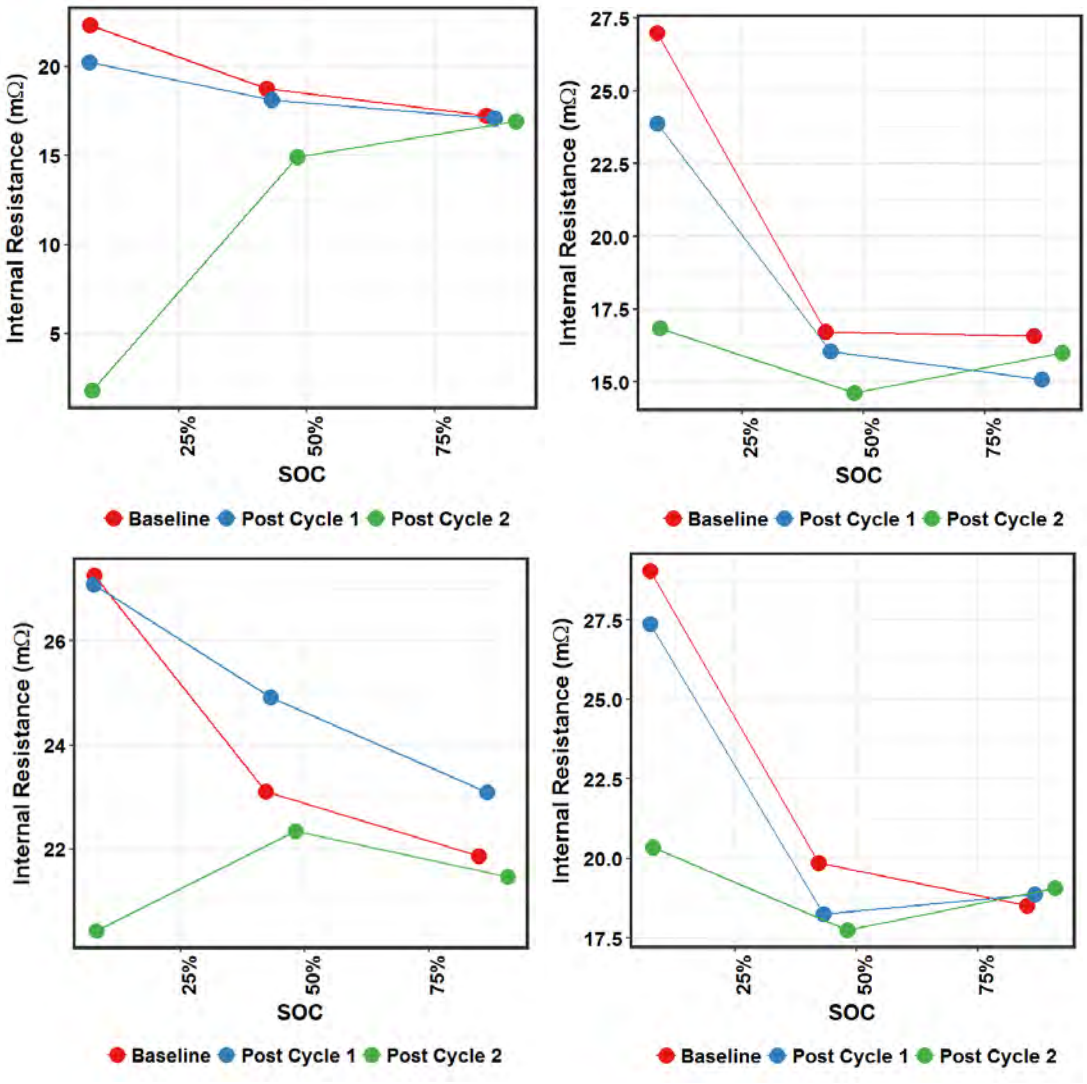

Figure 2.49. Internal Resistance from Pulse Testing of MESA-1a (left) and MESA-1b (right). Top: 10 Second Pulse, Bottom 20 Second Pulse

The corresponding internal resistance values for MESA-1a and 1b are shown in Figure 2.49, with the top graphs showing results for 10 second pulses, and the bottom for 20 second pulses. The internal resistance values for MESA-1a and 1b are nearly the same for 85 percent and 50 percent discharge for the 10-second pulse. For 10 second charge pulse at 8 percent SOC, MESA-1a internal resistance is one order of magnitude lower than the value for 1b. At 20 seconds, MESA-1b resistance at 85 percent and 50 percent discharge is lower by 10 percent and 30 percent respectively, while the internal resistance is nearly the same for charge at 8 percent SOC. Note that the MESA-1a current is lower by around 7 percent. It is known that the charge transfer resistance drops with increasing current. Hence, it is possible that this could be the reasons for higher internal resistance for 1a. The other effect could be the higher temperature associated with higher current through MESA-1b.

To investigate the reason for the precipitous drop in internal resistance at the 10 second charge for 1a, the voltage versus current curves are plotted in Figure 2.50 for post Cycle 1 and post Cycle 2 for 1a and 1b. For 1a post Cycle 2, the change in voltage at 2V is an order of magnitude lower than the 22-24V change for baseline (not shown) and post Cycle 1 pulse tests. For 1b, changes in voltage and current are lower for

post Cycle 2. This is probably because due to the very low internal resistance of 1a initially, more current flow through 1a (11.2 kA vs. 9.2 kA through 1b). At t = 20 seconds, the current through 1a and 1b are 10.8 kA and 11.4 kA respectively, and both 1a and 1b resistance are identical at 20.3 milliohms. As seen earlier, the power flow between 1a and 1b is not uniform at the start of various capacity tests. Farther the total power is from rated power of 2,000 kW, greater the disparity in power flow, with the lower resistance battery taking up more power. As the total power approaches the 2,000 kW threshold, the power flow is more uniform between the two batteries, since the rated power is reached for the lower resistance battery. It is important that the internal resistance for both batteries be balanced to ensure uniform power flow between the two batteries. With non-uniform power flow, one battery is exercised more than the other, resulting in greater average depth of discharge, and potentially shorter life. Another reason for the low internal resistance for 1a could be that the voltage data is not updated correctly. Either the meter was not temporarily reading the correct value, or there was a time lag for the meter to update the correct reading. Considering the current data appears properly updated, it seems unlikely that the time lag could be an issue for voltage. Regardless, it is clear that the extremely low internal resistance for 1a during 10-s charge pulse does not last a long time, with the internal resistance increasing to the same level as 1b in 20 seconds.

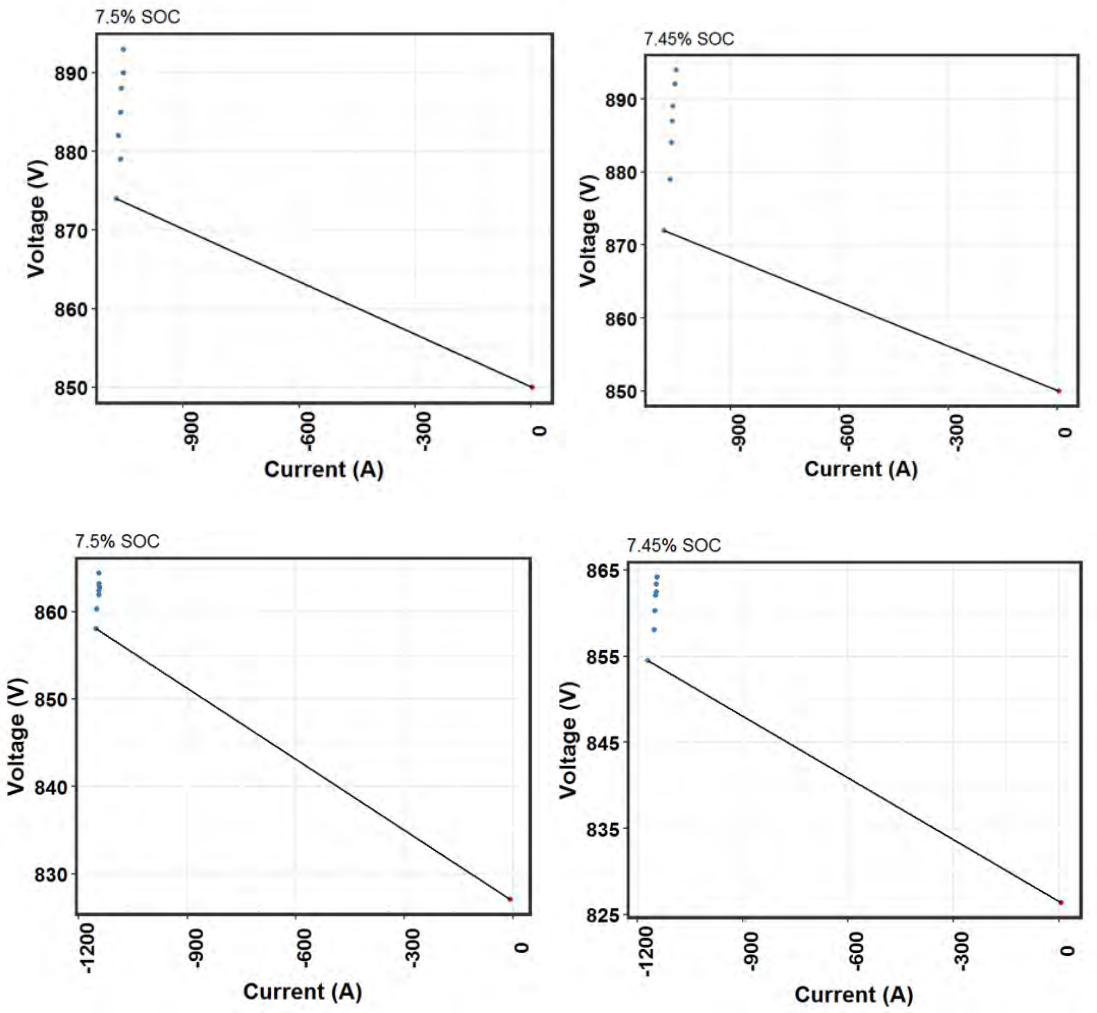

Figure 2.50. Voltage as a Function of Charge Current at 8% SOC for Post Cycle 1 (left) and Post Cycle 2 (right) for 1a (top) and 1b (bottom)

Degradation of a Li-ion cell or battery depends on various factors:

- Duration at various SOC/voltage, where voltage is a proxy for SOC
- Duration at various temperatures
- Operating power
- Number of cycles at various DODs
- Cumulative discharge energy throughput

As discussed earlier, initial charge and discharge power was higher for 1b. Additionally, from August 19, 2016 to August 25, 2016, there was power flow through only 1b. The cumulative discharge energy throughput through 1a and 1b is shown in Figure 2.51. The throughput for 1b of 215 MWh is 48 percent than the 145 MWh discharged by 1a. So far, this has not adversely affected the state of health (SOH) of 1b. However, this metric should be closely monitored as testing proceeds.

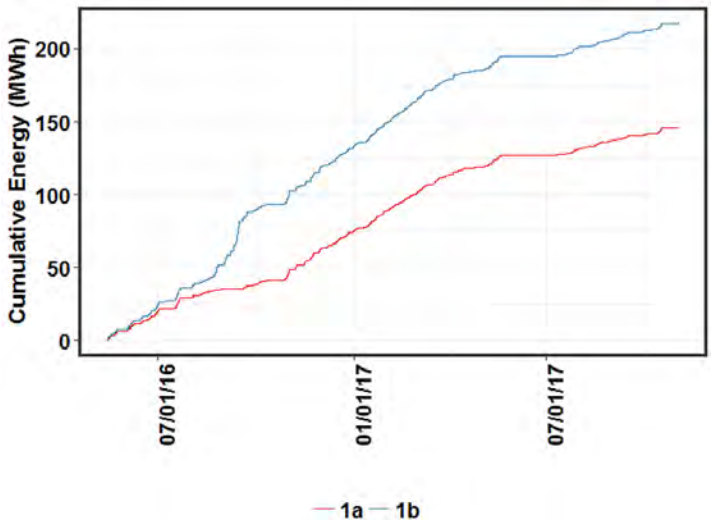

Figure 2.51. Cumulative Discharge Energy Throughput through 1a and 1b

To verify that charging is endothermic, a regression analysis was done for rate of change of temperature as a function of power and average temperature. A third order polynomial was used for power. From Table 2.21, the negative coefficient of P^1 shows the endothermic effect. The rate of change of temperature is plotted as a function of power below. As expected, at higher average temperature, the rate of change of temperature is lower.

Table 2.21. Cooling Effect of Charging

Term	Estimate	Std. Error	Pr(>|t|)
(Intercept)	0.040558	0.001609	1.82E-97
Average Temperature	-0.00013	5.43E-06	1.38E-94
Power	-0.00025	0.000341	0.458598
$Power^2$	0.033715	0.000474	2.26E-303
$Power^3$	0.002715	0.000346	1.85E-14

An analysis was done on the duration during testing when there was no power flow between the BESS and the grid. The auxiliary power through each battery is > 15 kW. Hence, by using a 10 kW cutoff, the percent of time the auxiliary power flow was < 10 kW was determined for 1a and 1b. For the duration of this project, from June 14, 2016 to May 16, 2017, 1a was disconnected from the grid 53 percent of the time, while 1b was disconnected 58 percent of the time. The numbers for the time period May 13, 2016 to November 1 2017 were 52 percent and 60 percent, respectively, for 1a and 1b.

3.0 Lessons Learned

This section provides an at-a-glance view of important lessons learned on the technical aspects of MESA-1 BESS based on the experiences gained during the testing process and the test results. Conclusive remarks on the overall testing effort and the importance of the test results are provided at the end of this section.

3.1 Lessons Learned from Test Results

1. The BESS was discharged between 92.5 percent and 7.5 percent SOC (85 percent DOD). The estimated discharge energy at 100 percent DOD was calculated by dividing the measured energy by the DOD of 85 percent. Including the auxiliary losses, 970 kWh was delivered at the C rate. Excluding auxiliary consumption, the energy delivered is within 5 kWh of the rated energy of 1000 kWh.
2. The RTE ranged from 66 to 91 percent, depending on the power, and whether the rest periods and auxiliary consumption were included. The BESS retained its energy content during post Cycle 1 and Cycle 2 capacity tests, with a similar RTE range. The RTE at C/4 rate was lowest for baseline tests, because of higher auxiliary power consumption during summer.
3. When auxiliary consumption during rest periods were excluded, the RTE rose by 3 to 5 percent, with the highest increase for baseline tests performed in summer, with higher auxiliary load. When the auxiliary consumption was excluded throughout the test period, the RTE increased by 6 to 16 percent, with the difference increasing with decreasing rate. At less than or equal to C rate, the increase in RTE was highest for baseline tests, which had auxiliary load
4. MESA-1a battery absorbs and provides less power than MESA-1b battery for power levels less than or equal to C/2 rate. This is because its initial SOC is higher at the start of charge, and lower at the start of discharge. For runs where MESA-1a starting SOC during charge was lower, it did absorb greater power during charge. This indicates that DERO distributes power between 1a and 1b based on reported SOC values.
5. For all cases, the initial SOC during charge is higher for 1a, and during discharge is lower for 1b. Hence, the starting power for both charge and discharge is lower for 1a. The exception is 2C rate charge. Since 1b is already at its maximum rating of 1,000 kW, the remaining 1000 kW has to be absorbed by 1a. Once 1a SOC reaches 55 percent, the power starts tapering, while 1b maintains 1,000 kW throughout charge. This shows the difference is the BMS, which reduces the power to C rate at 55 percent. For discharge at 2C, due to limitations in the SNOPUD system where the smallest time interval for commands is 15 minutes, discharge power was set lower than 2000 kW. Hence MESA-1b starting power was close to 1000 kW, with 1a initial power being in the 750 kW to 780 kW range. At 1C and 2C rates, even though average power for 1a lower than 1b during charge and discharge, temperature for 1a higher – higher internal resistance for 1a.
6. The MESA-1b BESS is more well suited for high power applications.
7. Auxiliary power consumption decreases during winter – less cooling needed.
8. Auxiliary power consumption increases with increasing charge or discharge power – more cooling needed.
9. Charging has an endothermic effect.

10. The shapes of the charge energy vs power curves are dominated by 1a when auxiliary power is included. That is because 1a requires more auxiliary power at high power, due to greater rise in temperature (high internal resistance). When auxiliary power consumption is excluded, the behavior of the BESS again is dominated by MESA-1a.
11. The discharge energy as a function of power curves is dominated by 1a, which peaks at 1C rate, whereas 1b discharge energy increases with discharge power. The exception again is post Cycle 1 which occurs at cold ambient temperature. The discharge energy for both 1a and 1b peak at 1C rate for post cycle 1.
12. The RTE as f(power) follows the shape of the discharge energy as f(power)
13. MESA-1a SOC range specifications was 10 to 90 percent, while 1b range was 10 to 95 percent. However, as testing proceeded, 1b lower SOC limit was extended t0 5 percent, while 1a, after its steep drop in SOC after charge, had an SOC of 85 percent.
14. The EPRI ESIC meeting held November 16, 2017 in Cleveland identified SOC calibration procedure, seasonal testing for auxiliary load, SOC loss rate due to reactive power injection and state of health definition and tests as key gaps that merit further studies. This project addressed all these gaps. Two more gaps identified by ESIC were:
    a. DC injection – can the BESS provide this service? Or can the BESS do any harm by injecting DC power into the grid?
    b. "Independent phase control for unbalanced loads – how can ESS balance loads in each phase of the distribution grid?

Would it help SnoPUD to do these studies?

<u>Anomalies</u>

This section describes the anomalies experienced during testing, such as power spikes, unexpected SOC relaxation trends during rest, high rate of decrease of SOC during reactive power flow and rest after discharge to low SOC.

1. For all rates, there is a spike in power after charge and discharge – a charge spike at the end of charge and discharge spike at the end of discharge. While the spike occurs more for 1b, it does occur for both 1a and 1b. At C/4 rate and C/3 rate, there is a spike at the end of charge and discharge. This is associated with power tapering at 1a, accompanied by power spiking at 1b. The spike magnitude is such that at times the total charge power or discharge power exceed requested power.
2. The rate of change of SOC increases when BESS is in power factor correction mode. During the same run, when BESS is not in power factor correction mode, the rate of change of SOC is lower. This probably has something to do with BESS being connected to the grid when power factor mode is on, and disconnected from the grid when it is not on power factor mode. This is a metric in the US DOE-OE protocol, the difference between rate of change of SOC with and without Volt-VAR or PF correction mode. Some examples of steep decrease in SOC during PF correction mode:
    a. Steep decrease in SOC from 50 percent to 10 percent with no real power flow, possibly due to PCS switching (November 18 2016 9 PM to November 19, 2016 5 AM).
    b. Steep decrease from 85 percent to 12 percent SOC in 48 hours between 3/11/17 to 3/13 17 with no real power flowing and PCS in switching mode.
3. The rate of change of SOC did not depend on the magnitude of the reactive power.

4. For all other runs when BESS was not placed in PF correction mode, during periods when real power flowed, reactive power was also exchanged. During rest after charge, no reactive power was exchanged, while after discharge there was exchange of reactive power. Thus, the BESS appears to go from grid connected mode to disconnected mode during rest after charge. Hence, the inverter is not being powered during rest or doing PF correction off mode for Use Case 3 Volt/VAR tests. It is still not clear why the rate of decrease of SOC during rest is greater when BESS is connected to grid (PF mode on). The PCS and auxiliary loads receive power separately. If BESS is powering auxiliary loads when PF mode is on, this should be reflected in discharge power at the inverter level but this is not the case.
5. Up to C/2 rate charge, there is a steep drop in SOC at the end of charge for MESA-1a. This indicates that the reported SOC during charge is greater than the actual SOC. This has the effect of underestimating the charge energy needed per unit SOC change for a fixed power level, thus making the charge look more efficient than it is.
6. At > C/2 rate charge, the drop in SOC is not as steep for MESA-1a. That is because at the end of charge, the reported SOC value is not as high as for C/4 and C/2 rates. This indicates the reported SOC, while still higher than actual, is closer to actual SOC than for lower charge rates. The SOC after rest is still lower for 1a, hence initial discharge power is also lower. The SOC at the end of discharge increases slightly for 1a.
7. At C rate charge, 1b SOC keeps increasing during the one hour rest. This indicates that the reported SOC value for 1b is lower than actual SOC. Hence, the charging appears more inefficient than it actually is based on Wh/delta SOC. For C rate discharge, the SOC keeps decreasing during rest. This indicates the reported SOC is higher than actual SOC, making the discharge more efficient in terms of Wh/delta SOC than actual.
8. At 2C rate, the trends are the same as for 1C, except after discharge, the SOC is stable for 1b for one run, and decreases a bit for another run.
9. For the PF Correction test, the volt-amperes-reactive (vars) requested were during Cycle 2 were lower than during Cycle 1, possible because Cycle 1 testing was done in winter, with higher need for PF correction.
10. A spike in discharge power during Cycle 1, to 50 kW, was accompanied by a decrease in vars and drop in apparent power to 1870 kVA (from close to 2000 kVA), indicating the DERO optimizer may be dropping var request more than the calculated available vars, in order to ensure the rated power of the BESS is not exceeded. This drop in apparent power was present for all occasions when discharge spikes were present, and did not occur when charge spikes were present. This appears to indicate that the required vars is lower when the BESS is discharging.
11. The PCS switches during normal operation and during PF mode. During rest after charge, the PCS does not switch. During rest after discharge, the PCS switches when the SOC at the end of discharge is within 2 percent of its lower limit, to prevent the SOC from decreasing below its lower limit.
12. To remove the PCS switching issue when no schedule files are being processed, a “0” schedule is placed on the project, which prevents the PCS from switching. This was done after about two months of testing to ensure the BESS SOC did not drift downward.
13. There were times when even with auto-scheduler on, the run started one hour earlier than intended

<u>Human and System Errors and Stoppages</u>

This category lists the various human errors that led to incorrect power requests from the BESS, some system errors such incorrect test start times, and various stoppages during testing.

1. For one capacity use case run (July 25-Aug 1, 2016), the charge energy used was the same as discharge energy, resulting in SOC dropping with time. The RTE was not used in determining charge power.
2. Testing times up to one week in a row were lost due to not loading schedules, Doosan being on site or other issues.
3. During testing, sometimes the BESS was taken offline by SnoPUD. During the time it was offline, the power swung from charge to discharge. The reason for the BESS being taken offline was not communicated by SnoPUD. The reason for the power swing while offline was also not communicated.
4. For one arbitrage run, a wrong day duty cycle was done for the last two days.
5. For some runs, the actual battery power lagged the scheduled power by an hour. This was because the person entering the commands was not able to enter the command within the correct hour, and so entered it the next hour. In some cases, the data led the scheduled power by an hour, indicating that the scheduler had entered the start time an hour earlier than intended. Also, at the 1C rate charge and discharge, the actual BESS power was only 87 percent of the recommended power in these cases (reason for this is not known). This happened when the schedule was entered manually to allow for switching back to optimizer scheduling for the BPA demand response test, which occurred Monday morning through Friday evening. It was communicated to PNNL that if PNNL sends a schedule that ran from Friday evening (post DR) through Sunday evening (before next DR starts), the "pre-input" of the schedule can be done "better". Hence this auto-scheduler method was followed in all subsequent scheduling when the BESS was set aside for DR during Tuesday-Friday.
    a. When running on a ***Resource Schedule*** the optimizer has been disabled and the resource is running to a written schedule.
    b. When running on an ***Override Schedule*** the optimizer is enabled but an override schedule has been entered. An override schedule should take precedence over any other recommendation but other algorithms continue to be in effect.
6. There were times when the testing was started at the incorrect SOC, once at 45 percent when the intended start SOC was 10 percent, and another times at 9- percent when the intended start SOC was 10 percent.

The number of days the BESS was not available for testing was determined. There were 88 days when the BESS was set aside for DR for BPA. Excluding these days, the number of days for testing were 242 from June 20, 2016 to May 20, 2017. The BESS was not available 38 percent of the 242 days, or a total of 92 days. Out of the 92 unavailable days, The BESS was not available for 16 days or 7 percent of the time due to BESS related issues, 12 days or 5 percent due to site/DERO-related issues, 6 days or 2.5 percent due to human error, while unknown reasons, which could be any of the categories listed, contributed 58 days or 24 percent of the time. When the days for DR were counted, the number of days for testing corresponded to 330 days (11 months). The BESS was not available to PNNL for testing 55 percent of the time, with stoppage-related unavailability corresponding to 5 percent due to BESS-related issues, 3.6 percent due to site/DERO-related issues, 1.8 percent due to human error, 18 percent due to unknown reasons, with the BESS performing DR for the remaining 27 percent of the time.

3.2 Lessons Learned in Design of Test Set-up and Data Transfer

1. SnoPUD provided PNNL a template to load schedule files. This template was further changed by SnoPUD prior to loading the file to operate the BESS. This led to different file formats – one sent by PNNL, and another created by SnoPUD. The file sent by PNNL had start times that were different

from the start times in the file generated by SnoPUD. The file name had numbers such as 1006 which was a 1E-1C identifier that would change with each test. This resulted in significant confusion in the beginning. Sometimes the start times would be changed multiple times, leading to further confusion.

2. The data historian at SnoPUD did not store the requested power. Hence, it was difficult to reconcile the actual power with requested power, resulting in an inefficient process. Charge and discharge steps had to be in 15-minute increments. Since the BESS at 2C takes less than 30 minutes to discharge, the discharge power had to be kept less than 2C (or 2,000 kW) in order to ensure the BESS was not overdischarged. Since the 1a and 1b discharge power did taper as SOC approached low values, 2,000 kW discharge power for 30 minutes could have been used without having to worry about the SOC excursion beyond its lower limit.
3. For Volt/var testing, the BESS was put on PF correction mode. The scheduled var was not shared with PNNL. It was subsequently learned that DERO stores this information for only one month. Information on where the PF was monitored, and if the Power factor remained within an acceptable range of target PF was also not shared. The Acceptance test shows that PF is being monitored at the Hardeson substation meter. Hence the PF at the Hardeson substation was tracked to look at the effectiveness of the ESS to provide PF correction.
4. The drawings provided to PNNL by SnoPUD had different labels for meters than the eDNA spreadsheet provided to PNNL. It was quite difficult to reconcile the drawings with the spreadsheet to identify what each point represents. The same issue is now arising with MESA-2.
5. There were about 40 periods during a test when data was missing. Most lasted one hour, while others lasted up to 12 hours. There was one data set when data was missing for 48 hours. There were some periods where the data within the hour was sampled twice. According to explanation from SNOPUD, data for PNNL is pulled from eDNA on an hourly basis for the previous hour and sent to a portal for PNNL to process. The PNNL interface runs at 20 minutes after each hour and pulls data from eDNA for the previous hour. Outage in the SNOPUD Batch Scheduling System caused the scheduled run that would normally occur at 5:20AM to be delayed well into the next hours. This resulted in data from one hour and from the following hour being processed twice. Since this was an intermittent issue occurring once a month, it was decided not to investigate this further.

3.3 Lessons Learned from Test Disruptions and Investigations

1. In the initial stages, some of the requested information such as battery SOC level was not provided to PNNL. This made it difficult to develop a schedule file.
2. PCS switching occurred after C/2 and C/4 discharge rates – this impacted the rate of change of SOC. PCS switching also occurs when BESS is under operation – real or reactive power.
3. The BESS stopped after a 100 kW charge due to a refrigerant leak in 1a. No lessons learned – just an example of disruption. 1a was offline for a week, so 1b was tested alone.
4. The BESS got an alarm July 21 early morning and was then taken offline few hours later. The lesson learned was unanticipated events do happen, and disrupt testing.
5. There were some occasions when the schedules were forgotten to be loaded (July 22, 2016). Resulting in different start times than our records.
6. On other occasions, Doosan site visit was announced after the fact and would create further delay (July 27, 2016).
7. For System Capacity test UC1, the charge energy was set equal to discharge energy, which resulted in BESS SOC decreasing more than expected.

8. There was an intermediate step between sending the schedule and executing the schedule. The BESS needed to be put on auto – which required coordination within SNOPUD between our POC and SNOPUD's field personnel initially, and Energy Control Center (ECC) Dispatcher later on. There were times (August 8, 2016) when our POC had not gotten a response from SnoPUD, hence the schedule was not executed.
9. Discrepancies between scheduled power and ESS actual power output were observed in a number of cases. Email discussions (January 24, 2017) with SnoPUD power scheduling personnel indicated there are two modes for running power schedules in DERO controller which controls the ESS. One is Resource Schedule mode where the DERO optimizer is disabled, and the resource runs to a written schedule, and the other is Override Schedule where the optimizer is enabled but an override schedule has been entered. An override schedule should take precedence over any other recommendation but, SnoPUD personnel witnessed, other algorithms continue to be in effect. Changing DERO controller mode from "Override" to "Resource" mode improved command following performance in some cases but not always.

4.0 Conclusions

SnoPUD obtains most of its power from BPA and provides balancing charges to BPA to account for difference in net load and scheduled net load (load – generation). SnoPUD is using the MESA-1 2MW/1 MWh BESS "to learn about energy storage and how it can be used to integrate renewable generation resources into its resource portfolio" (Zyskowski 2015). In addition to balancing, the BESS performance was evaluated for arbitrage, distribution upgrade deferral and PF correction. Since BESS are quite diverse in their characteristics, it was important to characterize their performance and stability over time using a DOE-OE standardized test procedure for energy storage.

This report investigated the technical performance of the SnoPUD MESA-1 BESS facility, consisting of two battery sub-systems 1a and 1b, based on a number of baseline and use case tests. Baseline tests were intended to assess the general technical capability of the BESS (e.g., stored energy capacity, ramp rate performance, ability to track variable charge/discharge commands, DC battery internal resistance) while the use case tests were intended to examine the performance of the BESS while engaged in a specific service (e.g., arbitrage, regulation, outage mitigation).

Parameters that are important for understanding BESS performance when subjected to actual field operation for economic purposes (e.g., RTE, auxiliary consumption, command tracking performance, temperature variations, parasitic power loss during power electronics switching during rest, SOC excursions, non-uniformity of power flow between the battery subsystems) were examined. Outcomes of these analyses will be beneficial for SnoPUD to understand the performance of the MESA-1 BESS at its current state and to apply these results in designing appropriate operational strategies. In addition, the results and lessons presented herein would also be beneficial for any task or effort that needs technical assessment on similar types of BESS based on field deployment results. Some specific conclusions are:

- The rated energy of 1 MWh was estimated to be delivered at the C rate at the PCS (excluding auxiliary losses) from 100 percent to 0 percent SOC, including the auxiliary losses, 970 kWh was delivered at the C rate.
- The BESS RTE ranged from 66 to 91 percent based on charge-discharge rate, auxiliary power consumption, and whether rest period and auxiliary load were included.
- Exclusion of 1-h rest period during baseline capacity tests increased RTE by 3 to 5 percent, while exclusion of auxiliary loads increased RTE by 6 to 16 percent, with higher increase in RTE at lower rates. This provides valuable insights in terms of how to operate the BESS optimally.
- The BESS RTE increases with cycling. However, when auxiliary power consumption is excluded, the RTE does not change with cycling.
- The RTE was computed including and excluding rest periods and auxiliary loads. The analysis shows that auxiliary losses eat into the RTE, which adversely affect arbitrage benefits, while long rest times at low SOC, in addition to auxiliary losses, also consume parasitic power that decreases SOC by nearly two orders of magnitude.
- RTE is maximum at 1,000 kW or C rate for this BESS.
- Power flow distribution through 1a at the start of charge or discharge is lower than through 1b, resulting in lower RTE at low power for 1a. This is related to lower SOC at the start of charge and higher SOC at the start of discharge for 1a.
- The internal resistance determined by 20-s pulse is lower for 1b, resulting in increasing RTE with power, while 1a RTE peaks at the C rate of 500 kW.

- The PCS is set in switching mode during PF correction; the SOC decreases at a rate of 1.62%/h, compared to 0.06%/h when the PCS is not in switching mode. Hence, this increases losses even when there is no power flow through the DC battery. This high rate of SOC decrease needs to be taken into account by the system operator when the BESS is in PF correction mode.
- Typically, the BESS PCS is set in switching mode at the end of discharge to the lower SOC limit to prevent the SOC from decreasing further, while after charge, this issue is not present. To avoid this unnecessary power consumption, it is desirable to not go below an SOC 5 percent above lower threshold so that the lower threshold will not be crossed for > 80 hours (5/0.06).
- Auxiliary consumption is higher in summer than in winter and spring by 6.5 kW. This reduces BESS RTE in summer.
- Spikes at the end of charge and discharge were present, primarily caused by power tapering in 1a necessitating 1b to spike in order to pick up necessary power. At low C rates, this spike results in total power flow exceeding requested power momentarily. Since the spikes do not exceed the PCS rating, no damage to the DC battery is anticipated. However, it is not known what the rapid power pulse does to the PCS hardware.
- System stoppages due to technical glitches mainly associated with PCS issues and DERO updates coupled with ongoing demand response deployment of the BESS resulted in loss of around 60 percent of testing time.
- The optimal spot for minimizing energy losses during operation is at 1,000 kW. This would change depending on the percent of time the BESS is at rest, whether PCS is in switched state during rest, and the time of the year.
- Due to differences in power flow between 1a and 1b, the throughput through 1b is 48 percent higher than the throughput through 1a, while its rated energy is 5 percent greater than 1a. This could eventually lead to greater degradation of 1b.
- A slight endothermic effect for charge existed, which could affect charge acceptance during winter.
- MESA-1b has better high rate performance than 1a, with RTE increasing as a function of power, while 1a RTE peaks at the C rate of 1,000 kW for the BESS.
- The BESS state of health has not degraded in the nearly one year of testing. It is recommended that PNNL analyze test results from May 2017 to present to assess degradation using in-situ pulse resistance results and energy per unit change in SOC and comparing with numbers to date. This will help firm up the degradation model PNNL is developing to predict performance as a function of battery operational history such as charge & discharge power levels, depth of discharge, number of cycles, energy throughput, time at various SOCs and temperature.
- A framework was developed to identify the various parameters that affect BESS performance and degradation to allow its optimal deployment.

5.0 References

1energy systems, Acceptance Test Report SN1B-QR-09, June 18, 2015

1energy systems, Acceptance Test Report SN1B-QR-09, February 9, 2016

Balducci PJ, MJE Alam, VV Viswanathan, AJ Crawford, D Wu, and TD Hardy. 2017. "Washington Clean Energy Fund: Energy Storage System Performance Test Plans and Data Requirements." PNNL-26492, Pacific Northwest National Laboratory, Richland, WA.

http://www.doosangridtech.com/products/ Accessed on Dec 16, 2016 (Doosan 2016a)

http://www.doosangridtech.com/products/distributed-energy/applications/ Accessed on Dec 16, 2016 (Doosan 2016b)

MESA Open Standards for Energy Storage http://mesastandards.org/wp-content/uploads/2016/11/MESA-ESS-Specification-November-2016-Draft-2.pdf Accessed on Dec 27, 2016 (MESA 2016)

Schweiger HO, O Obeidi, A Komesker, M Raschke, C Schiemann, M Zehner, M Gehner, M Keller, and P Birke. 2010. Comparison of Several Methods for Determining the Internal Resistance of Lithium Ion Cells. Sensors 2010, 10, 5604-5625. Accessed July 3, 2017 at http://www.mdpi.com/1424-8220/10/6/5604

http://mesastandards.org/wp-content/uploads/2017/09/SunSpec-Alliance-Specification-Energy-Storage-ModelsD4rev0.25.pdf Accessed on Feb 26, 2018 (SunSpec 2017)

Viswanathan VV, DR Conover, AJ Crawford, S Ferreira, and D Schoenwald. 2014. "Protocol for Uniformly Measuring and Expressing the Performance of Energy Storage Systems." PNNL-22010 Rev. 1, Pacific Northwest National Laboratory, Richland, WA.

Zyskowski, J. "Overview and Lessons Learned from Snohomish County PUD's First Energy Storage Project", accessed July 14 2017 at https://www.snopud.com/Site/Content/Documents/energystorage/SnoPUD-EnergyStorage013115.pdf.

Appendix A

Table A.1. Initial Baseline Capacity Test Results

Start Date	Duration (h)	Mean Temp. (°C)	Charge Energy (kWh)	Discharge Energy (kWh)	RTE (%)	Charge Energy No Rest (kWh)	RTE No Rest	Charge Energy No Aux (kWh)	Discharge Energy No Aux (kWh)	RTE No Aux (%)	Average Charge Power (kW)	Average Discharge Power (kW)
2016/06/14	2.9	28.4	1026	840	81.9	964	87.1	962	853	88.7	1694	1708
2016/06/14	2.9	29.2	1038	840	80.9	976	86.1	980	852	86.9	1779	1729
Mean 2000 kW charge, 1750 kW discharge 1/2h	2.9	28.8	1032	840	81.4	970	86.6	971	852	87.8	1736	1718
Cumulative	6.9	28.4	2088	1680	80.5	1938	86.7	1944	1705	87.7	1736	1718
2016/06/16	2.9	26.7	1026	845	82.4	969	87.2	966	859	88.8	1815	1691
2016/06/16	2.9	29.4	1025	833	81.3	956	87.1	953	848	89.0	1792	1663
2016/06/16	3.8	29.8	1072	837	78.1	965	86.7	972	851	87.6	1770	1672
Mean 2000 kW charge, 1750 kW discharge 1/2h	3.2	28.6	1041	838	80.6	963	87.0	964	852	88.5	1793	1675
Cumulative	8.9	28.6	3086	2513	81.4	2886	87.1	2876	2555	88.8	1828	1675
2016/06/23	9.6	21.1	1124	777	69.1	1075	72.3	1017	844	83.0	271	210
2016/06/23	9.6	21.7	1139	764	67.0	1087	70.2	1015	844	83.1	274	207
2016/06/23	9.6	21.6	1115	780	70.0	1069	72.9	1014	843	83.2	270	211
2016/06/24	9.5	21.5	1139	775	68.0	1086	71.3	1020	849	83.2	277	214
Mean 255 kW charge, 230 kW discharge 4h	9.6	21.5	1129	774	68.3	1079	71.7	1017	845	83.1	273	210
Cumulative	40.8	21.5	4591	3095	67.4	4318	71.6	4094	3380	82.6	273	210

After the peak shaving and pulse resistance tests, the baseline capacity tests at C/4 rate was repeated as shown in Table A.2. The charge and discharge energy and RTE without auxiliary losses was the same as the C/4 rate cycling results shown in Table A.1. However, due to higher auxiliary consumption, the charge energy from the grid is higher, and the discharge energy supplied to the grid is lower for the post peak shaving & pulse testing capacity tests. It is not clear why auxiliary consumption was higher for these tests.

Table A.2. Post Peak Shaving (PS) and Pulse Testing Baseline Capacity Tests

Start Date	Duration (h)	Mean Temp. (°C)	Charge Energy (kWh)	Discharge Energy (kWh)	RTE (%)	Charge Energy No Rest (kWh)	RTE No Rest (%)	Charge Energy No Aux (kWh)	Discharge Energy No Aux (kWh)	RTE No Aux (%)	Average Charge Power (kW)	Average Discharge Power (kW)
2016/06/28	9.6		1156	758	65.6	1100	68.9	1020	841	82.5	276	206
2016/06/28	9.6	21.6	1149	759	66.1	1092	69.6	1013	843	83.3	276	206
2016/06/29	9.6	21.5	1148	761	66.3	1094	69.5	1018	842	82.7	276	206
Mean 255 kW charge, 230 kW discharge 4h	9.6	21.6	1151	760	66.0	1095	69.3	**1017**	842	82.8	276	206
Cumulative	29.6	21.6	3484	2279	65.4	3285	69.3	3062	2526	82.5	276	206

Subsequent to the baseline tests conducted at C/4 rate and 2C rate prior to peak shaving and pulse testing, and C/4 rate after peak shaving and pulse testing, the energy capacity was determined at multiple power levels as shown in Table A.3. The trend of lower RTE at low power levels is clear. The highest RTE for charge and discharge at the C rate is achieved at 1,000 kW.

Table A.3. Multiple Charge-Discharge Rates July 4 Weekend and Mid July

Start Date	Duration (h)	Mean Temp. (°C)	Charge Energy (kWh)	Discharge Energy (kWh)	RTE (%)	Charge Energy No Rest (kWh)	RTE No Rest (%)	Charge Energy No Aux (kWh)	Discharge Energy No Aux (kWh)	RTE No Aux (%)	Average Charge Power (kW)	Average Discharge Power (kW)
2016/06/29	3.9	24.7	1058	880	83.2	1018	86.5	994	902	90.8	1018	868
2016/06/30	3.9	26.0	1044	875	83.8	1004	87.1	982	896	91.2	1004	868
2016/06/30	3.9	26.2	1043	866	83.0	1001	86.5	977	888	90.9	1001	866
Mean 1000 kW charge, 885 kW discharge 1h	3.9	25.6	1048	874	83.3	1008	86.7	984	895	90.9	1008	867
Cumulative	11.9	25.6	3148	2621	83.2	3023	86.7	2953	2685	90.9	1008	867
2016/06/30	5.9	23.7	1070	824	77.0	1016	81.1	979	869	88.8	503	419
2016/06/30	5.9	24.1	1075	835	77.7	1023	81.6	993	872	87.8	506	424
2016/07/01	6.9	24.3	1114	859	77.2	1036	83.0	1022	898	87.8	517	426
Mean 500 kW charge, 445 kW discharge 2h	6.2	24.0	1086	839	77.3	1025	81.9	998	880	88.1	508	423
Cumulative	17.9	24.0	3219	2511	78.0	3060	82.0	2967	2631	88.6	508	423
2016/07/01	7.8	22.6	1123	783	69.7	1064	73.5	1008	853	84.6	351	269
2016/07/01	7.9	22.9	1101	796	72.2	1048	75.9	995	854	85.9	351	273
2016/07/02	7.8	22.8	1098	790	71.9	1041	75.9	993	853	85.9	348	272
Mean 330 kW charge, 295 kW discharge 3h	7.8	22.8	1107	789	71.3	1051	75.1	999	853	85.4	350	271
Cumulative	23.8	22.8	3334	2368	71.0	3153	75.1	3001	2560	85.3	350	271
2016/07/2	19.1	20.8	1258	531	42.2	1215	43.6	1004	669	66.6	121	72
2016/07/14	21.1	20.5	1371	593	43.3	1326	44.7	1101	737	67.0	121	73
2016/07/15	21.0	20.7	1363	592	43.4	1319	44.9	1100	736	66.9	120	73
2016/07/16	21.0	20.8	1357	590	43.5	1311	45.0	1102	736	66.8	119	72

Start Date	Duration (h)	Mean Temp. (°C)	Charge Energy (kWh)	Discharg e Energy (kWh)	RTE (%)	Charge Energy No Rest (kWh)	RTE No Rest (%)	Charge Energy No Aux (kWh)	Discharge Energy No Aux (kWh)	RTE No Aux (%)	Average Charge Power (kW)	Average Discharge Power (kW)
Mean 100 kW charge, 91 kW discharge 10h, rest 1h	20.6	20.7	1337	577	43.1	1293	44.6	1077	719	66.8	120	72
Cumulative	69.0	20.7	4290	1776	41.4	3956	44.9	3387	2209	65.2	120	73
2016/07/17	3.4	26.2	1111	909	81.8	1045	87.0	1033	934	90.4	1307	1227
2016/07/17	4.4	27.5	1176	916	77.9	1071	85.6	1070	936	87.4	1253	1240
2016/07/17	4.4	27.9	1177	928	78.8	1078	86.1	1088	946	87.0	1263	1246
Mean 1500 kW charge, 1320 kW discharge 45 min, Rest 1h	4.0	27.2	1155	918	79.5	1064	86.2	1064	938	88.3	1275	1238
Cumulative	10.4	27.2	3366	2750	81.7	3168	86.8	3143	2812	89.5	1319	1239
2016/07/18	7.4	26.2	1166	835	71.6	975	85.6	1017	848	83.4	1577	1654
2016/07/18	3.9	29.3	1072	840	78.3	971	86.4	978	854	87.4	1723	1670
2016/07/18	3.8	29.8	1071	838	78.2	968	86.6	972	853	87.7	1765	1670
Mean 2000 kW charge, 1725 kW discharge 1/2h rest 1h	5.0	28.4	1103	838	76.1	972	86.2	989	852	86.2	1688	1665
Cumulative	13.4	27.7	3230	2505	77.6	2901	86.4	2934	2547	86.8	1740	1665
2016/07/18	9.6	22.5	1158	759	65.5	1103	68.8	1031	844	81.8	274	206
2016/07/19	9.6	21.7	1134	765	67.5	1079	70.9	1013	842	83.1	273	208
2016/07/19	9.6	22.0	1145	760	66.4	1090	69.7	1013	841	83.0	276	207
Mean 255 kW charge, 230 kW discharge 4h (2nd run post PS and Pulse test)	9.6	22.1	1145	761	66.5	1091	69.8	1019	842	82.7	274	207
Cumulative	29.6	22.1	3466	2284	65.9	3273	69.8	3070	2527	82.3	274	207

Start Date	Duration (h)	Mean Temp. (°C)	Charge Energy (kWh)	Discharge Energy (kWh)	RTE (%)	Charge Energy No Rest (kWh)	RTE No Rest (%)	Charge Energy No Aux (kWh)	Discharge Energy No Aux (kWh)	RTE No Aux (%)	Average Charge Power (kW)	Average Discharge Power (kW)
2016/07/20	3.9	24.9	1057	879	83.2	1016	86.5	995	902	90.7	1016	866
2016/07/20	3.9	25.9	1049	872	83.2	1006	86.7	983	896	91.2	1006	865
2016/07/20	3.9	26.1	1055	858	81.3	1001	85.7	975	886	90.8	1001	858
Mean 1000 kW charge, 885 kW discharge 1h (2nd run post PS and Pulse test)	3.9	25.6	1053	870	82.6	1008	86.3	984	895	90.9	1008	863
Cumulative	11.9	25.6	3164	2609	82.5	3024	86.3	2953	2683	90.9	1008	863
2016/07/20	5.9	23.8	1078	828	76.8	1022	81.0	991	869	87.7	495	421
2016/07/20	6.8	24.3	1127	854	75.8	1040	82.1	1019	900	88.3	518	421
2016/07/21	5.9	24.1	1071	826	77.1	1018	81.1	994	867	87.1	497	421
Mean 500 kW charge, 445 kW discharge 2h (2nd run post PS and Pulse test)	6.2	24.1	1092	836	76.6	1027	81.4	1002	879	87.7	503	421
Cumulative	17.9	24.1	3215	2488	77.4	3047	81.7	2961	2614	88.3	504	421
2016/07/21	7.8	22.9	1111	787	70.8	1057	74.4	990	848	85.7	352	271
2016/07/21	7.8	22.8	1104	788	71.4	1050	75.0	997	854	85.7	349	271
2016/07/22	7.8	22.7	1103	792	71.8	1049	75.5	997	856	85.8	349	271
Mean 330 kW charge, 295 kW discharge 3h (2nd run post PS and Pulse test)	7.8	22.8	1106	789	71.3	1052	75.0	995	853	85.7	350	271
Cumulative	23.8	22.8	3326	2366	71.1	3152	75.0	2984	2557	85.7	350	271
2016/08/13	14.0	23.5	909	576	63.4	697	82.7	678	599	88.3	662	576
2016/08/14	14.0	22.1	1086	598	55.1	714	83.8	718	615	85.6	687	584
2016/08/15	21.0	22.0	837	577	68.9	684	84.3	669	601	89.8	684	575

Start Date	Duration (h)	Mean Temp. (°C)	Charge Energy (kWh)	Discharg e Energy (kWh)	RTE (%)	Charge Energy No Rest (kWh)	RTE No Rest (%)	Charge Energy No Aux (kWh)	Discharge Energy No Aux (kWh)	RTE No Aux (%)	Average Charge Power (kW)	Average Discharge Power (kW)
Mean 330 kW charge, 295 kW discharge 3h	15.6	22.6	944	584	62.4	698	83.6	689	605	87.9	678	578
Cumulative (Start SOC 28 to 50%, end SOC 24 to 32%)												

* The cumulative analysis included runs with other power levels also. Hence it is not reported here.

From all the capacity tests done so far, the results for C/4, C/2, 1C and 2C rates are summarized in Table A.4 and Table 2.2. This includes results for all the runs, while Table 2.2 only provides the mean and cumulative results. The mean RTE is simply the average of RTE for each run, while cumulative RTE is the discharge energy divided by charge energy for all the runs combined. Note that at the end of each run, a charge or discharge energy is included to bring the SOC to the initial value. This charge or discharge at the end to bring the SOC to the initial value is actually not carried out, but is the estimated value based on the collected data, and is typically very small, since the BESS starts and ends at the low end of the SOC range for most tests. Note that when rets time and auxiliary losses are included, the maximum discharge energy available from the BESS is 971 kWh at the C rate, while when Auxiliary losses are excluded, the maximum energy available from the BESS is 1000 kWh. To calculate the maximum available energy, the measured energy is divided by the DOD of 82.5% (92.5 % SOC at the end of charge minus 7.5% SOC at the end of discharge).

Table A.4. Consolidated Results for Baseline Capacity Tests Prior to Cycle 1 Use Case Testing

Start Date	Dura-tion (h)	Mean Temp. (°C)	Charge Energy (kWh)	Discharge Energy (kWh)	RTE (%)	Charge Energy No Rest (kWh)	RTE No Rest (%)	Charge Energy No Aux (kWh)	Discharge Energy No Aux (kWh)	RTE No Aux (%)	Average Charge Power (kW)	Average Discharge Power (kW)
2016/06/23	9.6	21.1	1124	777	69.1	1075	72.3	1017	844	83.0	271	210
2016/06/23	9.6	21.7	1139	764	67.0	1087	70.2	1015	844	83.1	274	207
2016/06/23	9.6	21.6	1115	780	70.0	1069	72.9	1014	843	83.2	270	211
2016/06/24	9.5	21.5	1139	775	68.0	1086	71.3	1020	849	83.2	277	214

Start Date	Dura-tion (h)	Mean Temp. (°C)	Charge Energy (kWh)	Discharge Energy (kWh)	RTE (%)	Charge Energy No Rest (kWh)	RTE No Rest (%)	Charge Energy No Aux (kWh)	Discharge Energy No Aux (kWh)	RTE No Aux (%)	Average Charge Power (kW)	Average Discharge Power (kW)
Mean 255 kW charge, 230 kW discharge 4h	9.6	21.5	995	747	75.1	995	75.1	927	816	88.0	275	212
Cumulative	40.8	21.4	3980	2991	75.2	3980	75.2	3706	3265	88.1	275	212
2016/06/28	9.6	21.6	1156	758	65.6	1100	68.9	1020	841	82.5	276	206
2016/06/28	9.6	21.5	1149	759	66.1	1092	69.6	1013	843	83.3	276	206
2016/06/29	9.6	21.6	1148	761	66.3	1094	69.5	1018	842	82.7	276	206
Mean 255 kW charge, 230 kW discharge 4h	9.6	21.6	1151	760	66.0	1095	69.3	1017	842	82.8	276	206
Cumulative	29.6	21.6	3484	2279	65.4	3285	69.3	3062	2526	82.5	276	206
2016/07/18	9.6	22.5	1158	759	65.5	1103	68.8	1031	844	81.8	274	206
2016/07/19	9.6	21.7	1134	765	67.5	1079	70.9	1013	842	83.1	273	208
2016/07/19	9.6	22.0	1145	760	66.4	1090	69.7	1013	841	83.0	276	207
Mean 255 kW charge, 230 kW discharge 4h (2nd run post PS and Pulse test)	9.6	22.1	1145	761	66.5	1091	69.8	1019	842	82.7	274	207
Cumulative	29.6	22.1	3466	2284	65.9	3273	69.8	3070	2527	82.3	274	207
2016/06/30	5.9	23.7	1070	824	77.0	1016	81.1	979	869	88.8	503	419
2016/06/30	5.9	24.1	1075	835	77.7	1023	81.6	993	872	87.8	506	424
2016/07/01	6.9	24.3	1114	859	77.2	1036	83.0	1022	898	87.8	517	426
Mean 500 kW charge, 445 kW discharge 2h	6.2	24.0	1086	839	77.3	1025	81.9	998	880	88.1	508	423
Cumulative	17.9	24.0	3219	2511	78.0	3060	82.0	2967	2631	88.6	508	423
2016/07/20	5.9	23.8	1078	828	76.8	1022	81.0	991	869	87.7	495	421

Start Date	Dura-tion (h)	Mean Temp. (°C)	Charge Energy (kWh)	Discharge Energy (kWh)	RTE (%)	Charge Energy No Rest (kWh)	RTE No Rest (%)	Charge Energy No Aux (kWh)	Discharge Energy No Aux (kWh)	RTE No Aux (%)	Average Charge Power (kW)	Average Discharge Power (kW)
2016/07/20	6.8	24.3	1127	854	75.8	1040	82.1	1019	900	88.3	518	421
2016/07/21	5.9	24.1	1071	826	77.1	1018	81.1	994	867	87.1	497	421
Mean 500 kW charge, 445 kW discharge 2h (2nd run post PS and Pulse test)	6.2	24.1	1092	836	76.6	1027	81.4	1002	879	87.7	503	421
Cumulative	17.9	24.1	3215	2488	77.4	3047	81.7	2961	2614	88.3	504	421
2016/06/29	3.9	24.7	1058	880	83.2	1018	86.5	994	902	90.8	1018	868
2016/06/30	3.9	26.0	1044	875	83.8	1004	87.1	982	896	91.2	1004	868
2016/06/30	3.9	26.2	1043	866	83.0	1001	86.5	977	888	90.9	1001	866
Mean 1000 kW charge, 885 kW discharge 1h	3.9	25.6	1048	874	83.3	1008	86.7	984	895	90.9	1008	867
Cumulative	11.9	25.6	3148	2621	83.2	3023	86.7	2953	2685	90.9	1008	867
2016/07/20	3.9		1057	879	83.2	1016	86.5	995	902	90.7	1016	866
2016/07/20	3.9	24.9	1049	872	83.2	1006	86.7	983	896	91.2	1006	865
2016/07/20	3.9	25.9	1055	858	81.3	1001	85.7	975	886	90.8	1001	858
Mean 1000 kW charge, 885 kW discharge 1h (2nd run post PS and Pulse test)	3.9	26.1	1053	870	82.6	1008	86.3	984	895	90.9	1008	863
Cumulative	11.9	25.6	3164	2609	82.5	3024	86.3	2953	2683	90.9	1008	863
2016/06/14	2.9	28.4	1026	840	81.9	964	87.1	962	853	88.7	1694	1708
2016/06/14	2.9	29.2	1038	840	80.9	976	86.1	980	852	86.9	1779	1729

Start Date	Dura-tion (h)	Mean Temp. (°C)	Charge Energy (kWh)	Discharge Energy (kWh)	RTE (%)	Charge Energy No Rest (kWh)	RTE No Rest (%)	Charge Energy No Aux (kWh)	Discharge Energy No Aux (kWh)	RTE No Aux (%)	Average Charge Power (kW)	Average Discharge Power (kW)
Mean 2000 kW charge, 1750 kW discharge 1/2h	2.9	28.8	1032	840	81.4	970	86.6	971	852	87.8	1736	1718
Cumulative	6.9	28.4	2088	1680	80.5	1938	86.7	1944	1705	87.7	1736	1718
2016/06/16	2.9		1026	845	82.4	969	87.2	966	859	88.8	1815	1691
2016/06/16	2.9	26.7	1025	833	81.3	956	87.1	953	848	89.0	1792	1663
2016/06/16	3.8	29.4	1072	837	78.1	965	86.7	972	851	87.6	1770	1672
Mean 2000 kW charge, 1750 kW discharge 1/2h	3.2	29.8	1041	838	80.6	963	87.0	964	852	88.5	1793	1675
Cumulative	8.9	28.6	3086	2513	81.4	2886	87.1	2876	2555	88.8	1828	1675
2016/07/18	7.4	26.2	1166	835	71.6	975	85.6	1017	848	83.4	1577	1654
2016/07/18	3.9	29.3	1072	840	78.3	971	86.4	978	854	87.4	1723	1670
2016/07/18	3.8	29.8	1071	838	78.2	968	86.6	972	853	87.7	1765	1670
Mean 2000 kW charge, 1725 kW discharge 1/2h rest 1h	5.0	28.4	1103	838	76.1	972	86.2	989	852	86.2	1688	1665
Cumulative	13.4	27.7	3230	2505	77.6	2901	86.4	2934	2547	86.8	1740	1665

Pacific Northwest
NATIONAL LABORATORY

Proudly Operated by **Battelle** *Since 1965*

U.S. DEPARTMENT OF
ENERGY

902 Battelle Boulevard
P.O. Box 999
Richland, WA 99352
1-888-375-PNNL (7665)

www.pnnl.gov